Electrochemical Society

HELP

... on any customer's operating problem has top priority on the schedule of our technical service personnel. Your call triggers action—focuses attention on the answers you seek. For fast, effective, superior technical assistance, you can rely on GLC every time.

ELECTRODE GLC DIVISION

GREAT LAKES CARBON CORPORATION

18 EAST 48TH STREET, NEW YORK 17, N. Y. OFFICES IN PRINCIPAL CITIES

EDITORIAL STAFF

H. H. Uhlig, Chairman, Publication Committee

Cecil V. King, Editor

Norman Hackerman, Technical Editor

Ruth G. Sterns, Managing Editor

U. B. Thomas, News Editor

H. W. Salzberg, Book Review Editor

Natalie Michalski, Assistant Editor

DIVISIONAL EDITORS

W. C. Vosburgh, Battery

Milton Stern, Corrosion, I

R. T. Foley, Corrosion, II

T. D. Callinan, Electric Insulation

Seymour Senderoff, Electrodeposition

H C. Froelich, Electronics

Ernest Paskell, Electronics—Semiconductors

Sherlock Swann, Jr., Electro-Organic, I

Stanley Wawzonek, Electro-Organic, II

John M. Blocher, Jr., Electrothermics and Metallurgy, I

A. U. Seybolt, Electrothermics and Metallurgy, II

N. J. Johnson, Industrial Electrolytic

C. W. Tobias, Theoretical Electrochemistry, I

A. J. deBethune, Theoretical Electrochemistry, II

ADVERTISING OFFICE

ECS
1860 Broadway, New York 23, N. Y.

ECS OFFICERS

W. C. Gardiner, President
Olin Mathieson Chemical Corp., Niagara Falls, N. Y.

R. A. Schaefer, Vice-President
The Bunting Brass and Bronze Co., Toledo, Ohio

Henry B. Linford, Vice-President
Columbia University, New York, N. Y.

F. L. LaQue, Vice-President
International Nickel Co., Inc., New York, N. Y.

Lyle I. Gilbertson, Treasurer
Air Reduction Co., Murray Hill, N. J.

I. E. Campbell, Secretary
National Steel Corp., Weirton, W. Va.

Robert K. Shannon, Executive Secretary
National Headquarters, The ECS, 1860 Broadway, New York 23, N. Y.

Manuscripts submitted to the Journal should be sent, in triplicate, to the Editorial Office at 1860 Broadway, New York 23, N. Y. They should conform to the Instructions to Authors, last published in the August 1959 issue, pp. 232C-233C. Manuscripts so submitted become the property of The Electrochemical Society and may not be published elsewhere, in whole or in part, unless permission is requested and granted by the Editor.

Inquiries re positive microfilm copies of volumes should be addressed to University Microfilms, Inc., 313 N. First St., Ann Arbor, Mich.

Journal of the

Electrochemical Society

OCTOBER 1959 **VOL. 106 • NO. 10**

CONTENTS

Editorial

Report from Alaska 264C

Technical Papers

The Oxide Films Formed on Copper Single Crystal Surfaces in Pure Water, I. Nature of the Films Formed at Room Temperature. *J. Kruger* 847

An Electron Microscopic Study of the Formation of Oxide on Copper Single Crystals Immersed in an Aqueous Solution of Copper Sulfate. *G. T. Miller, Jr., and K. R. Lawless* 854

Influence of Silicon on the High-Temperature Oxidation of Copper and Iron. *J. W. Evans and S. K. Chatterji* 860

Translucent Phosphor Coatings in High-Pressure Mercury-Vapor Lamps. *C. H. Haake* 866

The Use of Organo-Substituted Hydrolyzable Silanes on Silicon Devices. *B. Schwartz* 871

Arc Decomposition of Rhodonite. *V. Harris, J. D. Holmgren, S. Korman, and C. Sheer* 874

On the Measurement of the Temperatures of Unenclosed Objects by Radiation Methods. *A. G. Emslie and H. H. Blau, Jr.* 877

The Behavior of Rhenium in Electron Tube Environments. *G. B. Gaines, C. T. Sims, and R. I. Jaffee* 881

Oxides on the Silver Electrode. *C. P. Wales and J. Burbank* 885

Hydrogen Overvoltage on Bright Platinum, III. Effect of Hydrogen Pressure. *S. Schuldiner* 891

A Porcelain Reference Electrode Conductive to Sodium Ions for Use in Molten Salt Systems. *R. J. Labrie and V. A. Lamb* 895

Galvanic Behavior in Fused Electrolytes, II. Discharge of the System Mg/LiCl-KCl-K_2CrO_4/Ni. *S. M. Selis and L. P. McGinnis* 900

Technical Notes

The Diffusion of Corrosion Hydrogen in Aluminum Alloys. *W. E. Tragert* 903

On the Crystallization of Simple Rhombohedral Boron from Platinum. *F. H. Horn.* 905

Technical Review

Report of the Chlor-Alkali Committee of the Industrial Electrolytic Division for the Year 1958. *C. A. Hampel and N. J. Ehlers* 906

Brief Communication

Action of Alkali on Caustic Cell Slimes. *S. Wawzonek and P. D. Klimstra* 910

Current Affairs 270C-277C

Published monthly by The Electrochemical Society, Inc., from Manchester, N. H., **Executive Offices, Editorial Office** and **Circulation Dept.,** and **Advertising Office** at 1860 Broadway, New York 23, N. Y., combining the JOURNAL and TRANSACTIONS OF THE ELECTROCHEMICAL SOCIETY. Statements and opinions given in articles and papers in the JOURNAL OF THE ELECTROCHEMICAL SOCIETY are those of the contributors, and The Electrochemical Society assumes no responsibility for them. Nondeductible subscription to members $5.00; subscription to nonmembers $18.00. Single copies $1.25 to members, $1.75 to nonmembers.

Copyright 1959 by The Electrochemical Society, Inc.

Entered as second-class matter at the Post Office at Manchester, N. H., under the act of **August 24, 1912.**

NOW...A COMPLETE LINE OF STANDARD SILICON INDUSTRIAL RECTIFIERS, 25KW TO 500KW, BY PERKIN

Lower initial cost, lower operating cost . . .
negligible maintenance . . . 94-97% efficiency!

Silicon's long life, stability and ruggedness have made possible industrial rectifiers which far outperform older conversion equipment both in reliability and efficiency. Perkin silicon rectifiers cover the full useful range of all other types of converters, cost less, install easily, are self-contained in a single compact enclosure (require no control panel), and are virtually maintenance-free. Use them for greater economy and dependability in powering chemical processes, machine tools, elevators, dc motors and controls – in fact, in *any* dc power application. Prompt delivery anywhere.

Overload protection to NEMA standards

All units completely self-protected for short circuits – coordinated protection of diode fuse, output fuse and input breaker.

Elements stay cool under severest conditions

To realize the long-life potential of silicon rectifier elements, Perkin fan-cools them during operation to just 40% of the manufacturer's recommended temperature rise!

Forced balance of voltage and current

Forced equality of voltage and current distribution prevents overloading or damaging of rectifier elements, even under severest conditions – no need to match replacement junctions.

Suppression of surges and transients

Capacitors and nonlinear resistor suppressors together with high-voltage-capacity rectifier elements make equipment fully surge proof.

Highest quality silicon diodes

All equipment uses the finest high-temperature, hermetically sealed silicon rectifier elements. Bond is metal-to-glass – no organic binders or potting compounds are used.

Optional Features

Where you need extreme reliability, Perkin can add a spare rectifier element in each string. If one element fails, remaining units maintain voltage. Fuse indicator lights pinpoint the bad element. In rectifiers of 200kw and over, an optional feature lets you replace elements and fuses *under load* safely and without interrupting operation.

Model IR25W

NOW... A STANDARD SILICON RECTIFIER FOR EVERY PURPOSE!

MODEL NUMBERS

KW Rating	DC OUTPUT VOLTAGE			
	125 V 2-wire	250 V 2-wire	125/250 V 3-wire	600 V 2-wire
25	IR25W	IR25X	IR25Y	
50	IR50W	IR50X	IR50Y	
75		IR75X	IR75Y	
100		IR100X	IR100Y	IR100Z
150		IR150X	IR150Y	IR150Z
200		IR200X	IR200Y	IR200Z
300		IR300X	IR300Y	IR300Z
400		IR400X	IR400Y	IR400Z
500		IR500X	IR500Y	IR500Z

Available ac input voltage (3 phase, 60 cps)

208v	to	600v	for	25,	50,	&	75kw
440v	to	600v	for	100,	150,	&	200kw
440v	to	13,800v	for	300,	400,	&	500kw

PERKIN

Model IR5002

Overload: 125% for 2 hrs., 200% for 1 min. Meets all NEMA standards.
Efficiency: 94-97% at rated load.
Power factor: 94% at rated load.
Voltage ripple: 2% rms.
Regulation: 5% from 15% F.L. to F.L.

In addition to the standard industrial rectifier line above, Perkin has also furnished many secondary to the chemical, steel, shipyard, utility and other industries. Installations which have been in operation for many years include 10,000 amp. up to 40 volt duplex tap Aluminum Ziegler Crystallization, and 20,000 amp. shipside dip-type. Perkin has recently produced series connected 4,000 amp. silicon rectifiers for two major Chemical firms.

Write on your letterhead for detailed technical information regarding your specifications, or for a copy of our latest technical article "Industrial Semi-Conductor Rectifiers."

PERKIN
ENGINEERING CORPORATION
[illegible] El Segundo, California
[illegible] or PAlfgate 2-1375
EAST PA ENGINEERING OFFICE
[illegible] Pennsylvania
NEW [illegible] OFFICE
[illegible] Massachusetts

Editorial

Report from Alaska

NOW that Alaska is a State, it may be expected to grow in population and in industry at a faster pace than before. We have received a 200-page report entitled "Economic Analysis of Fairbanks and Contiguous Area, Alaska," which was prepared for the Golden Valley Electric Association, Inc.[1] Fairbanks is situated well in the interior, and is the second largest city in Alaska with a population of about 17,000. The suburban area has another 12,000 people; the University of Alaska is located at College, which is in this area (Alaska is now building a second university at Anchorage, on the south coast). Several military bases in the Fairbanks area have a combined personnel of 32,000. Fairbanks has its own electric supply; Golden Valley is a rural electric cooperative which was organized in 1947 to serve the suburban and outlying districts, and has been financed by the U. S. Rural Electrification Administration.

The Fairbanks area has tremendous growth potentialities. Before you engage transportation, remember that the climate and way of life would be considered quite rigorous by some people; the average temperature is −11°F in January, 58°F in July. The growing season is only 105 days but, since the summer days are very long, with sunshine up to 22 hours, many familiar field and garden crops are grown, as well as beef and poultry. Agriculture is not easy; the permafrost line varies from a few inches to several feet below the surface and, in places, the ground may be frozen to a depth of 200 feet. Permafrost recedes on cleared land, especially on southern slopes, and if the soil can be made black to absorb the sun's rays. Precipitation is not large, and if rain and melted snow cannot be absorbed they run off rapidly, allowing the soil to dry out in the summer to the point where irrigation is needed.

There is great need for more agriculture and for food processing plants, even grain mills; for local partial manufacture of many items, from imported raw materials or concentrates; and for expansion of service industries, as well as those which are basic or primary such as mining. Cement and other building materials must be transported long distances, although most of the raw materials for making them are probably accessible. Lumber of fair quality is available and could be used more advantageously with improved methods of processing. Coal is plentiful and is the chief source of heat, power, and electricity, although considerable oil is brought in by tanker and rail. It is believed that eventually oil and gas will be distributed widely by pipeline. Hydroelectricity has not yet been developed in the Fairbanks area, although a number of sites within 100 miles are probably suitable for such plants.

Several metals and ores are mined and exported, but there are no iron ores in this part of Alaska. Gold is the second largest mineral output in value, sand and gravel being first. Much more gold could be produced at $50 an ounce.

It seems obvious that production of electricity, and industries based on the use of electric power, will grow rapidly in the Fairbanks area and other parts of Alaska. It will probably be a long time before large-scale electrochemical industries are established.

—CVK

[1] Report prepared and distributed by Ivan Bloch and Associates (member of North Pacific Consultants), 611 Park Bldg., Portland 5, Ore. In bound mimeograph form, $3.50.

how do you look at ANODES?

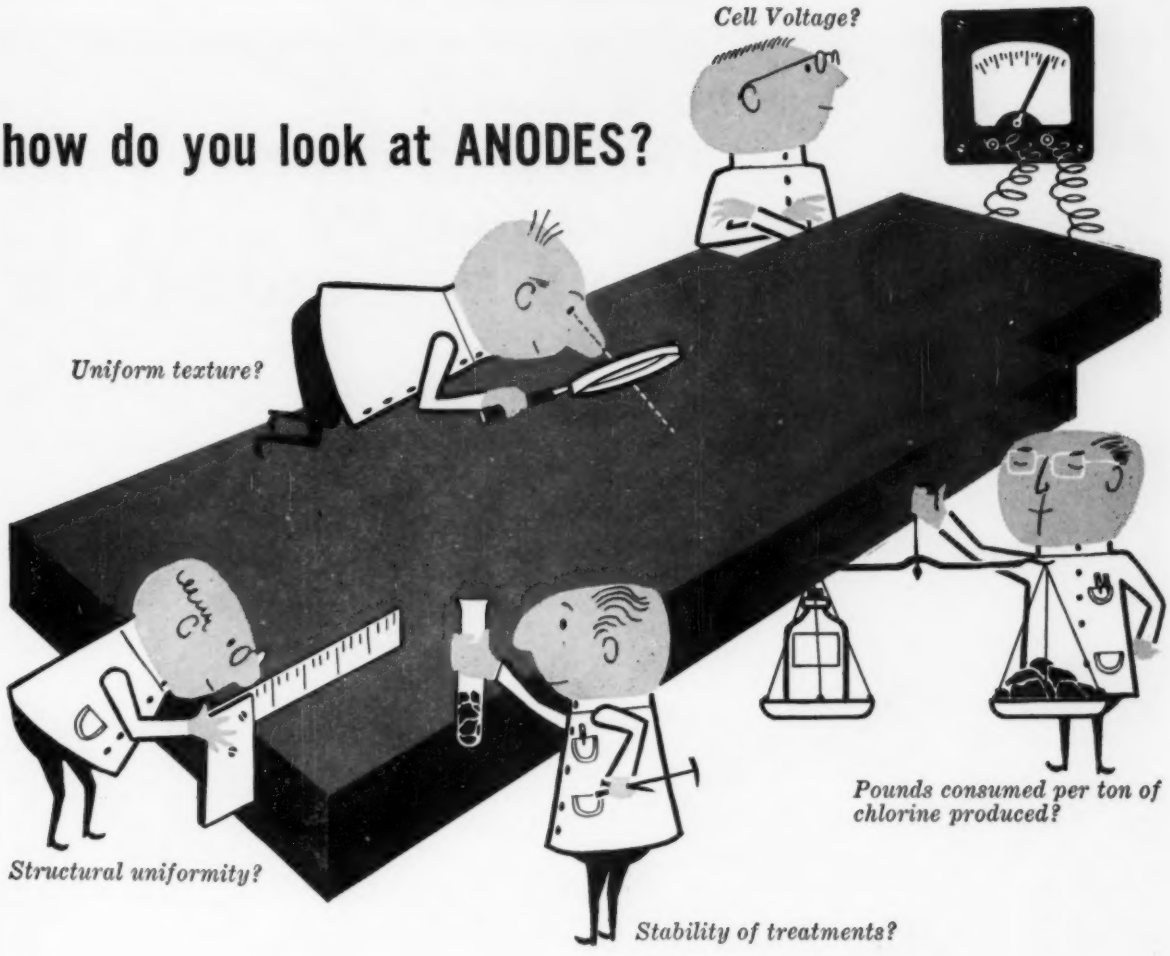

Judged by Cell Maintenance Costs Alone,

the highly stable impregnants used in Stackpole GraphAnode reduce diaphragm clogging to a bare minimum. The graphite is consumed slowly and evenly. Because GraphAnode anodes present uniform, low-porosity surfaces to the electrolyte, the graphite does not slough off to clog the diaphragm or to contaminate the cell.

Judged by Anode Cost and Performance,

Stackpole GraphAnode proves second to none whether you figure in terms of anode life, or in tons of chlorine produced per pound of graphite consumed. You get maximum anode life . . . and with the added advantage of low cell voltages. Stackpole engineers stand ready to offer a convincing demonstration on your equipment.

Stackpole Carbon Company, St. Marys, Pa.

STACKPOLE
GraphAnode®

ELECTROCHEMICAL ANODES FOR DIAPHRAGM, MERCURY, MANGANESE DIOXIDE, & SODIUM CHLORATE CELLS. OTHER TYPES FOR CATHODIC PICKLING, ALUMINUM ANODIZING, AND OTHER USES.

CATHODIC PROTECTION ANODES • FLUXING & DE-GASSING TUBES • SALT BATH RECTIFICATION RODS • ROCKET NOZZLES • RISER RODS • GRAPHITE BEARINGS & SEAL RINGS • ELECTRODES & HEATING ELEMENTS • WELDING CARBONS • VOLTAGE REGULATOR DISCS • "CERAMAGNET"® CERAMIC MAGNETS • ELECTRICAL CONTACTS • BRUSHES for all rotating electrical equipment • and many other carbon, graphite and electronic components.

INTRODUCING–

The New SARGENT Model XV RECORDING POLAROGRAPH®

Developed by E. H. Sargent & Co., the designers and manufacturer of the Models III, XII and XXI Polarographs, this new instrument becomes a companion to these long familiar Polarographs.

This completely new Polarograph has been designed with maximum simplicity of operation for the routine analyst. It includes full facilities for application to every phase of conventional polarography with full size recording and analytical accuracy at an economical price. The design is flexible and adaptable to future accommodation of specialized techniques as they become useful. It permits direct alternate use as a recording potentiometer of 2.5 millivolt range.

For Complete information write for Sargent Polarograph Booklet

SARGENT SCIENTIFIC LABORATORY INSTRUMENTS • APPARATUS • SUPPLIES • CHEMICALS

E. H. SARGENT & COMPANY, 4647 W. FOSTER, CHICAGO 30, ILLINOIS
DETROIT 4, MICH. • DALLAS 35, TEXAS • BIRMINGHAM 4, ALA. • SPRINGFIELD, N. J.

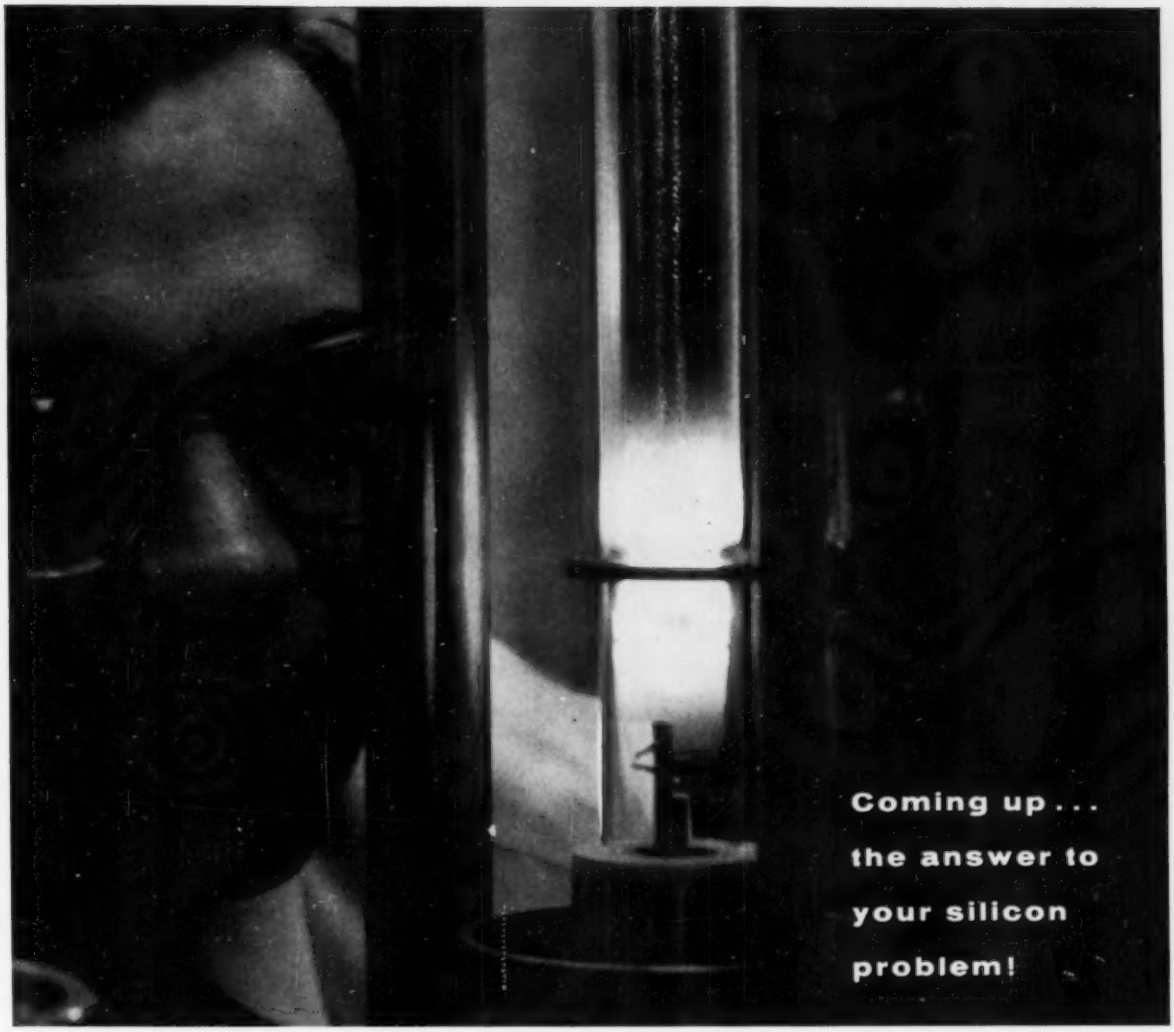

Du Pont . . . manufacturer of Hyperpure Silicon offers the services of technical specialists

When you specify Du Pont HYPERPURE Silicon, you get a product of highest dependability as well as expert technical assistance, when needed. Experienced Du Pont Technical Specialists will gladly discuss techniques of crystal growing and materials processing with you. What's more, you can take advantage of Du Pont's new $3,000,000 Technical-Service Laboratory designed for researching customer problems.

Floating zone single crystals of Du Pont HYPERPURE Silicon are available in a wide range of resistivities. Du Pont HYPERPURE Silicon is also supplied in densified cut rods . . . and rods suitable for float zone refining. They're offered in several grades with carefully controlled purity levels.

Here's more news: Du Pont's new Brevard, N. C., plant has a capacity of 70,000 lbs. of HYPERPURE Silicon per year. That means you're assured of a prompt supply of high-purity silicon in the form you need. For more information, write Du Pont . . . pioneer producer of semiconductor-grade silicon.

Free booklet is available upon request. It describes the manufacture, properties and uses of HYPERPURE Silicon. E. I. du Pont de Nemours & Co. (Inc.), Pigments Dept., Silicon Development Group, Wilmington 98, Delaware.

HYPERPURE SILICON

DU PONT

REG. U.S. PAT. OFF.

BETTER THINGS FOR BETTER LIVING
. . . THROUGH CHEMISTRY

WHATEVER FORM OR SIZE YOU NEED

there are "Plus-4"® (Phosphorized Copper) Anodes to help you cut the costs of acid-copper electroplating—at the same price as ETP copper anodes

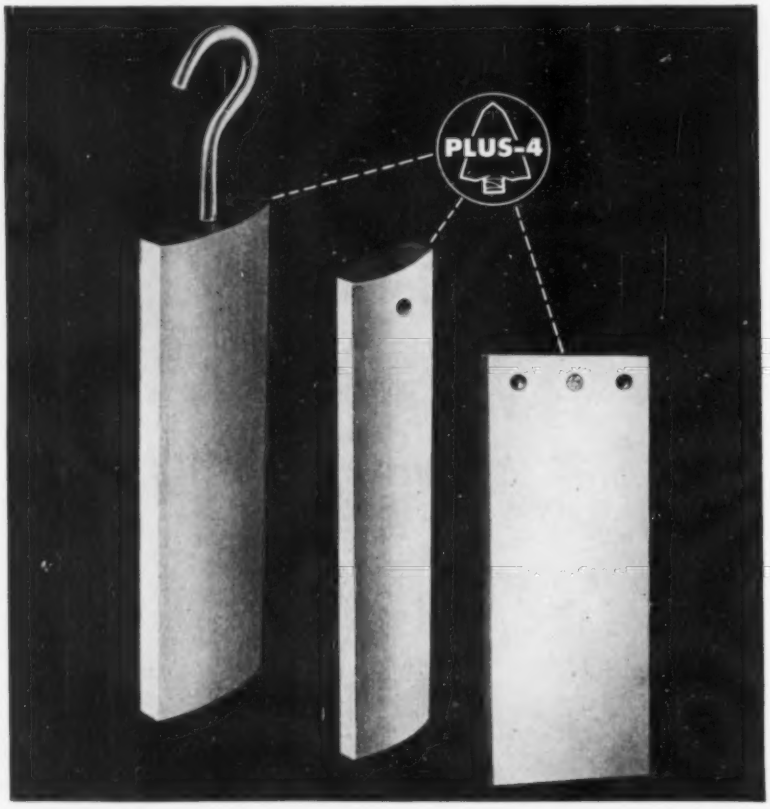

"Plus-4" Anodes in commercial use in practically all types of acid-copper electroplating have proved their advantages over wrought or cast electrolytic tough pitch copper anodes. The four advantages indicated by the name are:

+ 1 No anode sludge (no "bagging" or diaphragms required).
+ 2 No copper build-up in the solution.
+ 3 Smooth, heavy cathode deposits.
+ 4 Up to 15% more cathode deposit.

THE REASON for the elimination of sludge formation is that an anode of phosphorized copper develops an adherent dark brown film during electrolysis, which prevents the formation of free copper particles, but which in no way interferes with the plating operation or increases the electrical resistance of the bath. The phosphorized copper anode also corrodes more evenly, depositing more copper per pound on the cathode; gives a smooth, heavy deposit free from roughness due to lodgment of copper sludge particles; and leaves a small, compact "fish." There is no copper sludge or build-up of copper sulfate in the electrolyte.

WRITE FOR INFORMATION on how you can obtain a test quantity to supply one tank. Address: The American Brass Company, Waterbury 20, Conn. In Canada: Anaconda American Brass Ltd., New Toronto, Toronto 14, Ontario.

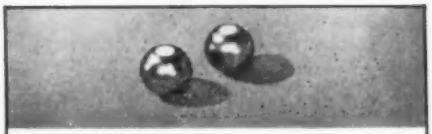

FORGED BALL ANODES

Anaconda ETP Copper Ball Anodes, used widely in cyanide plating, are cold forged from wrought metal. The result is a homogeneous, fine-grain structure, free from voids. Consequently they corrode very uniformly without disintegration. The balls are 2" diameter and weigh 1¼ pounds each. Identify them by the spearhead trademark.

ANACONDA®
"PLUS-4" ANODES
Phosphorized Copper
Made by The American Brass Company

The Oxide Films Formed on Copper Single Crystal Surfaces in Pure Water

I. Nature of the Films Formed at Room Temperature

Jerome Kruger

National Bureau of Standards, Washington, D. C.

ABSTRACT

A study was made of the nature of the films that formed on carefully prepared surfaces of single crystals of copper immersed in water containing varying amounts of oxygen, with the surrounding atmosphere both controlled and uncontrolled. It was found that the amount of oxidation depended on the crystallographic orientation of the metal surface. Cu_2O was the oxide observed if pH $\leqq$ 5.7. Intense white light markedly retarded film formation in water. When Cu_2O was formed, it had a preferred orientation and exhibited epitaxial relationships to the metal similar to those found in high-temperature oxidation. The films formed were not continuous but were composed of small nuclei of Cu_2O. Both Cu_2O and CuO were formed at pH 7 when the water was in equilibrium with an atmosphere of pure O_2. Lowering the pH converted CuO to Cu_2O.

The oxide films that form on a metal surface are one of the very important factors influencing most corrosion processes. These films affect the potential that the surface exhibits and influence the transport of metal ions away from it. Both of these aspects are interrelated and have an important influence on the corrosion of metals. In connection with work on the fundamentals of corrosion sponsored by the Corrosion Research Council, the subject selected for study was the growth of films on metal surfaces in contact with pure water containing oxygen. This system was chosen because most corrosion encountered in practice involves metal, water, and oxygen, plus a number of other substances. Thus if some understanding can be gained of this simple system, it would serve as a basis for study of the complicated systems that are related more closely to practical cases.

The metal chosen to initiate this study was copper, because it has a simple structure, and high-purity metal is available from which single crystals may be prepared easily. Its oxides are few and simple, and a great deal of fundamental data on its properties is available.

Work on the growth of films on Cu in water in the past (1-4) has been done generally on poorly characterized metal surfaces under conditions where the nature of the surrounding atmosphere and the purity of the water was not rigidly controlled. Much work has been done on the corrosion of Cu in aqueous solutions of many different compositions. However, with the possible exception of the work of Miller and Lawless (5) on single crystals, the surfaces used were in general poorly characterized. As a consequence the studies carried out are not as significant from a fundamental standpoint as they should be.

The work described here employs surfaces whose nature is better known than the surfaces used in most of the corrosion studies of Cu in aqueous media. The approach in this investigation was to use single-crystal surfaces, carefully prepared so that they would be as clean as possible and free from strain (6). This paper is concerned with some qualitative studies of the nature of the films formed on Cu in pure water containing oxygen. A subsequent paper will report studies of the rate of film formation.

Experimental Procedure

Materials.—The crystals used in this investigation were grown using OFHC Cu which has a purity of 99.99%.[1] The Bridgman technique of slowly cooling a melt was used to grow crystals in the shape of spheres ⅜ in. in diameter with a cylindrical shaft ¼ in. in diameter and ¾ in. in length. The water was obtained from the Physical Chemistry Section of the National Bureau of Standards and had a conductivity of 7×10^{-7} mhos.

Preparation of the metal surface.—In a number of experiments the as-cast single-crystal sphere was used after following appropriate cleaning and polishing procedures. These consisted in washing the crystal successively in water, ethyl alcohol, diethyl ether, and again in ethyl alcohol and water prior to electrolytically polishing the crystal in a phosphoric acid-water solution 50% by volume. After the electrolytic polishing was completed (1 hr the first time after casting, 10-20 min all times thereafter) the crystal was washed very carefully to remove traces of phosphate ions, following the schedule described by Young, Cathcart, and Gwathmey (6), who found that this washing procedure left a surface that oxidized reproducibly. In the case of experiments carried out in the room atmosphere, the crystal was immediately immersed while still wet in distilled water. When it was introduced into

[1] Spectrographic analysis showed that the Cu used contained 0.001 to 0.01% Ag and < 0.0001% Si, Al, Fe, Mg, Ni, and Pb.

the reaction chamber of the apparatus designed for carrying out the process under controlled conditions, the water remaining on the crystal was evaporated by evacuation of the system. Whenever the crystal was handled, preflamed gold-plated tongs were used to hold the shaft of the crystal.

For some studies three flat surfaces were cut parallel to the {111}, {110}, and {100} crystallographic planes. After cutting these surfaces the crystal was etched in nitric acid to remove the strained layer resulting from this operation. The orientations of the surfaces were checked and corrected, if they differed by more than 2° from the desired orientation. These surfaces then were polished mechanically with metallographic polishing papers through No. 0000 and lapped on a metallographic wheel with a water suspension of Linde B abrasive. From this point on the procedure was as described above.

Reaction apparatus and procedure.—Two different groups of experiments were carried out using Cu crystal surfaces prepared as described above. In the first group the nature of the surrounding atmosphere was not controlled. The procedure in this case was simply to immerse the crystal after electropolishing and washing directly, and while still wet, in 100 ml of distilled water. The crystals were mounted in glass holders and gas washing bottles were used as reaction vessels.

In the second group of experiments the nature of the surrounding atmosphere was controlled by carrying out the reaction in the enclosed apparatus shown in Fig. 1. The crystal, after polishing and washing, was introduced together with the glass crystal holder into the reaction chamber through its top, using a preflamed platinum hook. Introducing the crystal into the apparatus in this manner eliminated the need for greased ground joints with the attendant possibilities for contamination. The top of the chamber then was sealed. An oxy-hydrogen flame was used in the sealing process rather than the ordinary natural gas-oxygen flame because the latter was found to introduce contaminants. The high-purity water was introduced into the freeze-down tube and boiled before sealing and pumping. Half of the water in this tube was distilled in vacuum into the water-introduction tube by placing a Dewar flask of liquid nitrogen around this tube.

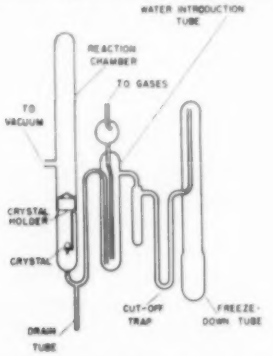

Fig. 1. Apparatus for oxidizing Cu single crystal in water under controlled conditions.

The frozen water so collected was thawed and then pushed into the reaction chamber by helium. The purpose of this part of the procedure was to rinse off any impurities that might have collected on the crystal during the time when it was being placed into the reaction chamber. The water was removed by breaking open the drain tube and pushing it out with a positive pressure of helium. The drain tube then was resealed, and the water remaining in the freeze-down tube was kept frozen in liquid nitrogen until required. Liquid nitrogen also was placed around the cut-off trap as an added measure to prevent any water from reaching the reaction chamber while it was being baked at 500°C overnight at a pressure of 10^{-5} mm. After this baking procedure, with the water still frozen in the freeze-down tube, the crystal was annealed in purified dry hydrogen at 500°C for 2 hr to remove the air-formed oxide film present on the crystal surface. The system then was evacuated, brought to room temperature, and the water in the freeze-down tube distilled over to the water-introduction tube by cooling this tube in liquid nitrogen. This water was thawed, pushed into the reaction chamber by the desired gas (e.g., dry purified oxygen), and the corrosion process allowed to start. To halt the reaction, the water was drained by cracking open the drain tube, resealing, and evacuating the system to dry the crystal. The crystal then was removed for examination by cracking open the top of the reaction chamber.

Results

Corrosion in Water with the Surrounding Atmosphere Uncontrolled

In these experiments, which were essentially preliminary in order to explore and determine the nature and magnitude of the effects to be studied, the Cu was immersed in water that was in contact with the room atmosphere. The spherical single crystal offers an ideal tool for exploratory experiments of this type because all of the crystallographic planes are represented as poles on the surface of the sphere and thus all of them can be studied simultaneously.

The following results were obtained from these experiments:

1. Oxidation was the most readily apparent reaction taking place.

When a crystal was placed in water deoxygenated by boiling, and either hydrogen or helium was bubbled in, no film formation was observed and the crystal remained bright. When oxygen was present, however, a film whose presence was indicated by the appearance of interference colors on the Cu was formed after exposure to the water.

2. At room temperature, oxide films formed on the Cu surface considerably faster in water than in air.

If a Cu crystal was allowed to stand in dry air or oxygen at room temperature no interference colors, which give an indication of the thickness of the films growing on the metal surface, were observed after weeks of standing. In water, however, colors

started to develop after standing only 30 min. Within 6 hr films exhibiting interference colors indicating thicknesses greater than 1000Å were observed.

3. The rate of oxidation varied with the crystallographic plane.

The thickness and thus the color of films formed on Cu exposed to air-saturated water varied with the crystallographic plane on which they were growing. Since all of the crystallographic poles could be observed simultaneously on the spherical crystal these differences could be seen easily. After a given time of exposure a symmetrical pattern made up of many different colors was obtained on the sphere, thus indicating a variation in the amount of film growth with crystallographic orientation. Such a pattern is shown in Fig. 2. Because the patterns formed on the single crystal spheres were extremely sensitive to a very minute change in environment or surface condition, many different patterns were observed unless the nature of the surrounding atmosphere, and the cleanliness of the water and the metal surface, were controlled rigidly. Thus, on the basis of these preliminary experiments carried out in the room atmosphere, it is not possible to list definitely the various crystallographic planes in the order of their relative rates of oxidation.

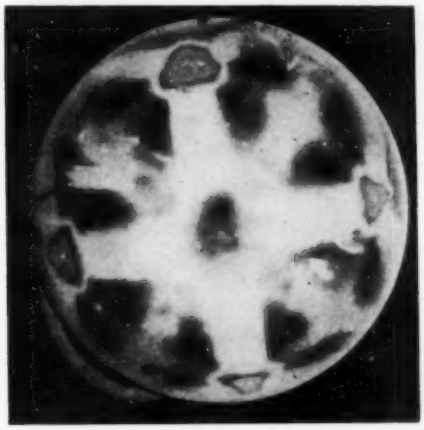

Fig. 2. Pattern formed when Cu single-crystal sphere is corroded in air-saturated distilled water at room temperature.

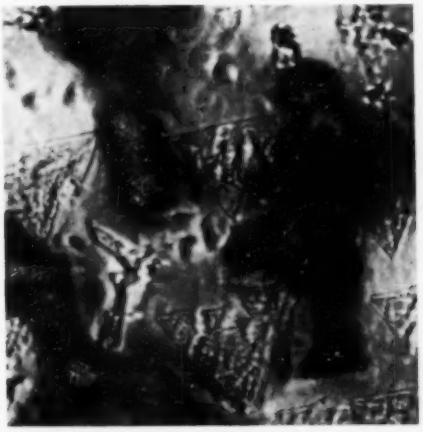

Fig. 3. Oxide crystals* formed on {111} plane of Cu crystal oxidized in water. Magnification 1000X before reduction for publication.

Fig. 4. Oxide crystals* formed on {110} plane of Cu crystal oxidized in water. Magnification 1000X before reduction for publication.

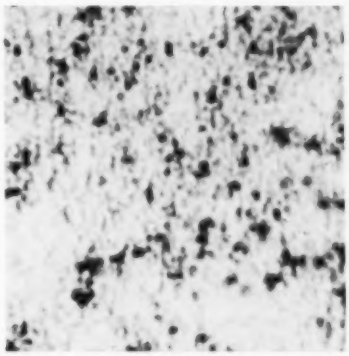

Fig. 5. Oxide crystals* formed on {100} plane of Cu crystal oxidized in water. 1000X.

4. The oxide films were not continuous.

When observed with unaided eye, the oxide films appeared to be uniform. However, microscopic examination indicated that the oxide films were made up of particles or nuclei. Figures 3, 4, and 5 show these oxide nuclei formed on a Cu surface exposed to water on three different crystallographic planes.

5. The degree of orientation and epitaxy of the oxide films depended on the crystal faces upon which they were grown.

X-ray diffraction studies, using the oscillating crystal technique described by Lawless and Gwathmey (7), were carried out to determine the chemical nature of the films and their epitaxial relationship to the metal substrate. Studies of the films formed on Cu crystals exposed to distilled water in an uncontrolled atmosphere for 18 hr showed them to be composed of Cu_2O made up of many crystallites exhibiting a preferred orientation with respect to the Cu substrate. In general, the degree of preferred orientation was higher for the {111} and {110}

* Note that the shape of some of the crystallites are indicative of the symmetry of the crystallographic orientation of the plane on which they are growing.

Table I. Epitaxial relationships between Cu and Cu_2O

Crystal face of Cu	Crystal face of Cu_2O parallel to Cu
{111}	{111}
{110}	{110}
{100}	{111}

planes than that for the {100} plane. The epitaxial relationships, i.e., the mutual orientation relationship between the Cu_2O and the Cu substrate, are shown in Table I.

These relationships agree with those found by others (7-9) on Cu single crystals oxidized in dry oxygen at temperatures considerably above room temperature.

6. Light had a marked influence on the oxidation process in water.

A number of attempts were made to obtain time-lapse motion pictures of the corrosion process of a Cu single crystal in air-saturated water. These were not successful because it was found that the light used to illuminate the crystal had a marked influence on the corrosion process (10). As a consequence, it was decided to study the effect of light on the oxidation process of Cu in water. A water-jacketed vessel, light-tight except for a small hole which allowed light to impinge on half of a crystal sphere, was employed, as shown in Fig. 6. When the crystal was immersed in air-saturated water in this vessel, illuminated by a tungsten 3200°K lamp, and kept at room temperature by the water jacket for 3 hr, the amount of oxidation on the area of the sphere exposed to the light was markedly different from that of the shaded area (see Fig. 7 and 8). Using a simple electroreduction technique similar to that of Miley and Evans (11) to estimate film thickness, it was found that the illuminated part of the crystal had a thickness of roughly 120Å or less,

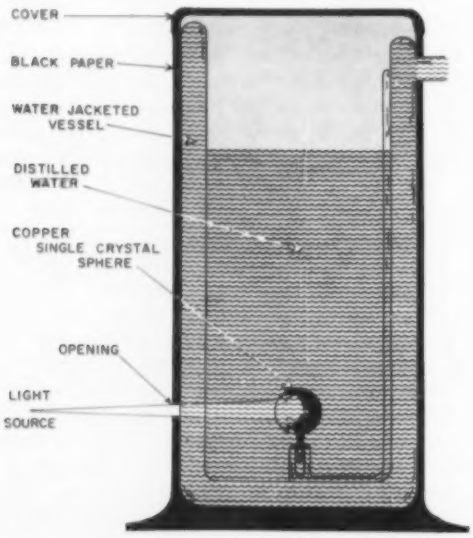

Fig. 6. Apparatus for studying influence of light on oxidation of Cu crystal in water.

Fig. 7. Copper single crystal oxidized in air-saturated distilled water at 25°C. Lower side was exposed to light from a 3200°K tungsten lamp, upper side kept dark.

Fig. 8. Boundary between dark and illuminated areas of Cu single crystal surface oxidized in air-saturated distilled water at 25°C. Upper region kept dark, lower illuminated. 500X.

while the part that was kept dark had an average thickness of approximately 550Å. Further, if light were allowed to impinge on part of a Cu crystal immersed in water and already containing a water-formed oxide film about 1000Å thick or greater, some of the oxide on the illuminated portion dissolved after a period of 2-3 hr and became thinner than the part kept dark. X-ray diffraction studies of the films formed on both the dark and the illuminated parts of the crystal showed that the films were composed of well-oriented Cu_2O.

Mott's theory (12) for Cu-Cu_2O photocells may provide an explanation for this effect. On the basis of this theory, illumination would cause a flow of electrons from the semiconductor film, Cu_2O, into the metal. A flow of electrons in this direction when the film is growing would thus inhibit growth. It is interesting to point out that for Al_2O_3 and Ta_2O_5, which are cation excess semiconductors, illumination enhances oxidation, while Cu_2O, a cation deficient semiconductor, oxidation is inhibited. Besides

this explanation, based on the effect of illumination on the electrons on the solid side of the solid-liquid interface, another explanation based on the influence of light on chemical reactions at the metal-solution interface should be considered also. These reactions may be important, for it is known (13) that light promotes the oxidation of cuprous ions to cupric. Thus any Cu_2O that forms may be oxidized to CuO. Since the latter is the more soluble of the two, it may go into solution rather than form a film, as in the case of the Cu_2O.

Corrosion in Water with Surrounding Atmosphere Controlled

In these experiments the techniques described in the Experimental Section for preparing the crystal surface and reacting it with pure water in a controlled atmosphere were utilized. The results obtained differed considerably from those observed under uncontrolled conditions.

In the controlled experiment the Cu crystal was immersed in high-purity water, which was stirred and kept saturated by bubbling O_2 through it at a rate of approximately 50 ml/min at 1 atm and 25°C. Oxidation was considerably slower in these experiments than in the experiments where the nature of the atmosphere was uncontrolled. It was found that after 1 hr the film thickness was roughly 70Å, and after 8 hr the thickness had not changed appreciably. After 50 hr of exposure the average value of the thickness was about 110Å. Also it was noted that some solid powder had settled to the bottom of the reaction chamber. The electroreduction technique was used to estimate the film thicknesses. This method was not precise enough to allow any definite statements to be made regarding the differences in the thickness of the films on the three crystallographic planes since the differences between them were less than the experimental error.

When the solution, saturated and in equilibrium with 1 atm of O_2, was not stirred but instead allowed to remain quiescent, the corrosion process was quite similar to that in the stirred solution for the first few hours, but after 7 hr a visibly thick brownish black to purplish black film of oxide had formed. This film had a powdery appearance and could be removed partially by wiping with a tissue. Beneath it another film exhibiting interference colors could be observed sometimes.

If the partial pressure of the O_2 in equilibrium with the water were reduced by introducing mixtures of O_2 and He containing varying proportions of these two gases, the time required for the appearance of CuO increased as the partial pressure of O_2 decreased. Thus, with 100% O_2, 7 hr elapsed before CuO was observed by the unaided eye, while with 20% O_2 the time was twice as long, and with 10% O_2, over 24 hr elapsed.

X-ray diffraction examinations of {111}, {110}, and {100} faces, reacted in the presence of oxygenated water under controlled conditions, revealed the presence of polycrystalline randomly oriented CuO. In a few cases Cu_2O also was found to be present along with the CuO. When this was so, the Cu_2O showed the same type of preferred orientation and epitaxial relationships as described for the experiments conducted in uncontrolled atmospheres. This Cu_2O probably was responsible for the film that exhibited the interference colors when the CuO was wiped off. When CuO was present, the film, as observed by the unaided eye and by microscopic examination, was thinnest on the {110} planes and thickest on the {100}, with that on the {111} being intermediate. The electroreduction technique could not be used to measure CuO film thickness because of the great difficulties encountered in reducing the CuO.

It is believed that the reason CuO was not formed on the Cu surface when the solution was agitated was that cuprous ions, on reaching the solid-liquid interface through the Cu_2O film, were caused by the agitation to oxidize in the body of the solution and precipitate as $Cu(OH)_2$ or CuO, whereas under quiescent conditions the cuprous ions were oxidized to cupric ions at the interface and formed CuO there. In all cases Cu_2O is present next to the Cu as CuO is reduced in the presence of Cu.

It is evident that the behavior of the Cu was markedly different when immersed in oxygenated water in the room atmosphere than when the environment was controlled more rigidly. In the first case films of oriented Cu_2O were formed on the Cu surface after a relatively short exposure to water. These films exhibited interference colors and formed beautifully symmetrical patterns. When the conditions were controlled, the Cu oxidized much more slowly and formed dark randomly oriented CuO films. Beneath the CuO films thin films of Cu_2O probably were present also. In an effort to duplicate the experiments in which the water was in contact with the room atmosphere under controlled conditions, it was found that by lowering the pH to 5.7 (the pH observed in water exposed to the room atmosphere), Cu_2O was observed. The *pH* was lowered by the introduction of CO_2. With still lower pH's, Cu_2O also was observed. The influence of CO_2 was demonstrated by an experiment in which CuO was formed on Cu in a closed system by exposing the Cu to water saturated with pure oxygen. Carbon dioxide was bubbled in for 1 min and the corroded crystal then was exposed to this water for 24 hr. At the end of this period, all of the CuO had been converted to Cu_2O. X-ray diffraction examination of the Cu_2O formed in this fashion revealed, however, that it was much more poorly oriented

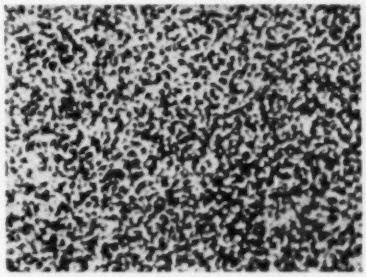

Fig. 9. {100} plane of Cu oxidized in oxygen-saturated water under controlled conditions. 1000X.

Fig. 10. {111} plane of Cu oxidized in oxygen-saturated water under controlled conditions. Magnification 1000X before reduction for publication.

than where CO_2 was present from the beginning of the oxidation process.

The morphology of the oxide films as revealed by the microscope was of great interest. After the oxidation had proceeded to the point where CuO could be observed, the film on the {110} plane was similar to that on the {100} plane (Fig. 9). Most of the surface of the {111} plane, however, was covered with the black CuO film but, as shown in Fig. 10, there were triangular areas that appeared Cu colored. It is interesting to note that some of the triangles had orientations that are 180° with respect to each other. This indicated that perhaps some nuclei of Cu_2O existed next to the Cu surface. Cu_2O could exist in these two orientations because of the epitaxial relationships found between Cu_2O and a {111} plane of Cu (7). Figures 11, 12, and 13 show the {111}, {110}, and {100} faces, respectively, after the CuO had been converted to Cu_2O by the introduction of CO_2.

Discussion

The first fact which was noted from these studies concerned with the nature of the oxides is that Cu_2O was formed when Cu was exposed to water in equilibrium with air, the pH of the water being about 5.7. This is the oxide formed initially by dry air oxidation. Further, the epitaxial relationships between the Cu_2O and the metal substrate were the same both for oxidation in solutions and in dry gases. Finally, the extent of oxidation depended on the crystallographic orientation of the surface in both cases.

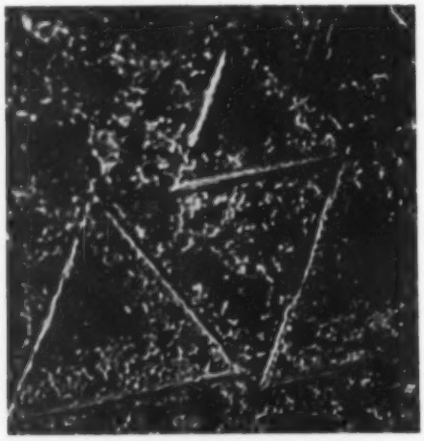

Fig. 11. Cu_2O formed on {111} plane of Cu by conversion of CuO which was present initially. The change was caused by introduction of CO_2 into aqueous solution. Magnification 1000X before reduction for publication.

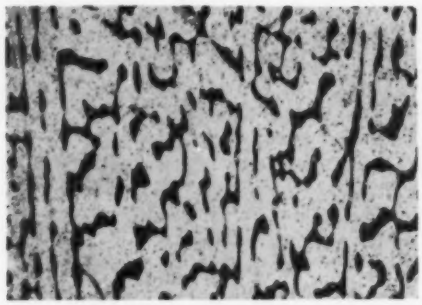

Fig. 12. Cu_2O formed on {110} plane of Cu by conversion of CuO which was present initially. The change was caused by introduction of CO_2 into aqueous solution. Magnification 1000X before reduction for publication.

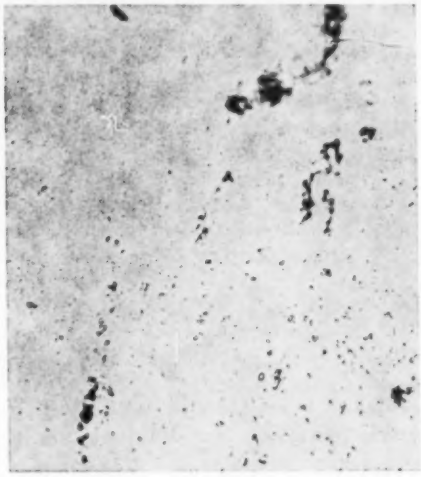

Fig. 13. Cu_2O formed on {100} plane of Cu by conversion of CuO which was present initially. The change was caused by introduction of CO_2 into aqueous solution. 1000X.

The one very evident difference between oxidation in air and oxidation in water was that at room temperature oxidation occurred more rapidly in water (exposed to air) than it did in air. It is also known from the work of Miller (14) that, if Cu is immersed in a solution of cupric sulfate, the reaction is even more rapid than if Cu is immersed in pure water. Cu_2O is the product formed in copper sulfate solution and the epitaxial relationships between oxide and metal are the same as those mentioned above. The nuclei contained in films formed during oxidation in solutions were larger than those formed during oxidation in gases. Finally, the influence of light was much more pronounced when oxidation occurred in solutions than when it occurred in gases. A few attempts were made to see if illumination had any influence on the oxida-

tion of Cu in pure oxygen at 250°C but no marked effects were noted.

These differences between oxidation in air-saturated water and oxidation in air, are probably due to the ability of metal ions during aqueous oxidation to move through the water and take part in reactions at sites on the surface that differ from those from which these ions emerged initially. This transport of ions through a solution is, of course, an all-important factor in electrochemical reactions occurring on metal surfaces immersed in an electrolyte. It is not the purpose of this paper to discuss the mechanism of oxidation in water but to be concerned only with the nature of the films formed. However, because of the ability of the water to transport ions, soluble substances can be removed from a surface or insoluble substances can be deposited onto a surface. On account of these processes the oxides formed in water in equilibrium with 1 atm of pure oxygen at room temperature differ from those formed by gaseous oxidation at room temperature. Thus, besides the Cu_2O commonly present at room temperature CuO was also observed.

This has not generally been found in most of the previous studies of the films that form on Cu in contact with aqueous solutions because most of these experiments were carried out under conditions where the presence of CO_2 was not rigorously excluded. The formation of CuO when CO_2 is absent is to be expected on the basis of the diagram of Pourbaix (15). This diagram enables the prediction of the thermodynamically stable phases present under a given set of conditions. On the basis of this diagram it may also be concluded that by lowering the pH and the partial pressure of oxygen there would be a tendency for the CuO to go over to Cu_2O.

However, the thermodynamic considerations on which the Pourbaix diagram is based are not sufficient to allow the prediction of the solid phases present. Thus, for the conditions existing during the oxidation of Cu in water saturated with air and exposed to the room atmosphere (pH = 5.7, $pO_2 = 10^{-0.69}$ atm) the formation of CuO would be expected, although Cu_2O was observed. The rate at which cupric ions build up in solution is also of utmost importance in determining the oxide observed. Thus, if enough time were allowed and if all of the components of the system were kept in intimate contact with each other, CuO would be observed at pH 5.7 in air-saturated water. Actually, what appeared to happen was that at this pH the CuO was soluble to such an extent and the rate of cupric ion formation by oxidation of cuprous ions was sufficiently slow so that only the considerably less soluble Cu_2O was observed.

At a pH of 7, however, the solubility of CuO is less than at the lower pH and with the water in equilibrium with 1 atm of oxygen, the time required to observe the formation of CuO visually was about 7 hr. Experiments with pure water in equilibrium with different partial pressures of oxygen show that apparently the rate of cupric ion formation did depend on the partial pressure of the oxygen, for the time to observe CuO formation increased with a decrease in partial pressure. During this time, before the appearance of CuO, only Cu_2O was observed. When the pH was lowered from 7, after the formation of CuO by the introduction of CO_2, the solubility of CuO was increased and it went into solution.

The Cu_2O that is always next to the Cu was then the only oxide observed and its thickness actually started to increase at the lower pH where it was still quite insoluble. This indicated that the rate of cuprous ion formation was probably faster than the rate of oxidation of cuprous ions to cupric. This question of the rate of film formation and the rate of cupric and cuprous ion formation will be discussed in a more quantitative fashion in the next paper in this series. These details must be investigated before a more nearly complete understanding of the corrosion of Cu can be achieved.

Acknowledgment

The author wishes to thank the Corrosion Research Council which supported this work in part.

Manuscript received Feb. 20, 1959. This paper was prepared for delivery before the Buffalo Meeting, Oct. 6-10, 1957.

Any discussion of this paper will appear in a Discussion Section to be published in the June 1960 JOURNAL.

REFERENCES

1. G. D. Bengough and O. F. Hudson, *J. Inst. Metals*, **21**, 37 (1919).
2. L. W. Haase, *Z. Metallkunde*, **26**, 185 (1934).
3. A. Quartoroli, *Korrosion u. Metallschutz*, **18**, 368 (1942).
4. L. Tronstad and R. Veimo, *J. Inst. Metals*, **66**, 17 (1940).
5. G. T. Miller, Jr., and K. R. Lawless, *J. Applied Phys.*, **29**, 863 (1958).
6. F. W. Young, Jr., J. V. Cathcart, and A. T. Gwathmey, *Acta Metallurgica*, **4**, 145 (1956).
7. K. R. Lawless and A. T. Gwathmey, *ibid.*, **4**, 153 (1956).
8. N. B. Gorney, *Soviet Phys. JETP*, **2**, 687 (1956).
9. E. Menzel, *Ann. Physik (Leipzig)*, **5**, 163 (1949).
10. J. Kruger, *J. Applied Phys.*, **28**, 1212 (1957).
11. U. R. Evans and H. A. Miley, *J. Chem. Soc.*, **1937**, 1295.
12. N. F. Mott, *Proc. Roy. Soc. (London)*, **A171**, 281 (1939).
13. J. W. Mellor, "A Comprehensive Treatise on Inorganic and Theoretical Chemistry," p. 160, Longmans, Green and Co., London (1923).
14. G. T. Miller, Jr., Dissertation, University of Virginia (1958).
15. M. J. N. Pourbaix, "Thermodynamics of Dilute Aqueous Solutions," p. 59, Edward Arnold and Co., London (1949).

An Electron Microscopic Study of the Formation of Oxide on Copper Single Crystals Immersed in an Aqueous Solution of Copper Sulfate

G. Tyler Miller, Jr.[1], and Kenneth R. Lawless

Cobb Chemical Laboratory, University of Virginia, Charlottesville, Virginia

ABSTRACT

Electron microscope and electron diffraction techniques were used for the examination of the different faces of a single crystal of copper which had been immersed in an aqueous solution of $CuSO_4$ containing dissolved oxygen. During the reaction a thin film of Cu_2O was formed initially and continued to grow in the form of well-defined oriented polyhedra of oxide. For immersion times of 24 hr or more, etching of the metal surface and of the oxide polyhedra occurred due to a decrease in the pH of the solution. An attempt was made to interpret the oxide growth in terms of the electrochemical theory of corrosion and the dislocation theory of crystal growth.

Although the reactions of metals with aqueous salt solutions are among the commonest of reactions and have been the subject of many investigations, the influence of surface structure on these reactions is only poorly understood. Most previous studies have been carried out on fine-grained polycrystalline specimens, and the interpretation of the results is complicated by the presence of grain boundaries and by differences in activity of the different crystal faces. In addition to this, an understanding of the reactions involved is frequently difficult because little or no information is available on the structure of the surface before and after the reaction.

This study is concerned with the electron microscopic and electron diffraction examination of the different faces of a carefully prepared single crystal of copper which has been immersed in an aqueous solution of copper sulfate containing dissolved oxygen. During the reaction oxide is formed and some etch pits are developed. The epitaxial relationship of these oxide films with the metal surface as determined in this study are described in detail in another paper (1).

Interesting types of oxide structures were found, and an attempt was made to interpret the oxide growth in terms of the electrochemical theory of corrosion, the structural relationships of the oxide to the underlying metal, and the dislocation theory of crystal growth. The results indicate clearly that the understanding of one of the simplest of reactions, important in an understanding of corrosion, is dependent on a careful study of surface structure.

Experimental Procedure

The experimental procedure consisted of exposing known crystallographic surfaces of copper single crystals to an aqueous solution of cupric sulfate at a known concentration, temperature, and pH. The oxygen concentration in the solution was approximately constant. After definite periods of immersion the surfaces of the specimens were examined with the aid of optical and electron microscopes and by electron diffraction.

Copper single-crystal rods of 99.999% copper were grown from the melt and machined into the form of spheres $\frac{5}{8}$ in. in diameter. Flat faces parallel to specific crystallographic planes were cut on the spheres. The surfaces of these crystals were mechanically polished and then electrolytically polished, followed by thorough washing and drying as previously described (2). The Laue back-reflection technique was used to take x-ray diffraction photographs after every three or four experiments to make sure that each face remained within 1° of the desired orientation. Great care was taken in the preparation of these specimens in order to obtain known surfaces as free as possible from chemical contaminations and structural imperfections.

The copper specimens after being washed and dried were placed in a Pyrex reaction chamber. The system was then evacuated, purified hydrogen admitted, and the specimen annealed at 500°C for 1 hr to remove any oxide present on the surface and to relieve any residual strains in the crystal. The specimen was cooled to 25°C in an atmosphere of hydrogen, and then, without exposing it to the air, the crystal was lowered to the bottom of the reaction chamber which was immersed in a water thermostat maintained at 25° ±0.02°C. An aqueous solution of $CuSO_4$ could be admitted into the reaction chamber through a Pyrex tube which was ring-sealed to the base of the chamber. The top end of the tube was ground flat so that a flat face of a crystal could be placed on it and a reaction carried out on only one face. A glass cup was sealed to the upper part of this tube so that the crystal could be suspended within the cup and sufficient solution admitted to cover the whole crystal if desired. After being exposed to the aqueous solution for the de-

[1] Present address: Department of Chemistry, Hampden-Sydney College, Hampden-Sydney, Virginia.

sired length of time, the crystal was removed, washed thoroughly in distilled water to remove any $CuSO_4$, and dried in a jet of nitrogen.

Solutions of $CuSO_4$ were prepared using 50 g/liter of doubly recrystallized reagent grade $CuSO_4 \cdot 5H_2O$ and distilled water. The pH of the solution was measured before and after each experiment with a L&N pH indicator. The pH of the solution initially was 3.8 for all experiments. The oxygen concentration in this solution was approximately 10^{-4} moles per liter.

After reaction the surfaces of the copper crystals were examined using both optical and electron microscope techniques and in many cases electron diffraction techniques. It was not possible to examine the surfaces directly with the electron microscope, and it was therefore necessary to use a replica technique. For all of these studies carbon replicas approximately 100Å thick were made of the surfaces (3). These were removed using a stripping solution such as 10% KCN, 1:1 orthophosphoric acid water or 10% ammonium persulfate. The stripped replicas were mounted on the usual 200 mesh, ⅛ in. diameter grids, and these were then shadowed with Cr, Pt-20% Pd, or Pd (4). The angle of shadowing varied from 5° to 30°, depending on the appearance of the surface as indicated in the optical microscope, the lower shadowing angle being used for the smoother surfaces. The shadowed replicas were examined with the RCA EMU-3B electron microscope operated at 50 or 100 kv.

In a few cases, the reaction product was stripped from the copper surface using a modification of the electrolytic stripping technique described by Harris, Ball, and Gwathmey (5). These stripped films were then examined by transmission electron microscopy and electron diffraction. In order to determine the surface products and their structural relationships to the metal substrate, representative specimens were examined with high voltage electron diffraction (60-80 kv), utilizing reflection techniques (6). In these cases, after reaction, washing, and drying, the specimens were transferred immediately to the diffraction apparatus in order to minimize the possibility of surface contamination.

To determine the importance of copper ions in the solution, several experiments were carried out using a solution of 50 g/liter of K_2SO_4 instead of $CuSO_4$.

Experimental Results

Oxidation of a spherical crystal of copper in dry oxygen gas gave a symmetrical "oxidation pattern" of brilliant colors (2). A black and white photograph of such a pattern is shown in Fig. 1a. Such a pattern was due to the interference colors formed with different thicknesses of oxide on different crystal faces. In the present study, similar oxidation patterns were formed when electropolished crystals were immersed in an aqueous solution of $CuSO_4$ at 25°C which contained dissolved oxygen. With careful surface preparation, these patterns were easily reproducible. A typical oxidation pattern formed under these conditions after an immersion time of 1 min is shown in Fig. 1b. Reflection electron diffraction showed that the surface product was Cu_2O. It was obvious for the immersed specimens that there were differences in the oxidation on the different crystal faces, although the patterns were not as striking as in the case of dry oxidation in oxygen. Transmission electron diffraction studies on stripped oxide films and measurements of shadow heights on electron micrographs of replicas indicated that most of the oxide was greater than 1000Å thick after an immersion time of 5 min in the $CuSO_4$ solution. This is to be compared with an oxide thickness of less than 100Å for dry oxidation of copper at 25°C over a period of months, (7) and of 70Å for oxidation of copper in pure water at 25°C for a period of 8 hr (8). The rate of oxidation was therefore much faster for crystals immersed in $CuSO_4$ solution than for those exposed to dry oxygen or to water containing oxygen at the same temperature.

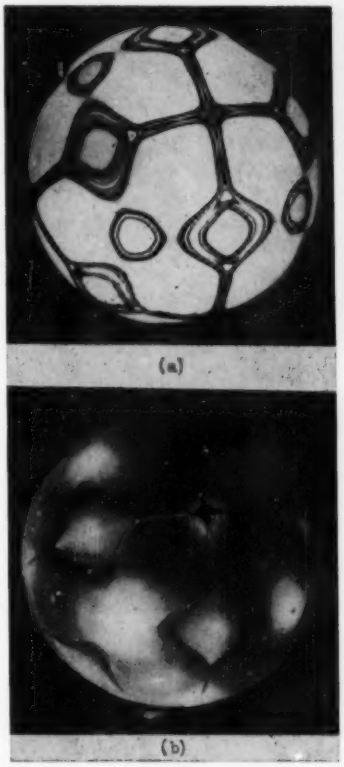

Fig. 1. Oxidation patterns on spherical copper single crystals: a, 20-min oxidation in oxygen at 250°C at atmospheric pressure; b, 1-min oxidation in aqueous $CuSO_4$ at 25°C, pH 3.8.

In order to observe the structural details of the oxide formation on the different crystal faces of copper, flat faces parallel to specific crystal planes were immersed in $CuSO_4$ solutions. In this way differences due to crystal face and the effects of time of immersion could be studied.

Back reflection x-ray diffraction patterns of the flat faces indicated that the cold worked surface layer produced by the mechanical polish was removed by the electropolish. Electron micrographs of

carbon replicas of the metal surface after electropolishing and annealing show no indications of pitting, facet development, or other type of roughness. The surfaces were very smooth with only a slight waviness of the order of 2°. The micrograph is not reproduced here since it would appear only as a plain gray area. Electron diffraction patterns showed sharp Kikuchi lines.

The effect of time of immersion on the oxidation was studied on five crystal faces, the (110), (100), (111), (210), and (311) for immersion times from 30 sec to 90 hr at a solution temperature of 25°C. Figure 2 shows the results of this study on the (110) face for representative immersion times of 30 sec, 24 hr, and 60 hr. Figure 3 shows the results on the (100), (111), (210), and (311) faces for an immersion time of 60 hr. The results at 30 sec and 24 hr for these faces were similar to the (110), the major differences being the shapes of the oxide growths and the relative coverage of the surface by the oxide.

Well-shaped polyhedra of Cu_2O single crystals varying in diameter from 300-3000Å were present on all faces after 30 sec in $CuSO_4$. The coverage of the surface varied from face to face, but in no case was there a complete coverage of the surface by the polyhedra. For oxide crystals 1000Å in diameter the heights of these polyhedra as determined from shadow lengths were roughly 500-700Å. The oxide polyhedra grew larger with time. This growth was both parallel and normal to the copper surface. After 24 hr the oxide polyhedra had grown together so as to give a more complete coverage of the surface, with many individual crystals 20,000-30,000Å in diameter, although some of 1000Å or less were still present. The pH of the solution had changed from 3.8 to 3.4 in this period of time.

After 60 hr in $CuSO_4$, the appearance of the surface was much more complicated. The coverage of the surface was rather uneven, some areas being almost completely covered with large oxide polyhedra which had grown together as in Fig. 3b and 3c. Other areas were only partially covered as in Fig. 3a and 3d, and some areas were almost free of large oxide figures as shown in Fig. 4. These latter regions frequently showed a considerable amount of etching of the metal surface, in addition to small oxide polyhedra. This etching was usually in the form of well-shaped etch pits. This is shown in Fig. 4. It was also apparent that some etching of the larger oxide polyhedra had taken place (Fig. 3c). Some of the oxide crystals were as large as 300,000Å (30 μ) in diameter, whereas others were only of the order of 1000Å. The pH of the solution at the end of 60 hr had changed from 3.8 to 3.2.

After 90 hours' immersion the specimen surfaces were similar to the 60-hr specimens, except that considerably more etching both of the oxide and of the metal surface had taken place.

Both optical and electron microscopic examination of specimens after 24-, 60-, and 90-hr immersion showed that the larger oxide polyhedra usually had complex step and spiral structures present on their surfaces. In most cases the spirals were present on the (111) surfaces of the oxide. The spirals were observed only once on another oxide face, the (100). Figure 5 shows an example of a spiral on the (111)

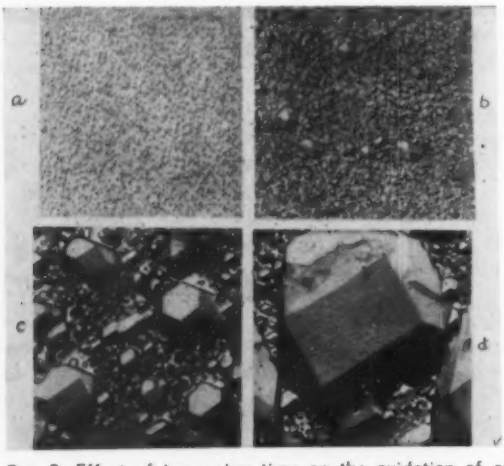

Fig. 2. Effect of immersion time on the oxidation of annealed (110) face of copper in $CuSO_4$ solution at 25°C: a, 30 sec, pH 3.8; b, 24 hr, pH 3.4; c and d, 60 hr, pH 3.2. Magnification 3500X before reduction for publication.

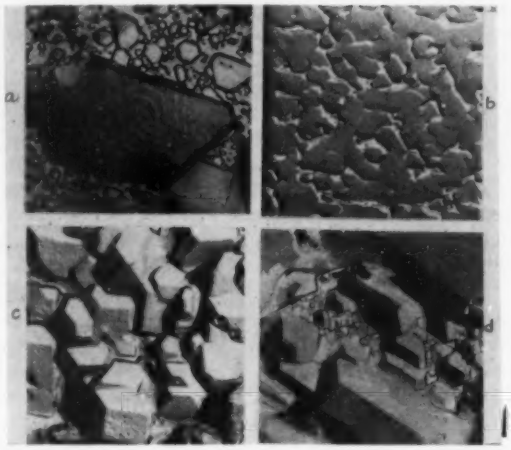

Fig. 3. Appearance of surfaces after 60-hr immersion in $CuSO_4$ solution at 25°C, pH 3.2; a, (100) face; b, (111) face; c, (210) face; d, (311) face. Magnification 3500X before reduction for publication.

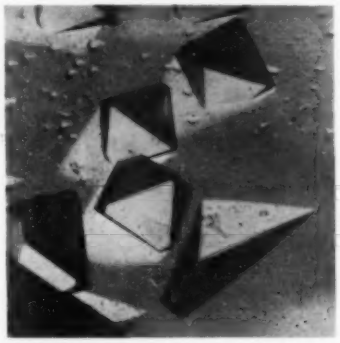

Fig. 4. Etch pits and oxide polyhedra on (210) face after 60-hr immersion in $CuSO_4$ solution at 25°C, pH 3.2. Magnification 6200X before reduction for publication.

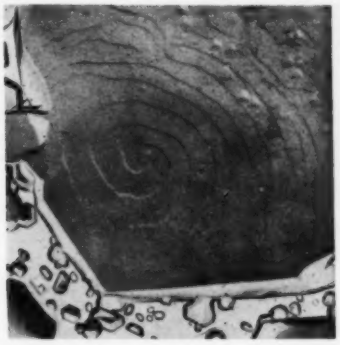

Fig. 5. Spiral growth on (111) surface of Cu_2O formed on the (100) face of copper immersed for 60 hr in $CuSO_4$ solution at 25°C, pH 3.2. Magnification 6200X before reduction for publication.

face of Cu_2O. The step height of the spirals was determined from the shadows and was in the range 100-200Å. No spirals were observed on the smaller oxide growths. In general the spiral systems were more complex than that shown in Fig. 5 and frequently more than one spiral system was present on a given oxide crystal. A more complex spiral system can be seen on the large oxide polyhedron in Fig. 3a.

Both electron diffraction and electron microscopy showed that the oxide grew such that there were specific epitaxial relationships between the oxide and the metal on the different crystal faces. These results will be reported in more detail elsewhere (1). In general the orientation relationships were the same as those previously determined for dry oxidation by Lawless and Gwathmey (9), and for oxidation in pure water by Kruger (8), and Lawless (7).

The very early stages of the oxide growth were studied on specimens which had been immersed for 15 sec. The oxide film was stripped from the copper electrolytically and examined by the electron microscope. Figure 5a shows the appearance of the oxide on the (100) face of copper. The similarity of this to electron micrographs of the early stage of dry oxidation at 150°C (5, 7) was striking. At higher magnifications the dark oxide crystals showed the same shapes as appear in Fig. 3. Electron diffraction (Fig. 6b) indicated that not only well-oriented single crystal particles of oxide but also a continuous polycrystalline thin film of Cu_2O were present. These diffraction studies indicated that the thickness of this thin film was certainly less than 50Å and probably less than 20Å.

Cu_2O also formed on crystals which were immersed in an aqueous solution of K_2SO_4, but at a rate much slower than that for crystals immersed in an aqueous solution of $CuSO_4$. The amount of oxide formed in an hour was of the same order of magnitude as the amount formed on a crystal immersed in distilled water (8).

The oxide on the surface of a copper crystal could be dissolved by dipping the crystal in a 10% HCl solution for about 15 sec. When this experiment was carried out for a crystal on which oxide had been formed by immersion in $CuSO_4$, the oxide dissolved leaving a bright copper surface showing no apparent roughness or etching of the metal surface. When the same experiment was carried out using a crystal with an oxide film of comparable thickness which was formed by oxidation in dry oxygen gas, the surface appeared roughened and faceted.

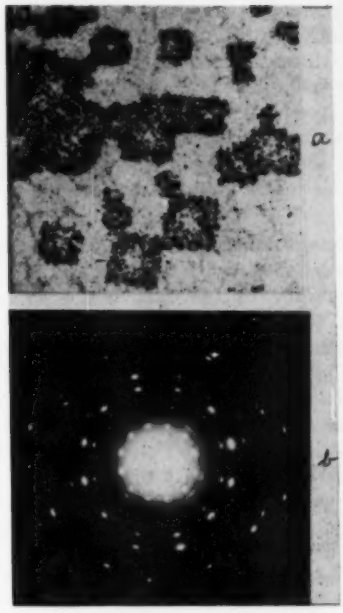

Fig. 6. Oxidation of (100) face of copper in aqueous $CuSO_4$ solution at 25°C, immersion time 15 sec: a, electron micrograph of stripped oxide, magnification 12,000X before reduction for publication; b, transmission electron diffraction pattern of stripped oxide.

Discussion

The results of this study revealed some of the extreme complexities arising in the oxidation of a metal in an aqueous salt solution. Any completely satisfactory mechanism for the reaction of copper in aqueous $CuSO_4$ solution must explain the rapid growth of individual Cu_2O polyhedra, the presence of spirals on the oxide, and the presence of both etch pits and oxide figures on the same surface.

Formation of oxide on the copper immersed in this solution was dependent on the pH of the solution. Cu_2O was the only oxide observed in these studies in which the pH ranged from 3.8 to 3.2. At a pH below 3 only etching of the copper was observed. The results under these conditions do not appear to be important to this discussion and will be treated elsewhere. The formation of Cu_2O only was to be expected on the basis of the work of Pourbaix (10) since this is the only oxide stable in the pH range 3.8 to 3.2.

It was obvious from the irregular thickness of the oxide as shown in the micrographs that rate measurements, in the usual sense of the word, would have limited value for reactions of this nature, even when made on carefully prepared single-crystal surfaces. However, it was apparent that the total amount of oxidation on a given area of surface

was much greater when the crystal was immersed in the $CuSO_4$ solution than when immersed in pure water or when oxidized in dry oxygen at the same temperature for the same length of time. The role of the aqueous salt solution is probably a twofold one of providing an easier path for the flow of electrons and ions and a readily available source of copper ions, thus enabling a more rapid oxidation to occur.

A consistent mechanism which can explain the oxide formation can be arrived at from the data available in the micrographs and diffraction patterns and from theoretical considerations. A thin polycrystalline film of Cu_2O, 20-30Å thick, was formed almost immediately, covering the whole metal surface. The electron diffraction patterns indicated that such a film was formed in these studies, and experimental and theoretical work by Hoar and Evans (11) suggested that the formation of a thin compact oxide film was the initial stage for many reactions in aqueous salt solutions. Studies on oxidation in dry oxygen (5) also indicated that the formation of a thin polycrystalline oxide was the initial stage of oxidation in that case.

This initial oxide film contained many grain boundaries and probably a large number of imperfections. In air at 25°C the subsequent growth of this base film was extremely slow, whereas in aqueous $CuSO_4$ solution certain oxide nuclei in the base film continued their growth at a very rapid rate, as seen in Fig. 2-6. Why should certain of these oxide crystals have continued to grow rapidly while others essentially stopped growing or, at best, grew only slowly? First, it was apparent from the diffraction patterns that the crystals which grew rapidly were well oriented with respect to the base metal. Second, during the later stages of growth it was apparent that imperfections in the oxide polyhedra were playing an important role in the continued growth of the oxide. It is probable that imperfections in the initial thin film were important as well. It seems likely, therefore, that the oxide crystals in the base film which continued to grow rapidly were those which had a specific orientation with respect to a particular face, and which had the proper number and type of imperfections necessary for continued rapid growth.

It is now necessary to explain how these specific oxide crystals could grow so much faster in aqueous $CuSO_4$ than in pure water or dry oxygen. The fact that oxide formation was much slower in an aqueous solution of K_2SO_4 than in $CuSO_4$ is an indication of the importance of the copper ions in the solution. In addition, the fact that the metal surface was not roughened appreciably by the formation of a thick oxide is perhaps further evidence that the bulk of the copper ions converted to oxide came from the solution rather than from the metal. It seems likely, therefore, that after the initial formation of the thin oxide film, for which copper ions would be available both from the metal and from the solution, the bulk of the oxide is produced by reaction of copper ions from the $CuSO_4$ solution.

The initial oxide film could be produced either by reaction of copper with oxygen adsorbed on the surface from solution

$$2Cu + \tfrac{1}{2} O_2 \rightarrow Cu_2O \qquad [1]$$

or by reaction of cuprous ions with water or hydroxyl ion

$$2Cu^+ + 2\,OH^- \rightarrow Cu_2O + H_2O \qquad [2]$$

In these experiments it was not possible to distinguish between these possibilities.

The subsequent growth of the oxide could take place either by reaction [2] above or by the reaction of Cu^{++} ions with water at suitable sites on the surface where electrons would be available [3].

$$2Cu^{++} + 2e^- + H_2O \rightarrow Cu_2O + 2H^+ \qquad [3]$$

This is of course essentially the same reaction as [2], only assuming the reduction of cupric ion to cuprous ion at suitable reduction sites on the oxide surface. Since this is a reduction, an oxidation reaction is necessary also. Two possible oxidation reactions are

$$Cu \rightarrow Cu^+ + e^- \qquad [4]$$

and

$$Cu \rightarrow Cu^{++} + 2e^- \qquad [5]$$

According to Hoar and Evans (11) it would be possible for metal ions to go into solution with migration of these ions through an oxide film on the metal surface. This would be expected to take place at imperfections in the oxide such as would be created by lattice defects or grain boundaries, or at very thin regions of the oxide. Since we are concerned with a very thin oxide film, tunnelling of electrons can take place setting up a strong electric field which would assist the movement of metal ions through the oxide (12).

If the copper surface is not completely covered with an oxide film, in addition to reactions [4] and [5], an additional reaction can occur

$$Cu + Cu^{++} \rightarrow 2Cu^+ \qquad [6]$$

Although it seems likely that in the oxygen containing $CuSO_4$ solution a continuous film of oxide would be present on the copper surface, it is not possible from these experiments to conclude definitely that there are no regions on the surface which are free of oxide. There is therefore a possibility that reaction [6] does occur in the aerated solution. The fact that appreciable etching of the copper surface does not occur until the pH has decreased considerably would indicate that the extent of this reaction is at best rather small in the early stages of the reaction. If a copper crystal having a thin air-formed oxide film on its surface is immersed in aqueous $CuSO_4$, additional oxide is formed. This is further evidence that reaction [6] is not important in the early stages of the reaction.

In some preliminary experiments using deaerated aqueous $CuSO_4$ it was found that oxide formed on the copper crystal apparently as rapidly as in the experiments with aerated $CuSO_4$. Similarly, over a

period of 24 hr the pH of the deaerated solution decreased from 3.8 to 3.2. Electron microscope observations of the surfaces of copper crystals immersed in deaerated $CuSO_4$ solution showed the same type of oxide structures as observed with oxygen containing solutions. The regions between the oxide polyhedra seemed, however, to be etched to a greater extent in the experiments with deaerated solution. This could be a result of reaction [6].

The similarity between the behavior of copper in aerated and deaerated $CuSO_4$ solutions indicated that basically the same oxide formation process was occurring in both cases. This is apparently reaction [2],

$$2Cu^{+} + 2\,OH^{-} \rightarrow Cu_2O + H_2O \qquad [2]$$

El Wakkad (13), however, states that the solubility product for this reaction is not exceeded for solutions of the concentration and pH used in these experiments. Since Cu_2O is definitely formed in these experiments it seems probable that the value for K_{sp} of 7.18×10^{-14} taken by El Wakkad (13) is too large and that the value given by Feitknecht (14) of 1.5×10^{-15} is more reasonable.

A calculation of the thickness of oxide formed on the copper based on the stoichiometry of Eq. [2] was made from the pH change and gave a figure of the right order of magnitude. It was not possible to make an exact comparison since the thickness irregularity of the oxide growths made it impossible to get more than an approximate average thickness for the actual oxide formed. The exact concentration of Cu^{+} ion in the original solution was not measured, but the maximum concentration possible can be calculated from the solubility product. This amount of Cu^{+} ion is less than the amount needed to form the observed amount of oxide and therefore additional Cu^{+} ions must be formed either from the metal by reaction [4], from the solution by reduction of Cu^{++} ions at suitable reduction sites on the surface, or by reaction [6] if bare places are available on the metal surface.

It is possible that in the aqueous solution of $CuSO_4$ containing oxygen which was used for most of these experiments that the reaction

$$\tfrac{1}{2}O_2 + H_2O + 2e^{-} \rightarrow 2\,OH^{-} \qquad [7]$$

is of importance. This reaction at the oxide surface could produce locally a higher OH^{-} concentration making it easier to exceed the K_{sp} in aerated solutions. From the experiments with deaerated solutions, however, reaction [7] does not seem to be necessary for the oxide formation in these experiments.

It seems probable, therefore, that reaction [2] is the main process responsible for the oxide formation with either reaction [3], [4], or [6] being responsible for the conversion of additional copper or cupric ions to cuprous ions. This latter point cannot be settled conclusively from the experimental data available at this time. This reaction [2] would lead to a decreased pH as observed. The reaction would take place on the surface of particular oxide crystallites where the oxide growth is energetically most favorable. The oxide will form rapidly since initially copper ions are readily available from the solution for reaction without the necessity for diffusion through the bulk of large oxide crystals. The oxide polyhedra can then continue to grow provided a suitable mechanism for their growth is available.

It has been shown theoretically (15) and experimentally (16) that the emergence of a screw dislocation on a crystal face provides a mechanism for continued rapid crystal growth without the necessity of two-dimensional nucleation on the surface. In this study the larger oxide polyhedra invariably showed spiral or step growth features for times of immersion of 24 hr or more. This indicated strongly that the rapid growth of these polyhedra in the later stages of growth was due to the presence of screw dislocations in the oxide. The presence of complete spirals on the surfaces was also a good indication that the growth was continuing by means of volume diffusion of copper ions and not by surface diffusion or diffusion through the bulk of the oxide. It is probable that the spirals were not observed at the earlier stages of oxidation because of the small size of the oxide particles and the difficulty of shadowing such small step heights. The screw dislocations apparently had large Burgers vectors which were stabilized by the presence of impurities (17). This type of imperfection could arise at any stage in the oxide growth because of stresses in the oxide or the growing together of two or more slightly disoriented oxide crystals.

Copper specimens immersed for 24 hr or more in the $CuSO_4$ solution showed etching of both the metal and the oxide polyhedra. This occurred with an attendant decrease in the pH of the solution. According to reaction [2], a decrease in the pH of the solution was to be expected because of the decrease in hydroxyl ion during the reaction. At a pH of 3.2, a state very close to equilibrium is attained and it might be expected that some solution of the oxide would occur at high energy sites of the oxide. Since the thin oxide film probably consisted of many imperfect crystals with numerous grain boundaries. it would be more subject to attack than the more perfect oxide polyhedra. Thus the thin oxide would dissolve or partially dissolve at specific sites and etching of the metal could occur. The thin oxide film is probably re-formed at these sites fairly rapidly after its solution. Imperfections in the oxide polyhedra would also provide high energy sites which would be subject to attack by the H^{+}, as observed.

The exact function of the dissolved oxygen in the $CuSO_4$ solution is not understood. It will be necessary to continue experiments in which the oxygen has been removed completely from the solution before this point can be clarified.

Summary

When a copper crystal was immersed in an aqueous $CuSO_4$ solution of pH 3.8, a thin film of Cu_2O, 20-30Å thick, formed immediately over the whole surface. Particular oxide crystals in the base film continued to grow at a rapid rate forming well-defined oriented polyhedra showing only (111),

(100), and (110) faces. Growth spirals were observed on the larger oxide polyhedra after immersion time of 24 hr or more. With long periods of immersion in the aqueous solution the pH of the solution decreased to 3.2, and etching of both the metal surface and the oxide occurred. The rapid formation and growth of the isolated oxide polyhedra was explained on the basis of a readily available supply of copper ions, both from the metal and from the solution, an electrochemical mechanism of reaction, and a dislocation mechanism of crystal growth.

This investigation has indicated the importance, and indeed the necessity, of using both electron microscope techniques and carefully prepared single-crystal surfaces if studies of surface reactions are to have any meaning. Details of the metal surface or of the thin oxide film structure, which are too small to be resolved or seen clearly with the optical microscope, can be of the utmost importance in determining the course of a chemical reaction such as oxidation or etching. It is through the study of such structural factors at the high magnifications possible only with the electron microscope, that a better understanding of corrosion processes can be obtained.

Acknowledgment

The authors would like to thank Drs. A. T. Gwathmey, N. Cabrera, and R. E. Cunningham for many discussions pertaining to this work. We would also like to thank Dr. R. H. Kean for carrying out the preliminary studies with the deaerated $CuSO_4$ solutions. This research was supported by a grant from the Office of Naval Research.

Manuscript received Oct. 20, 1958.

Any discussion of this paper will appear in a Discussion Section to be published in the June 1960 JOURNAL.

REFERENCES

1. K. R. Lawless and G. T. Miller, Jr., *Acta Cryst.*, to be published.
2. F. W. Young, J. V. Cathcart, and A. T. Gwathmey, *Acta Met.*, **4**, 145 (1956).
3. D. E. Bradley, *J. Inst. Metals*, **83**, 35 (1954).
4. C. E. Hall, "Introduction to Electron Microscopy," McGraw-Hill Book Co., New York (1953).
5. W. W. Harris, F. L. Ball, and A. T. Gwathmey, *Acta Met.*, **5**, 574 (1957).
6. Z. G. Pinsker, "Electron Diffraction," Butterworths Scientific Publications, London (1953).
7. K. R. Lawless, Unpublished results, University of Virginia.
8. J. Kruger, Private communication.
9. K. R. Lawless and A. T. Gwathmey, *Acta Met.*, **4**, 153 (1956).
10. M. J. N. Pourbaix, "Thermodynamics of Dilute Aqueous Solutions," Edward Arnold and Co., London (1949).
11. T. P. Hoar and U. R. Evans, *This Journal*, **99**, 212 (1952).
12. N. Cabrera and N. F. Mott, *Repts. Progr. Phys.*, **12**, 163 (1948-49).
13. A. R. Tourky and S. E. S. El Wakkad, *J. Chem. Soc.*, **1948**, 740; S. E. S. El Wakkad, **1950**, 3563.
14. W. Feitknecht, *Chimia*, **6**, 3 (1952).
15. W. K. Burton, N. Cabrera, and F. C. Frank, *Phil. Trans.*, **A243**, 299 (1951).
16. A. R. Verma, "Crystal Growth and Dislocations," Butterworth Scientific Publications, London (1953).
17. G. T. Miller, Jr., and K. R. Lawless, *J. Appl. Phys.*, **29**, 863 (1958).

Influence of Silicon on the High-Temperature Oxidation of Copper and Iron

J. W. Evans and S. K. Chatterji

Department of Metallurgy, University of Manchester, England

ABSTRACT

The effects of 1 at. % of silicon on the oxidation behavior of pure copper at 850°-1000°C and of pure iron at 950°-1200°C have been studied by means of a thermobalance. Silicon has a marked effect on the oxidation of iron but relatively little on that of copper. The distinctive behavior is attributed mainly to the different diffusivities of oxygen in the base metals. The depth of subscale formed in the iron alloy suggests that the diffusivity of oxygen in iron is much faster than is commonly supposed.

The high-temperature oxidation resistance of many metals is improved by small additions of silicon. The beneficial effects of Si in steel have been demonstrated frequently and the general pattern of oxidation behavior established (1-5). During oxidation several distinct layers are formed. At the outside surface there is a very thin Fe_2O_3 layer; next to this is a somewhat thicker magnetite layer and this is followed by the thickest layer adjacent to the metal (about 90% at 800°-1000°C) which is wüstite or nonstoichiometric FeO. Because the oxidation of the Fe in the Si steel occurs almost entirely by the outward diffusion of ferrous ions to the surface, the Si concentrates at the oxide-metal interface to form a thin, coherent layer. This layer may consist of fayalite ($2FeO \cdot SiO_2$) or silica, depending on the Si content and temperature.

Silicon has less effect on the oxidation resistance of Cu than it has on Fe. A review of the oxidation behavior of Cu alloys relating to work up to about 1950 has been given by Tylecote (6). The oxidation of a Cu-Si alloy proceeds similarly to that of Fe in

which cationic diffusion outwards of Cu ions occurs. The scale is principally cuprous oxide with a thin outer layer of cupric oxide. Unlike Si in Fe, however, the Si does not invariably concentrate at the oxide-metal interface but may well accumulate in the alloy, the precise behavior depending on the Si concentration initially and the temperature. For example, Preece and Dennison (7) found that a 2% Si-Cu alloy gave a layer of silica at the metal-oxide interface only below 800°C. This layer was absent above this temperature, and above 900°C the Si accumulated in the alloy to such an extent that a liquid Cu-Si phase was formed.

A distinctive feature of the oxidation of Cu alloys is the formation of an extensive subscale caused by the relatively rapid inward diffusion of oxygen into the alloy which precipitates finely disseminated silica throughout the metal matrix. Subscale formation in Cu alloys has been investigated thoroughly by Rhines, Johnson, and Anderson (8), who demonstrated that the depth of subscale was determined principally by oxygen diffusivity. Subscale formation in Fe-Si alloys has been observed but not quantitatively investigated.

In this present work, precise rate laws and their temperature dependence have been determined for pure Cu and Fe. The influence of about 1 at. % Si on the oxidation rate of the pure metals has been studied at temperatures between 800° and 1200°C. The distinctive behavior of Si in each of these metals is shown to be dependent on the extent of subscale formation and this behavior has been partly confirmed by selectively oxidizing Si in the alloys by the use of a controlled gas mixture of hydrogen and water vapor.

Experimental

Materials.—High-purity iron (C, 0.003%; Si, 0.002%; Mn, 0.004%; S, <0.005%; P, <0.001%; Cr, 0.001%; Al, 0.001%) was obtained from the National Physical Laboratory, England.

High-purity (OFHC) Cu and high-purity Fe-Si and Cu-Si alloys containing 0.52% and 0.61% Si, respectively, were supplied by Johnson & Matthey Ltd.

Specimens for oxidation tests were cut from ⅛ in. rolled strip, polished with metallurgical emery paper, and finished with 4-0 grade to give a mirror finish. Specimens were degreased with carbon tetrachloride and acetone immediately before inserting in the furnace.

Oxygen and hydrogen (<10 ppm oxygen) of commercial purity were supplied by the British Oxygen Company.

Apparatus.—The reaction rate of the pure metals and alloys was determined by means of a thermobalance. A Pt-wound resistance furnace was used with an impervious mullite reaction tube mounted vertically. Temperature control was maintained to ±5°C over a 3 in. central zone by means of a mechanical controller operated by a Pt/Rh thermocouple. Connections to the mullite tube were made in Pyrex glass with Araldite cement and these joints were water cooled.

The balance consisted simply of a precision glass spring (obtained from Still and Cameron, London) suspended from the inside of a ground glass joint above the furnace. The sensitivity of the spring was approximately 43 mg/cm extension under a load of 1 g; Hooke's law was obeyed over extensions of several centimeters. The entire spring was maintained virtually at room temperature, and specimens were suspended in the hot zone of the furnace by a fine silica rod; Pt wire was used to support the samples. The weight changes were obtained by measuring the changes in spring extension with a traveling microscope focused on a fine datum mark on the spring. Weight changes of better than 0.1 mg could be observed without difficulty.

The usual arrangements were made for evacuating the furnace tube and for passing dry or wet gases through the system.

The usual procedure for making a measurement was as follows. The furnace was brought to temperature and the ground glass joint removed. The spring with its silica rod and metal sample suspended from it was carefully attached to the hook. While a rapid stream of argon was flowing through the furnace tube, the joint and spring assembly were lowered into position. This could be done in a few seconds and the furnace then was evacuated. The traveling microscope was focused on the mark on the spring to obtain the initial reading. Dry oxygen was admitted and the weight gains followed by adjusting the microscope at suitable intervals to coincide with the datum mark; initially, readings were taken every minute and for longer intervals after the first hour; runs up to 5 hr were made. Pretreatment of certain specimens was carried out by heating them in a stream of hydrogen, saturated with water vapor at room temperature, for 3 hr at the temperature of subsequent oxidation.

Microsections were studied on many specimens and the thickness of various oxide layers estimated.

Results

Pure Copper.—The oxidation of pure Cu followed a smooth parabolic law; results for 906°, 960°, and 1002°C are shown in Fig. 1. The logarithm of the

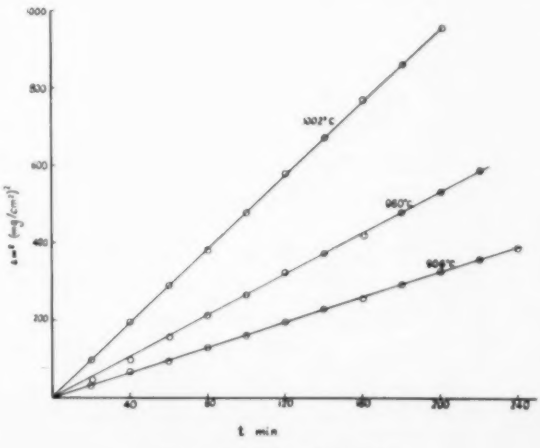

Fig. 1. Oxidation of pure Cu

Table I

Temperature, °C	CuO, mm	Cu_2O, mm
906	0.019	0.286
960	0.003	0.337
1002	0.002	0.622

Table II

Temperature, °C	CuO, mm	Cu_2O, mm	Subscale mm
862	0.003	0.167	0.010
912	0.004	0.257	0.117
952	—	—	0.137
1006	0.002	0.456	0.143

parabolic rate constant is plotted against the reciprocal of the absolute temperature in Fig. 3; from the slope of this line, the usual Arrhenius equation yields an activation energy of 34.8 kcal for the oxidation process. In all cases the oxide scale was firmly adherent and when broken disclosed a dark red layer of Cu_2O underneath the gray-black surface CuO. The relative thicknesses of the two oxide layers are given in Table I.

Copper—0.61% silicon.—As with pure Cu the oxidation of the alloy followed a smooth parabolic law: results for 862°, 912°, 952°, and 1006°C are shown in Fig. 2. The rates are slightly but significantly slower than the corresponding values for pure Cu.

The logarithm of the parabolic rate constant against the reciprocal of the absolute temperature is plotted in Fig. 3. The slope of this line is very close to that for pure Cu, giving a calculated activation energy of 36 kcal for the process.

The oxide scale was similar to that on Cu but was less adherent and tended to flake off during cooling. In addition to the characteristic oxide layers of Cu_2O and CuO, the microstructure of the underlying metal showed a clearly defined subscale, presumably of precipitated silica at grain boundaries.

The relative thicknesses of the various layers are given in Table II.

Copper—0.61% silicon after pretreatment in wet hydrogen.—Even after pretreatment in wet hydrogen, the oxidation proceeded smoothly following a parabolic rate law; results for 952° and 1006°C are shown in Fig. 4. The rates are slower than for both pure Cu and the untreated alloy.

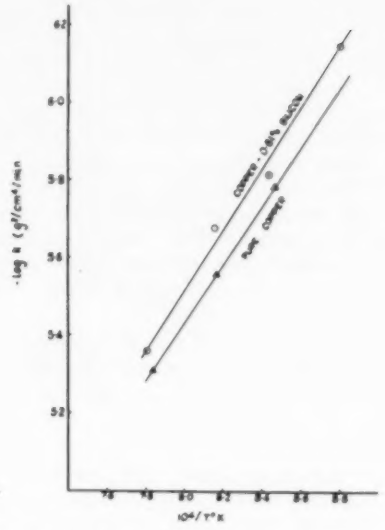

Fig. 3. Log k vs. 1/T for Cu and Cu-0.61% Si

After pretreatment, but before oxidation, the metal surface appeared quite bright and free from a surface film.

Pure iron.—The oxidation curves for pure Fe followed smooth parabolas; results for 810°, 864°, 910°, 984°, and 998°C are shown in Fig. 5. From the graph of the logarithm of the rate constant against the reciprocal of the absolute temperature (Fig. 6), the activation energy for the process is calculated to be 34.3 kcal.

Below 900°C, the surface layer had a velvet, dark red appearance whereas above this temperature the color was metallic gray. The scale was firmly adherent, but it could be removed by light hammering. Microscopically, three oxide layers could be readily distinguished, viz., a very thin outer layer of Fe_2O_3, a thicker layer of Fe_3O_4, and finally a mixed layer of FeO and Fe_3O_4 adjacent to the metal.

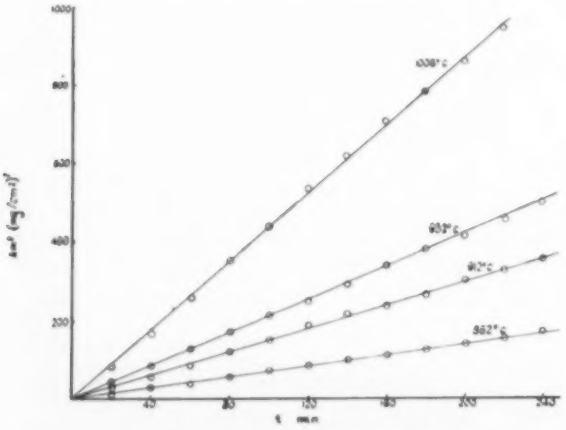

Fig. 2. Oxidation of Cu-0.61% Si alloy

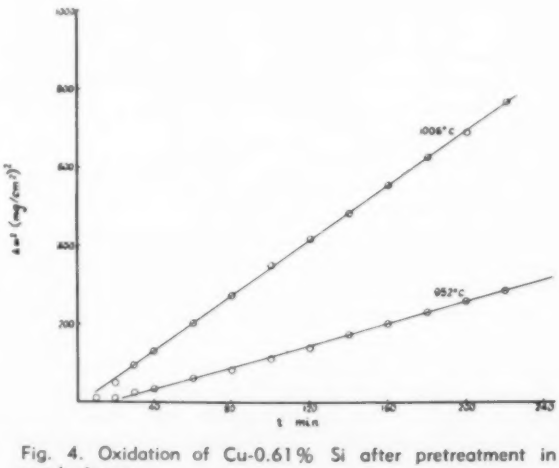

Fig. 4. Oxidation of Cu-0.61% Si after pretreatment in wet hydrogen.

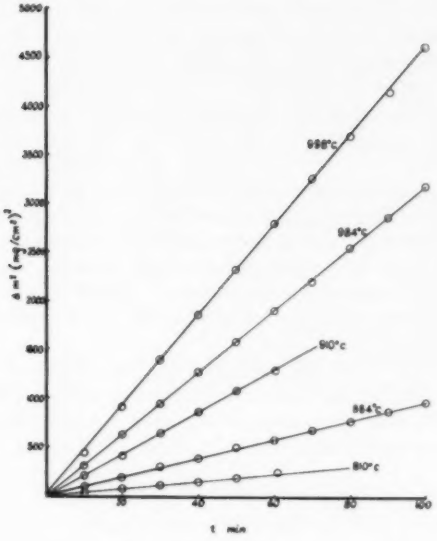

Fig. 5. Oxidation of pure Fe

This latter mixed layer may well result from the partial decomposition of wüstite on cooling. There appears to be no abnormal change in the oxidation process at the α-γ transition in Fe (910°C), but a small difference would be undetected.

Iron—0.52% silicon.—Unlike the behavior of Si in Cu, Si in Fe has a pronounced effect on both the rate and mechanism of oxidation of Fe.

Results for 950°, 998°, 1055°, 1103°, 1131°, and 1165°C are shown in Fig. 7. Up to about 1100°C, the reaction is initially quite slow; after a time depending on the temperature, the oxidation increases, following an approximately smooth curve. At higher temperatures, this initial slow period disappears. At about 1170°-1180°C, the oxidation was catastrophic and no rate data could be obtained above this temperature, because of the melting point of fayalite (1180°C).

The scale was grayish black and closely adherent but could be removed by slight hammering. The exposed metal surface was roughly corroded; there were no obvious signs of silica precipitation at the metal interface, but on the specimen oxidized at

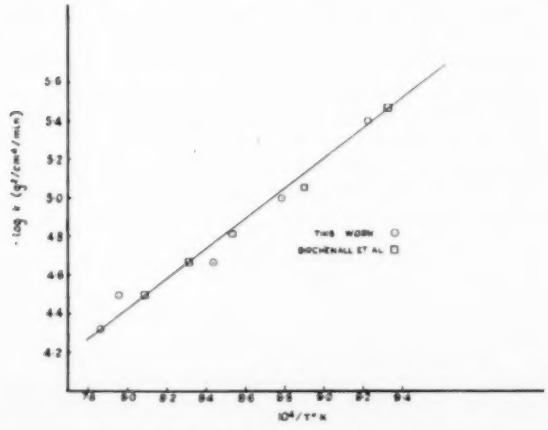

Fig. 6. Log k vs. 1/T for pure Fe

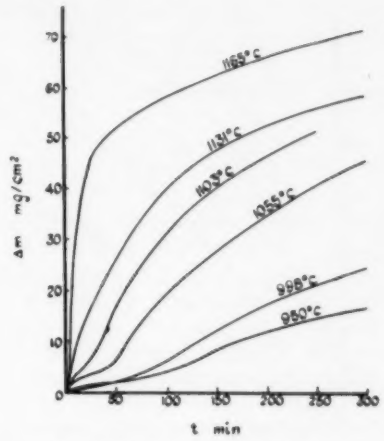

Fig. 7. Oxidation of Fe-0.52% Si

1160°C specks of a partly molten phase could be seen. A microsection of the oxidized specimen showed a number of oxide layers. The external layer was a very thin compact layer of hematite which occasionally showed needle-like growths on specimens oxidized above 1050°C. Beneath this, there was a dense layer of magnetite; below this was a less well-defined and rather more porous structure of wüstite mixed with some magnetite, and finally, adjacent to the metal, there was a thin compact layer of wüstite with fayalite. Within the metal there was a very thin subscale. Approximate relative thicknesses of the various layers are shown in Table III.

Iron—0.52% silicon after pretreatment in wet hydrogen.—After pretreatment in wet hydrogen the oxidation curves showed very similar behavior to that of the untreated alloy, although the rates of oxidation appear somewhat faster. Results are shown for temperatures of 1010°, 1060°, and 1110°C in Fig. 8. The curves are irregular and the oxide scales showed cracking and blistering.

Discussion

Oxidation of Pure Copper and Iron

The parabolic rate constants for pure Cu and Fe derived from the experimental results are:

For Cu (900°-1000°C) $k = 0.076 \exp(-34{,}800/RT)$ g² cm⁻⁴ sec⁻¹

For Fe (800°-1000°C) $k = 0.578 \exp(-34{,}300/RT)$ g² cm⁻⁴ sec⁻¹

The results for Cu are in general agreement with other workers, e.g., Valensi (9) and Feitknecht (10).

Table III

Temperature, °C	Fe_2O_3, mm	FeO, mm	FeO + Fe_2SiO_4, mm	Subscale, mm
950	0.010	0.060	0.081	0.018
998	0.011	0.072	0.133	0.036
1055	0.020	0.082	0.347	0.030
1103	0.052	0.252	0.131	0.061
1131	0.086	0.361	0.107	0.065
1165	0.253	0.040	0.540	0.120

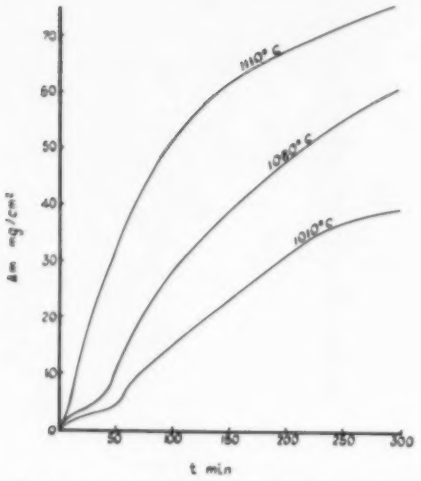

Fig. 8. Oxidation of Fe-0.52% Si after pretreatment in wet hydrogen.

In this temperature region the growth of the oxide layer is controlled by the diffusion of cuprous ions through cuprous oxide. Moore and Selikson (11) measured the diffusivity of Cu^+ in Cu_2O using radiocopper and obtained an activation energy of 36.1 kcal for the diffusion process which agrees reasonably well with the experimental activation energy of 34.8 kcal for the scaling process.

For pure Fe the results compare well with the measurements of Davies, Simnad, and Birchenall (12) in this temperature range; their results are plotted in Fig. 6. Himmel, Mehl, and Birchenall (13) have shown that the controlling process in the oxidation of Fe is the diffusion of ferrous ions in wüstite. They have measured the diffusion rates of cations in the various Fe oxides and obtained a value of 29 kcal for ionic diffusion in wüstite which may be compared with the value of 34.3 kcal for the oxidation process.

Many workers have studied the oxidation of Fe in air, oxygen, and at other controlled oxygen pressures, but the results have not been concordant; part of the discrepancy almost certainly arises from the relative purity of the Fe employed and to a less extent to the use of humid air or oxygen.

When the slight difference in activation energy is taken into account, the parabolic rate constant for the oxidation of Fe is about ten times that for Cu at corresponding temperatures. In both oxides the controlling process is cationic diffusion through a nonstoichiometric oxide, probably via vacant lattice sites. From a consideration of Wagner's theory of parabolic oxidation, it is clear that the difference in scaling rates of the two metals lies in the different ionic conductivities of the two oxides. For FeO the electrical conductivity (13) is 107 ohm^{-1} cm^{-1} for an oxygen partial pressure corresponding to the dissociation pressure of magnetite at 1000°C and the cation transport number is 2×10^{-4}; for Cu_2O the conductivity (14) is 4.8 ohm^{-1} cm^{-1} at an oxygen partial pressure corresponding to the dissociation pressure of CuO at 1000°C and the cation transport number is 4×10^{-4}.

Oxidation of Silicon Alloys

The oxidation of Cu and Fe containing a small amount of Si differs significantly. Silicon in Cu has little effect on the scaling rate of pure Cu, whereas Si in Fe modifies the oxidation mechanism as shown by the irregular oxidation curves. A further point is that the subscale in Cu is substantially thicker than in Fe for the corresponding temperature.

The difference in subscale thicknesses arises principally from the difference in diffusivities of oxygen in Cu and Fe, although the difference in oxygen solubility in both metals, the scaling rate of the base metal, and the relative diffusivities of Si all play their part.

Darken (15) has analyzed the formation of subscale in dilute alloys, and, with certain assumptions, showed that the depth of subscale x during scaling is given by the equation

$$x = (D/r) \ln (1 + u/v)$$

in which D is the diffusivity of oxygen in the alloy, r is the scaling rate, u is the solubility of oxygen in the pure base metal, and v is the initial concentration of Si. This relation shows that the depth of subscale increases with increasing diffusivity and solubility of oxygen and decreases with increasing rate of scaling and Si content of the alloy.

From the diffusivities and oxygen solubilities at 1000°C shown in Table IV, the difference in oxygen diffusivity would appear to be decisive. The very large differences in oxygen diffusivities ought to be reflected in the relative depths of subscale. (Tables II and III, however, show that this is not so.) The value for oxygen in Fe in Table IV is based on one value of Bramley, *et al.* (17), but the depth of subscale in our experiments suggests that their value for diffusivity is at least 1000 times too low. This is partly confirmed by Darken (15) who implies a value for oxygen in iron of the order of 10^{-7} cm^2 sec^{-1} without citing experimental evidence.

The effect of Si in Cu is such that during scaling Si cannot accumulate at the oxide-metal interface but becomes progressively oxidized in depth by virtue of the rapid inward diffusion of oxygen. On the other hand, during the scaling of Fe, Si can diffuse and concentrate at the metal-oxide interface, becoming converted initially to silica which builds up a coherent and partially protective layer. The form of the Si-Fe oxidation curves suggests that, during the initial period of oxidation, silica is first precipitated at the interface and the oxidation rate is appreciably reduced because of the protective nature of the silica (18). However, after this slow initial period the silica undergoes a solid state reaction with FeO to form fayalite. This is itself a semiconductor, and the alloy then begins to oxidize at a

Table IV*

1000°C	D(Oxygen), cm^2sec^{-1}	D(Silicon), cm^2sec^{-1}	Oxygen solubility, wt %
Copper	10^{-5}	0.5×10^{-5}	0.009
Iron	10^{-10}	10^{-5}	0.003

* Data from Metals Reference Book (16).

Table V

Exptl. gas mixture	Cu-Cu_2O	Fe-FeO	Si(1 at. %)-SiO_2
H_2O/H_2 ratio at 1000°C	2.5×10^{-2}	5×10^{3}	0.5	7×10^{-5}

faster rate by ionic diffusion through this layer. The initial slow period decreases with increasing temperature which would be expected as the solid-state reaction becomes more rapid. A similar two-stage process was observed by Ipatev and Orlova (5) during the oxidation of a Si steel containing 1.4% Si.

Pretreatment in Wet Hydrogen

A controlled gas mixture capable of oxidizing Si but not Cu or Fe was obtained easily by saturating hydrogen with water at room temperature. The H_2O/H_2 ratio under these conditions is 2.5×10^{-2}. Corresponding ratios for the formation of cuprous oxide and ferrous oxide and for the precipitation of silica from a 1 at. % silicon alloy is shown in Table V.

The calculation for silica is based on approximate activity coefficient of Si in both Cu and Fe of 0.01 (19). It is clear from this table that wet hydrogen should, theoretically, readily precipitate silica but not form either copper or iron oxide.

The formation of subscale in the absence of continuous scaling of the base metal has been studied carefully by Rhines, Johnson, and Anderson (8). They studied a number of dilute binary alloys with Cu as the base metal and correlated their results with a theoretical equation which for Si alloys can be expressed:

$$x^2/t = (2D_o c_o - 1.92\, D_{Si}\, c_{Si})/(1.14\, c_{Si} + 0.33\, c_o)$$

where x is depth of subscale; t, time; D_o and D_{Si}, diffusivities of oxygen and silicon in the alloy, respectively; c_o, solubility of oxygen in the base metal and dependent on the external partial pressure of oxygen; c_{Si}, initial concentration of Si in the alloy.

Since c_o is usually much less than c_{Si}, the depth of subscale and indeed whether any subscale forms or not depends on the relative values of $D_o c_o$ and $D_{Si} c_{Si}$, i.e., not merely on the relative diffusivities of oxygen and silicon.

The solubility of oxygen in Cu at the limiting oxygen pressure of Cu_2O is 0.009%. It is reasonable to assume that oxygen dissolved in solid Cu obeys Sieverts' law, viz., the solubility is proportional to the square root of the partial pressure of oxygen. For H_2O/H_2 mixtures this means that the solubility will be simply proportional to the H_2O/H_2 ratio. From Table V it is seen that the maximum oxygen solubility under the experimental conditions is:

$$0.009 \times \frac{2.5 \times 10^{-2}}{5 \times 10^{3}} = 4.5 \times 10^{-7}\ \text{wt \%}$$

By substituting this value for c_o and the other values from Table IV it is seen that $D_o c_o$ is much less than $D_{Si} C_{Si}$ which implies that no subscale can form and Si will, therefore, diffuse to the surface of the alloy forming a layer of silica. The corrosion behavior of pretreated specimens in oxygen shows that they are significantly more resistant than the untreated alloy although a completely protective silica skin has not formed.

For Si-Fe the oxygen solubility under wet hydrogen conditions is

$$0.003 \times \frac{2.5 \times 10^{-2}}{0.5} = 1.5 \times 10^{-4}\ \text{wt \%}$$

With Bramley's value (17) for the diffusivity of oxygen, $D_o c_o$ is again much less than $D_{Si} c_{Si}$ so that no subscale would be expected, and silica should precipitate at the Fe surface. The oxidation of pretreated silicon iron, however, does not confirm this since the oxidation apparently is enhanced after pretreatment. These experimental results suggest that subscale has formed and depleted the surface of the alloy in Si. This could only happen if the diffusivity of oxygen was in fact much faster than Bramley's value or alternatively that the oxygen solubility was much higher.

Conclusions

Small amounts of Si affect the scaling of Cu and Fe in different ways. For Cu, Si in the alloy tends to be precipitated mainly as subscale during external scaling with the result that little or no silica is formed at the metal-oxide interface. Therefore, the oxidation rate compared with pure Cu is lowered only slightly and moreover the mechanism of oxidation is unchanged.

Because of the slower diffusivity of oxygen in Fe, silica tends to precipitate at the metal oxide interface to give some protection during oxidation. However, a solid-state reaction between iron oxide and silica occurs after a comparatively short time depending on the temperature, and the resulting iron silicate is sufficiently conducting to give a fairly rapid scaling rate. The extent of subscale formation in Fe-Si alloys suggests that the diffusivity of oxygen in Fe is much faster than is commonly supposed.

By the use of controlled oxygen pressures it is possible to selectively oxidize Si to form silica on the surface which may give some measure of protection. The conditions for this selective oxidation can be estimated reasonably from a knowledge of diffusivities of oxygen and Si in the metal. Preliminary experiments with higher Si-Cu alloys have demonstrated that a considerable improvement in oxidation resistance can be obtained in this way.

In an Fe-Si alloy it is a relatively easy matter to produce silica only, but as soon as normal oxidation occurs some iron oxide must form and consequently the highly protective silica is converted into the much less protective iron silicate.

Acknowledgment

Thanks are due to the Morgan Crucible Company Limited, London for financial support of this work. The authors are grateful to Dr. O. Kubaschewski for useful discussion.

Manuscript received Jan. 14, 1959.

Any discussion of this paper will appear in a Discussion Section to be published in the June 1960 JOURNAL.

REFERENCES

1. L. B. Pfeil, *J. Iron Steel Inst.*, **119**, 501 (1929).
2. A. Portevin, E. Pretet, and H. Jolivet, *ibid.*, **130**, 219 (1934).
3. E. Scheil and K. Kiwit, *Arch. Eisenhuttenw.*, **9**, 405 (1936).
4. T. Mishima and M. Sugiyama, *Tetsu to Hagane*, **36**, 184, 263, 317, 495 (1950).
5. V. V. Ipatev and O. M. Orlova, *J. Appl. Chem. U.S.S.R.*, **29**, 881 (1956).
6. R. F. Tylecote, *J Inst. Metals*, **78**, 259 (1950).
7. A. Preece and J. P. Dennison, *ibid.*, **81**, 229 (1953).
8. F. N. Rhines, W. A. Johnson, and W. A. Anderson, *Trans. A.I.M.E.*, **147**, 205 (1942).
9. G. Valensi, *Rév. Met.*, **45**, 10 (1948).
10. Feitknecht, *Z. Elektrochem.*, **35**, 142 (1929).
11. W. J. Moore and B. Selikson, *J. Chem. Phys.*, **19**, 1539 (1951).
12. M. H. Davies, M. T. Simnad, and C. E. Birchenall, *J. Metals*, 889 (October 1951).
13. L. Himmel, R. F. Mehl, and C. E. Birchenall, *ibid.*, **5**, 827 (1953).
14. H. Dünwald and C. Wagner, *Z. Phys. Chem.*, **B22**, 212 (1933).
15. L. S. Darken, *Trans. A.I.M.E.*, **150**, 157 (1942).
16. Metals Reference Book, C. J. Smithells, Editor, **2**, 533-560, Butterworth, London (1955).
17. A. Bramley, J. Heywood, W. R. Cooper, and O. P. Watts, *Trans. Faraday Soc.*, **31**, 707 (1935).
18. L. Himmel, R. F. Mehl, and C. E. Birchenall, *ibid.*, 1064 (1958).
19. B. Ellingsaeter and T. Rosenqvist, *J. Metals*, 1111 (August 1956).

Translucent Phosphor Coatings in High-Pressure Mercury-Vapor Lamps

C. H. Haake

Lamp Division, Westinghouse Electric Corporation, Bloomfield, New Jersey

ABSTRACT

The optical conditions in quasi-infinitely thick phosphor plaques and in translucent phosphor coatings of closed lamps are studied. Theory shows, and experiments carried out on magnesium fluorogermanate phosphors activated with Mn confirm, that the correlation between the brightness of plaques and of translucent coatings in closed lamps is rather involved. Although prolonged phosphor firing time monotonically increases the former, the latter reaches a maximum and then decreases. This and other unpredictable results render dubious the value of crude plaque brightness tests of phosphors meant for translucent coatings in lamps. Reliable measurements of phosphors for such coatings must include for the main wave lengths of excitation relative quantum efficiencies, reflectances of quasi-infinitely thick phosphor layers, and also differential reflectivities or absorptivities in a thin phosphor layer of a known density.

The intensity of the visible radiation from the discharge in high-pressure mercury-vapor (HPMV) lamps is about 60% of that of the ultraviolet radiation (1). Therefore, HPMV lamps are good light sources; however, they exhibit a radiation deficiency in the red region of the spectrum. To correct for this deficiency the outer bulb of HPMV lamps is often coated with a layer of an ultraviolet-absorbing, red-emitting phosphor (Fig. 1). The layer is kept so thin that an excessive loss of visible radiation is avoided and yet radiation is added in the red region of the spectrum which amounts to about 8% of the total luminous output of the lamp. (In the future, for the sake of simplicity, we will refer to the radiation of this part of the spectrum as "red-lumens".) Typical such phosphors are magnesium fluorogermanate (2) and magnesium arsenate (3) both activated with manganese.

An inherent difficulty when preparing these phosphors is the judgment of their expected performance. Ultimately one is interested only in the behavior of the phosphor in a coated lamp. Phosphor tests in lamps, however, are rather tedious and in practice one usually restricts the tests to the very conveniently and quickly carried out plaque brightness measurements (emission brightness of quasi-infinitely thick phosphor layers for given excitation conditions) (4). This method is sensible only if a direct correlation exists between the plaque brightness and the red emission of phosphor coatings in a finished lamp such that an increase of the former is concomitant to an increase of the latter.

The purpose of this study is the investigation of the

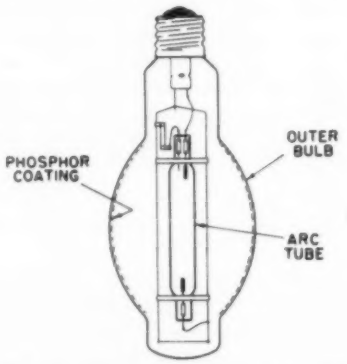

Fig. 1. High-pressure mercury-vapor lamp (Westinghouse JH-1, 400 watts).

behavior of thin phosphor layers in HPMV lamps. Equations which govern the emission from such layers are derived and discussed on the basis of experimental findings obtained from a Mn-activated magnesium fluorogermanate phosphor (MFG) in a Westinghouse 400-watt HPMV lamp. Particular interest is directed toward any possible significance of plaque brightness measurements on phosphors to be used in HPMV lamps.

Theory

The optical conditions of translucent phosphor coatings on plane substrates have been described and discussed by several authors (5, 6). The pertinent equations for the reflectance, transmittance, and absorptance[1] apply to grainy phosphor layers whose thickness is much larger than the average particle size of the phosphor crystals. The average density of the phosphor coating in HPMV lamps is about 1-2 mg/cm^2 and the particle size usually ranges from 3 to 5 μ. However, the particles in the layer do not arrange themselves in anything near a close-packed structure. When viewed under a microscope the layer appears porous and mountainous. The estimated average elevation of the phosphor layer over the surface of the bulb wall is about 30 μ. The coated bulb shows a fair degree of optical scattering and very little transparency. It seems, therefore, that in good approximation the existing equations for translucent phosphor coatings are also applicable to the present case. It will be assumed further that the reflection of the glass substrate for the exciting radiation is much smaller than that from the grainy layer and, therefore, can be neglected.

We will first present the equations for the reflectance, R, the transmittance, T, and the absorptance, A, of plane translucent phosphor coatings (6).

$$R = \frac{(r/p)\sinh(ps)}{\cosh(ps) + [(a+r)/p]\sinh(ps)} \qquad [1]$$

$$T = \frac{1}{\cosh(ps) + [(a+r)/p]\sinh(ps)} \qquad [2]$$

and

$$A = 1 - R - T \qquad [3]$$

where

$$p = \sqrt{a^2 + 2ar} \qquad [4]$$

The layer thickness is given by s, measured either in cm or mg/cm^2. The optical properties of the layer material are described by an absorptivity a and a reflectivity r, both measured either in cm^{-1} or in cm^2/mg, since as and rs are dimensionless arguments. These are the coefficients of absorption and reflection for a phosphor layer of the thickness ds. For practical purposes it is convenient to relate a and r to an easily measurable quantity, the reflectance, R_∞, of a quasi-infinitely thick phosphor layer. In this case $\sinh(ps) = \cosh(ps)$ and Eq. [1] gives

$$R = R_\infty = \frac{r}{p + a + r}$$

from which follow

$$\left.\begin{aligned} \frac{r}{a} &= \frac{2R_\infty}{(1-R_\infty)^2} \\ \frac{a}{p} &= \frac{1-R_\infty}{1+R_\infty} \\ \frac{r}{p} &= \frac{2R_\infty}{1-R_\infty^2} \end{aligned}\right\} \qquad [5]$$

If a thin phosphor layer is applied to the inside wall of the outer bulb of a HPMV lamp, any exciting radiation reflected from the layer will reach the layer somewhere on the opposite side of the bulb, etc. Hence, the effective transmittance of exciting radiation through the bulb becomes approximately

$$\tau = T\sum_{i=0}^{\infty} R^i = T/(1-R) \qquad [6]$$

With Eq. [1], [2], and [5] using exponential terms one finds

$$\tau = \frac{1 + R_\infty}{R_\infty \exp(-ps) + \exp(ps)} \qquad [7]$$

It is realized that the sum in Eq. [6] is somewhat affected by the uncoated portions of the bulb and the interior parts of the lamp. This effect, however, is small and will be neglected in the calculation, although later in this paper some comments will be made on this matter.

The effective absorptance of the phosphor coating on the bulb is

$$\alpha = 1 - \tau \qquad [8]$$

If $N(\lambda)$, the number of quanta per sec. emitted in the discharge line at λ, the effective absorptances $\alpha(\lambda)$ of the coating and the quantum efficiencies $\eta(\lambda)$ of the phosphor are taken into account, the total quantum emission, I_L of the phosphor coating becomes

$$I_L = \sum_i N(\lambda_i)\,\eta(\lambda_i)\,\alpha(\lambda_i) \qquad [9]$$

On the other hand, the quantum emission of a quasi-infinitely thick phosphor layer under the same excitation conditions is

$$I_p = \sum_i N(\lambda_i)\,\eta(\lambda_i)[1 - R_\infty(\lambda_i)]\cdot F(\lambda_i) \qquad [10]$$

$F(\lambda_i)$ is the ratio of the radiation generated to the radiation actually escaping the phosphor layer on the side on which the exciting radiation is incident. In the special case of MFG:Mn phosphors the quantum emission I_p is proportional to the plaque brightness since the emission spectrum is independent of the wave lengths of excitation (2).

Experimental Data

For a quantitative discussion of the equations and the dependence of their parameters on the preparation conditions of MFG:Mn, five phosphor samples of the same composition (3.5MgO, 0.5MgF_2, 1GeO_2, 0.01Mn) were studied. These samples were drawn from a large batch:

[1] These equations in a general form were originally derived by Schuster (7) although not specifically for phosphor powders.

Sample A: after 2 hr firing at 1100°C in air

Sample B: after 3 hr ball milling of sample A

Sample C: after 20 hr refiring of sample B at 1100°C in air

Sample D: after 12 hr refiring of sample C at 1100°C in air

Sample E: after 14 hr refiring of sample D at 1100°C in air.

Numerous quantities were measured:

(*a*) The relative plaque brightness, I_p (λ), of the quasi-infinitely thick phosphor layers for $\lambda = 254$, 313, 365, 405, and 436 mμ as exciting wave lengths; (*b*) the reflectance, R_∞ (λ), of the same phosphor layers for the same wave lengths as in (*a*); (*c*) the relative total lumens, I_T; and (*d*) the relative red lumens, I_R, of a HPMV arc tube with phosphor-coated bulbs; (*e*) the relative total lumens, I_{T_∞}, of the same HPMV arc tube with an uncoated bulb; (*f*) the effective transmittance, $\tau(\lambda)$, of the exciting Hg-lines through the coated bulbs; (*g*) the density, s, of the phosphor coating on the bulbs.

Methods of Measurement

(*a*) *and* (*b*).—The arc tube of a 400W HPMV lamp (Westinghouse EH-1) served as excitation source whose lines were selected and transmitted through an ultraviolet monochromator onto a thick phosphor layer. The emitted radiation, $I_p(\lambda)$, was measured as photocurrent from a photomultiplier (RCA 1P28). A cut-off filter prevented the exciting radiation from entering the photomultiplier. After this filter was exchanged for one which transmits only the exciting radiation, the reflected radiation was measured as photocurrent. The container with the phosphor was then replaced by a similar one filled with MgO and the photocurrent was read again. Multiplication of the ratio of the former reading to the latter by 0.95 (averaged reflectance of MgO in the wave-length range of interest) gave the reflectance, $R_\infty(\lambda)$, of the phosphor. The plaque brightness, $I_p(\lambda)$, is proportional to the quantum efficiency, $\eta(\lambda)$, to the exciting radiation absorbed in the phosphor layer, $1 - R_\infty(\lambda)$, and to the ratio $F(\lambda)$ (see Eq. [10]). An expression for F has been derived by Coltman, *et al.* (5) which, for thick phosphor layers, becomes

$$F(\lambda) = \frac{1}{2} \cdot \frac{1 + R'_\infty(\lambda)}{1 + p'(\lambda)/p(\lambda)}$$

The primed quantities are those for the emitted radiation. It could be shown that for the five samples studied $F(\lambda)$ did not change by more than 1% at any one particular wave length of excitation. Since in the following the quantum efficiencies η are given relative to those of sample E, the ratio $F(\lambda)$, therefore, need not be considered here.

(*c*), (*d*) *and* (*e*).—Each phosphor sample was ball milled in an equal amount of nitrocellulose for a given length of time under the same conditions. BT-37 bulbs (as used in Westinghouse 400W JH-1 and EH-1 lamps) were coated and lehred for 10 min at about 600°C. They were then sleeved over an EH-1 arc tube mounted in a 60 in. integrating sphere. The arc tube itself was sealed into a slender quartz tube. Relative lumens were measured in a conventional way Weston Photronic cell + Viscor filter #594 Y.R.V., for total lumens and Weston Photronic cell + Viscor filter #594 Y.R.V. + Corning filter #2418 for red lumens).

(*f*).—A double-monochromator with a photomultiplier (RCA 1P28) at its exit slit was placed in front of a small hole in the integrating sphere. A baffle in the sphere shielded the hole from direct light from the lamp. For $\lambda = 313$, 365, 405, and 436 mμ, photocurrent readings were taken with the coated bulbs and a clear bulb in place, respectively. The ratio of the two readings gave the effective transmittance, $\tau(\lambda)$, through the phosphor coated bulb. Since the bulb glass does not transmit the 254 mμ line, $\tau(254)$ could not be measured.

(*g*).—After completion of the measurements (*c*) to (*f*) the total amount of phosphor in each bulb was recovered and weighed. The weight divided by the known area coated (500 cm^2) gave the coating density, s, in mg/cm^2.

The data obtained are shown in Table I, II, and III. The first six columns of Table II show the sample identification; the wave length of excitation, λ; the plaque brightness, I_p; the reflectance, R_∞; the effective transmittance, τ; and the relative quantum efficiency, η, respectively. Since from samples A to E only the relative changes of the values measured or computed are of interest, I_p and η of the sample E were arbitrarily chosen to be 1.00 regardless of the wave length of excitation. In the 7th and 8th column are shown the differential absorptivity a, and the differential reflectivity, r, which one obtains from Eq. [5] after determining p by inserting s (Table I), τ and R_∞ in Eq. [7]. In the 9th column is tabulated $\eta\alpha = \eta(1 - \tau)$. These values show how for each wave length of excitation the emission intensity of the coating in the lamp changes from phosphor A to phosphor E. Since the varying density of the coating with phosphors A to E, as encountered here for experimental reasons, does not lend itself to arriving at general conclusions, one can compute the values of $\eta\alpha$ (listed in Table II as $\eta\alpha^*$) using η, a, τ, and R_∞ as determined earlier, and $\bar{s} = 1.290$ mg/cm^2 as mean coating density. If large numbers of lamps were to be prepared with phosphors A to E in the coatings, small variations of the density would cancel out and the averaged values of $\eta\alpha$ for each phosphor at each wave length of excitation would be $\eta\alpha^*$. Likewise on the basis of an averaged density $\bar{s} = 1.290$ mg/cm^2 computed values of τ are listed in the 11th column as τ^*.

It should perhaps be explained at this point to what extent the values of a, r, and particularly τ^*

Table I. Density, s, of the phosphor coatings

Phosphor	s (mg/cm^2)
A	1.385
B	1.235
C	1.190
D	1.310
E	1.330

Table II. Measured and computed data for phosphors and phosphor coatings

Samples	λ (mμ)	I_p	R_∞	τ	η (rel.)	$a\left(\frac{cm^2}{mg}\right)$	$r\left(\frac{cm^2}{mg}\right)$	ηa	ηa^*	τ^*
A		0.88	0.38	—	0.91	—	—	—	—	—
B		0.90	0.38	—	0.93	—	—	—	—	—
C	254	0.98	0.37	—	0.99	—	—	—	—	—
D		0.99	0.37	—	1.00	—	—	—	—	—
E		1.00	0.36	—	1.00	—	—	—	—	—
A		0.84	0.19	0.15	0.89	1.0	0.60	0.75	0.74	0.17
B		0.85	0.20	0.18	0.90	1.0	0.64	0.74	0.75	0.17
C	313	0.97	0.17	0.23	0.99	0.97	0.46	0.76	0.79	0.20
D		0.98	0.16	0.22	0.99	0.92	0.42	0.78	0.77	0.22
E		1.00	0.15	0.21	1.00	0.95	0.39	0.79	0.78	0.22
A		0.73	0.64	0.59	0.85	0.15	1.5	0.34	0.32	0.62
B		0.72	0.66	0.61	0.88	0.15	1.7	0.35	0.36	0.59
C	365	0.89	0.62	0.66	0.97	0.15	1.3	0.33	0.36	0.63
D		0.94	0.60	0.63	0.97	0.15	1.2	0.36	0.35	0.64
E		1.00	0.59	0.65	1.00	0.15	1.0	0.35	0.34	0.66
A		0.76	0.61	0.67	0.86	0.13	1.1	0.28	0.27	0.69
B		0.77	0.63	0.68	0.90	0.14	1.2	0.29	0.31	0.66
C	405	0.93	0.58	0.73	0.96	0.14	0.90	0.26	0.29	0.70
D		0.95	0.57	0.72	0.96	0.13	0.82	0.27	0.26	0.73
E		1.00	0.57	0.74	1.00	0.12	0.74	0.26	0.25	0.75
A		0.71	0.64	0.65	0.86	0.13	1.3	0.30	0.27	0.69
B		0.72	0.64	0.67	0.87	0.13	1.3	0.29	0.30	0.66
C	436	0.88	0.61	0.74	0.97	0.13	0.99	0.26	0.28	0.71
D		0.94	0.58	0.71	0.97	0.13	0.87	0.28	0.27	0.72
E		1.00	0.57	0.73	1.00	0.13	0.76	0.27	0.26	0.74

and ηa^* are affected by the somewhat idealistic assumption that no exciting radiation reflected from the phosphor coating into the lamp is lost for the process of interreflections, either by absorption in lamp parts or by transmission through the uncoated end parts of the lamp. Actually these losses do occur to some extent and they modify the equations slightly. It can be shown that the values of a and r are somewhat lower than those appearing in Table II. Conversely, within the accuracy desired, the values of τ^* and ηa^* remain unchanged. This is because p (and thence a and r) is obtained from the inverted Eq. [7]. Later after this equation has again been inverted one finds τ^* and thence ηa^* using an average coating thickness $\bar{s}$. Thus a modification of Eq. [7] due to losses has virtually no effect on τ^* and ηa^*.

In Table III are shown the red lumen percentages (based on the total lumens of a clear lamp as 100) of the coated bulbs, and also the per cent loss of total lumens due to absorbed visible radiation in the coating.

Discussion and Conclusion

It can be seen from Eq. [10] that, for constant quantum efficiencies $\eta(\lambda)$, the plaque brightness *increases* with decreasing reflectances $R_\infty(\lambda)$. On the other hand, an analysis of Eqs. [5] and [7]-[9] shows that, again for constant $\eta(\lambda)$, the emission from a phosphor bulb of a HPMV lamp *decreases* with decreasing reflectance, if, as often is the case, the absorptivity a remains essentially unchanged. This adverse trend of I_p and I_L rules out any meaningful judgment of phosphors based on measurements of plaque brightness, a method which still is widely practiced for selecting phosphors to be used in HPMV lamps [see, e.g., Ref. (4)]. Thus, if one were to choose certain conditions for preparing phosphors merely guided by plaque brightness measurements, phosphors might be discarded which would exhibit an excellent performance in translucent coatings on bulbs, and vice versa.

Table III. Lumen ratios of coated bulbs

Phosphor	$100\ I_R/I_{T_\infty}$	$100\ (1 - I_T/I_{T_\infty})$
A	8.5	5.0
B	8.7	5.0
C	8.6	2.5
D	8.9	2.5
E	9.0	2.5

Also in the present case the reflectances $R_\infty(\lambda)$ decrease (from B to E). At the same time, however, the efficiencies $\eta(\lambda)$ increase. Thus with prolonged firing time ηa^* and, hence, the red lumens emitted from a coated bulb should approach a maximum and then decrease. This maximum is concealed in the values of ηa and I_R/I_{T_∞} shown in Table II and Table III, because in the present experiments the coating thickness could not be held constant from A to E. However, the maximum clearly appears in the values of ηa^* as computed for a constant coating thickness. In order to further substantiate this result we coated eight bulbs with MFG:Mn phosphor which had been fired for 10 hr and for 48 hr, respectively. When we measured the red lumen percentage, we actually found a decrease from (9.9 ± 0.1) % for the phosphor fired for 10 hr to (9.2 ± 0.3) % for the phosphor fired for 48 hr. It, therefore, becomes apparent that a limited firing time is required for the

phosphors to obtain optimum performance. There is, however, also the requirement of as high a transmission through the coating for the visible radiation of the discharge as possible. As can be seen from the values of I_T/I_{T_∞} in Table III this transmission increases slightly from phosphors B to E with firing time, but it soon reaches a saturation at a point where the latter requirement may no longer be conflicting with the former.

There is another interesting phenomenon. The reflectance R_∞ at 405 mμ (violet) and 436 mμ (blue) decreases from phosphors B to E. This is tantamount to an increasing yellowish body color of the phosphors which usually is considered objectionable. When used for coatings in HPMV lamps the phosphor will absorb violet and blue radiation of the discharge which is needed for good color rendition. Since phosphor E exhibits a yellowish body color deeper than that of B, one is lead to believe that also in a thin coating phosphor E should show effective transmittances for violet and blue light which are lower than those of phosphor B. It is interesting to note from the values of τ^* in Table II that just the opposite holds true: τ^* (405mμ) and τ^* (436 mμ) *increase* from B to E. This seemingly odd behavior can again be explained by Eqs. [5] and [7]. Since the reflectances $R_\infty(\lambda)$ decrease from B to E and the absorptivities virtually do not change, p in Eq. [5] decreases and, hence, τ in Eq. [7] increases.

For the purpose of achieving good uniformity of the phosphor the MFG:Mn was ball milled between the first and second firing (sample B). Small pebbles were used whose main action was the breakage of agglomerates. This, as can be seen in Table II, leads to an increase of the reflectance, R_∞, to a decrease of the effective transmittance, τ^*, and hence to an increase of the effective absorptance, α^*, of the phosphor coatings. Since also the quantum efficiencies increase, one can expect a rather strong increase of $\eta\alpha^*$ and of red lumens emitted from the phosphor coating. In fact, phosphor B gives the highest values of $\eta\alpha^*$ for $\lambda_{ex} = 365$, 405, and 436 mμ. The increase of η induced by ball milling is rather surprising, as ball milling has a detrimental effect on other phosphors, particularly those of the ZnS type (8). At this time we cannot offer more than a suggestion as to the reason for the increase in η. The arrangement of the oxygen ions which surround the emitter ion (Mn^{++}) has a strong effect on the efficiency, η, of quantum conversion in the center. Any distortion of the system, possibly frozen in after firing, can result in a small η. It seems feasible that such internal strains are released during mild ball milling of the phosphors.

Summary

Translucent coatings of MFG:Mn phosphors such as are used for color correction in HPMV lamps exhibit performance parameters markedly different from those obtained with quasi-infinitely thick phosphor plaques. By firing the phosphor for a prolonged period of time the emission intensity of the coating increases to a maximum value and then decreases, whereas the emission intensity of the phosphor plaques increases monotonically.

Prolonged firing time will also lead to an increasingly yellow body color of the phosphor plaque, i.e., to an increasing absorption of violet and blue light. Contrary to this, the translucent phosphor coatings in lamps exhibit an increasing effective transmittance for the violet and the blue mercury lines with increasing firing time.

Therefore, a valid judgment of phosphors which ultimately will be used in translucent coatings of HPMV lamps cannot be based on simple plaque brightness measurements. It is mandatory to determine various phosphor parameters whose evaluation will result in the optimum preparation conditions of the phosphor, or to coat bulbs, sleeve them over the same arc tube, and measure the red lumen output.

Manuscript received March 23, 1959.

Any discussion of this paper will appear in a Discussion Section to be published in the June 1960 JOURNAL.

REFERENCES

1. W. Elenbaas, "The High Pressure Mercury Vapor Discharge," North Holland Publishing Co. (1951).
2. L. Thorington, *J. Opt. Soc. Amer.*, **40**, 579 (1950).
3. H. A. Klasens, *Philips Res. Repts.*, **9**, 377 (1954).
4. K. H. Butler and R. W. Mooney, *Sylvania Technologist*, **9**, No. 4 (1956).
5. J. W. Coltman, E. G. Ebbighausen, and W. Altar, *J. Appl. Phys.*, **18**, 530 (1947).
6. I. Broser, *Ann. Physik*, **5**, 401 (1950).
7. A. Schuster, *Astrophys. J.*, **21**, 1 (1905).
8. N. Riehl and H. Ortmann, *Ann. Phys.*, **29**, 556 (1937).

The Use of Organo-Substituted Hydrolyzable Silanes on Silicon Devices

B. Schwartz

Hughes Semiconductors, Newport Beach, California

ABSTRACT

The formation of silicone polymers directly from the monomers, on the surface of silicon diodes, has resulted in devices with low reverse currents. Transistors treated in this way react in different ways due to the conditions imposed by the specific surface potentials involved.

Silicone resins, varnishes, and greases have been used in the fabrication of semiconductor devices, since these materials provide a hydrophobic environment for the device and at the same time have the thermal stability necessary for proper operation. All these materials are in a polymeric form prior to application to the device. This paper concerns techniques for forming a silicone polymer directly on the surface of the device by the use of organo-substituted hydrolyzable silanes so that enhanced electrical properties result (1).

The general formula for an organo-substituted hydrolyzable silane, which is the starting point from which all silicones are derived (2), is $R_{4-i}SiX_i$ ($i=1, 2, 3,$), while R is an organic radical. For use on semiconductor devices a short-chain hydrocarbon is preferred, since the shorter the chain, the better the thermal stability. The X refers to the hydrolyzable part of the compound and can be a halide, ethoxide, or other radical which will react with water.

In order to see how a silicone polymer is formed from this class of compounds, consider the hydrolysis of the difunctional reagent dimethyldichlorosilane. In the presence of water this compound reacts spontaneously to form dimethyldihydroxysilane and HCl. The dimethyldihydroxysilane is unstable, and by intermolecular dehydration a silicone polymer is formed which in this case would be polydimethylsiloxane. Compounds also are available with either 1 or 3 organic radicals in the so-called monomer, so that not only can linear polymers be made, as just described, but space polymers can be realized also by having some trifunctional silane present during the reaction.

In the case of the ethoxy system, the reaction with H_2O is not so straightforward, and one must provide either an acidic or basic medium for the hydrolysis to proceed. Since most of the silicon device work to be reported on here was done using the chlorosilanes, all reference is to this system. Somewhat analogous results were obtained when the ethoxy system was used in place of the chloro system.

Methods and Results

The techniques that one might use in forming the silicone on the surface are: (*a*) exposure of a premoistened unit to the vapors of the silane mixture (3); (*b*) total immersion of the unit in the silane mixture itself; and (*c*) immersion of the unit in a solution of the silane mixture. The method of total immersion in the silane mixture has given the best results, and this technique is the one preferred to during the rest of this paper.

Figure 1 shows the effect of silaning on the electrical characteristics of a grown p'n silicon junction. Curve A illustrates the reverse diode characteristics of the unit before etching where the crystal surface contained a good deal of work damage. Curve B illustrates the junction properties after the unit had been acid etched to remove the work damage and baked at 200°C for 15 min. Curve C shows the properties of the same junction after it had been silaned with a mixture of methyl and phenyl chlorosilanes and baked for 1 hr at 250°C. In this particular measurement no attempt was made to reach the full breakdown voltage of the unit, since this device was to be used for a special series of surface experiments which required only a 500 v or better peak inverse voltage.

In Table I the reverse characteristics of 10 experimental large-area evaporative-fused-junction p'n silicon diodes are listed. E_b and E_r are the voltages necessary to pass 2 and 10 μa, respectively, in the reverse direction; I_b is the reverse current measured at 125 v. For the silaning operation a 50-50 mixture

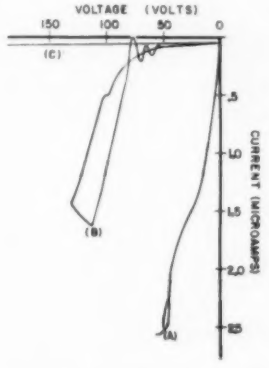

Fig. 1. Reverse characteristics of a group p+n silicon junction diode (A) before etching, (B) after etching in a mixture of hydrofluoric acid and nitric acid, and (C) after silaning.

Table I.

After standard treatment			Silaned with 50% dimethyldichlorosilane-50% methyltrichlorosilane and baked at 100°C for ½ hr		
E_a, v	E_b, v	I_b, mμa	E_a, v	E_b, v	I_b, μa
20	10	>50,000	500*	500*	21
4	2	>50,000	30	10	>50,000
8	3	>50,000	500*	500*	20
500	440	36	500*	500*	21
10	4	>50,000	500*	500*	21
52	20	>50,000	440	400	25
340	320	500	500*	500*	25
14	6	>50,000	32	14	>50,000
4	2	>50,000	500*	500*	22
8	2	>50,000	150	75	5,000

of dimethyldichlorosilane and methyltrichlorosilane was used. One should not attempt to compare the individual units in this table, since they were not tabulated in the same order before and after silaning. Notice that where originally there was only 1 unit with a reverse current less than 100 mμa, there were 7 units with reverse currents of less than 100 mμa after silaning. Again, these units were not tested above 500 v. Other units, similarly treated, were taken out to breakdown, and no adverse effects were noticed unless too much current was allowed to pass in the reverse direction.

Table II shows the necessity of a curing cycle to bring out the improvement in diode properties after silaning. The units were not kept in order so that individual comparisons are not valid. Here again a 50-50 mixture of methyl and dimethylchlorosilanes was used for surface treatment. Initially there were only 3 units that had reverse currents of 220 mμa or less. After silaning, but prior to baking, all the units had poor characteristics; but after baking for ½ hr at 100°C, there were 7 units with reverse currents of 220 mμa or less; in fact, 6 of the units showed less than 50 mμa reverse current.

Heat Treatment and Stability

Some experiments were performed to establish the influence of the baking part of the silane-treatment cycle without the silanes having been applied. Table III shows the results of an experiment where a lot of approximately 700 units, which had been processed simultaneously, was arbitrarily divided in two, and only one half were silaned, using a mixture of mono-, di-, and tri-methylchlorosilanes. Both sets

Table II.

After standard treatment	I_b mμa After silaning but no baking	After silaning and baked at 100°C for ½ hr
100	>50,000	2,000
120	>50,000	50
>50,000	>50,000	30
>50,000	25,000	220
>50,000	>50,000	>50,000
>50,000	>50,000	>50,000
220	12,000	26
>50,000	>50,000	30
>50,000	>50,000	23
>50,000	33,000	20

Table III.

I_b μa, silaned	I_b mμa, control	Percentage less than stated I_b
17	1120	10
24	2000	20
46	4440	50
190	5200	90

of units then were baked at 200°C for 2 hr.

It was also established by experimentation that prolonged air baking, of the order of hours, (i.e., 3 hr or more), at elevated temperatures (approximately 200° to 250°C) would result in improved devices, without silaning, but the reproducibility was poor and further heating might very well cause the units to deteriorate appreciably. Therefore, it is felt that the improvements noted after silaning were due to the formation of the silicone film on the surface of the device and were not merely the result of baking the unit for the stated periods.

Some silaned transistors which have been aging in air for more than two years since they were treated were retested recently. The emitter and collector diode reverse currents on these units were found to be essentially the same as when the units were first silaned, indicating a good stability factor for this type of treatment.

The thermal stability of silaned units was investigated by aging the units at elevated temperatures and periodically checking the reverse current for degradation. At 250°C and below, no noticeable degradation took place; in fact, if anything, the units improved. At 300°C degradation appeared after about 8½ hr of aging. For 350°, 375°, and 400°C, the times for the onset of degradation were approximately 6½ hr, 3½ hr, and ½ hr, respectively.

The solvent resistance of the silaned units was investigated by boiling the units in various solvents for 5 to 15 min, again using the diode reverse current as the indicator of stability. If the units were not properly cured before being exposed to the solvent, degradation was immediate and universal. If the units were cured properly, then boiling in acetone, carbon tetrachloride, benzene, methyl alcohol, or trichloroethylene had no adverse effect.

Surface Channels and Surface Recombination Velocity

In Fig. 2 the effect of silaning on channels (4) on a fused-junction rectifier is shown. To the left of the origin is the p-region and to the right is the n-region. Figure 2A is a plot of the photoresponse of the freshly etched silicon rectifier as a function of distance. The sharpness of the peak indicates the absence of a channel. Figure 2B is a plot of the photoresponse of the same diode after it had been allowed to age in air for two weeks. The channel-type response over the n-region, indicating p-type conversion at the surface, can readily be seen. In Fig. 2C the photoresponse of the same diode is plotted after re-etching and silaning. In Fig. 2D the photoresponse of the same silaned unit after it had been allowed to age in air for six months is plotted; notice the absence of the channel.

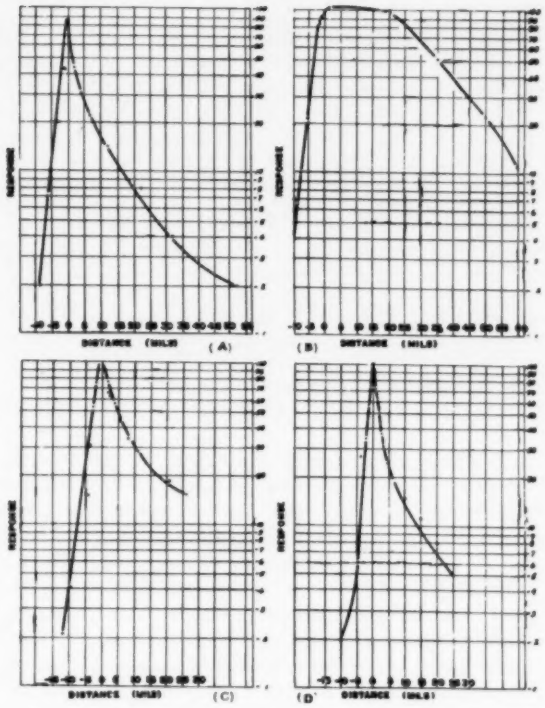

Fig. 2. Photoresponse of a fused p'n silicon junction diode as a function of distance from the junction.

A few experiments have been performed where the surface recombination velocity (s) of silicon filaments was measured before and after silaning. Improvement of s was noted, but stability was quite poor and degradation to the initial value occurred within 6 hr. When this treatment was tried on p-n-p transistors, units made by a diffusion technique showed improvement in the current amplification factor while evaporative fused junction transistors degraded in this parameter. These results can be explained on the basis that silaning causes the surface potential to become more positive, i.e., more n-type, a fact which can be seen by observing the results in Fig. 2 and which was verified in a gas cycling study (5). If the surface potential of the base region of the evaporative fused junction transistor is about −0.15 e.v.[1] and considering the relationships between current amplification factor, surface recombination velocity, and surface potential (6-9), then one can, by increasing ϕ_s, produce a decrease in the current amplification factor. It is believed, though, that the base region of the diffused device has a surface potential high enough (i.e., strongly n-type), due to the high doping density at the surface, that the "bell-shaped" functional relationship between surface recombination velocity and surface potential actually can result in an improvement in the current amplification factor by increasing the surface potential. The amount of change in surface potential due to silaning has not been measured as yet, so that more quantitative results cannot be stated at this time.

It has been observed that the structure of the polymer has an important influence on the resulting properties of the device. Long-chain polymers appear to reduce reverse currents more than short-chain systems. Also, stability appears to be structure dependent, and the presence of a tri-functional compound in the system seems to aid in achieving more stable properties in the units so treated. This agrees with the findings of Hall (10), who reports an actual bonding of the film that is formed into the surface of the substrate silicon when a tri-functional compound is present.

In conclusion, it is seen that when organo- substituted hydrolyzable silane monomers are polymerized on a silicon device, creating a silicon coating on the surface, the diode characteristics for the device can be improved. Furthermore, since this approach utilizes the so-called monomers of the silicones, additives and copolymerization agents can be chosen so as to produce additional benefits in semiconductor devices.

[1] "Channel" experiments in this laboratory always have shown conversion of type over the base region of these transistors. Preliminary experiments have shown that the surface potential is of this magnitude when the unit is allowed to age in air. These results will be published at a later date.

Acknowledgment

The author wishes to express his gratitude to Mrs. E. Lu for her assistance in this work, to Mr. A. Drasein for the data used in Table III, and to Mr. M. J. Barrett for the devices used in this study as well as his many helpful comments and suggestions.

Manuscript received June 2, 1958. This paper was prepared for delivery before the New York Meeting, April 27-May 1, 1958.

Any discussion of this paper will appear in a Discussion Section to be published in the June 1960 JOURNAL.

REFERENCES

1. B. Schwartz, U. S. Pat. 2,832,702, April 29, 1958; 2,854,358, Sept. 30, 1958; and 2,874,076, Feb. 17, 1958.
2. E. G. Rochow, "An Introduction to the Chemistry of the Silicones," John Wiley & Sons, Inc., New York (1946).
3. F. J. Norton, *General Electric Rec.*, **47**, p. 6 (1944).
4. A. L. McWhorter and R. H. Kingston, *Proc. I.R.E.*, **42**, 1376 (1954).
5. R. Solomon, Private communication.
6. W. M. Webster, *Proc. I.R.E.*, **42**, 914 (1954).
7. D. T. Stevenson and R. J. Keyes, *Physica*, **20**, 1041 (1954).
8. A. Many and D. Gerlick, *Phys. Rev.*, **107**, 414 (1957).
9. T. M. Buck and F. S. McKim, *This Journal*, **105**, 713 (1958), using a value of the order of 10^5 for the ratio of the capture cross section for holes to that of electrons.
10. T. C. Hall, Private communication.

Arc Decomposition of Rhodonite

Victor Harris, John D. Holmgren, Samuel Korman, and Charles Sheer

Vitro Laboratories, Division of Vitro Corporation of America, West Orange, New Jersey

ABSTRACT

A developmental pilot line for the arc treatment of Colorado rhodonite has been built and operated to investigate the applicability of the high-intensity arc process to the extraction of manganese from siliceous ores. The rhodonite is incorporated into 2-in. diameter electrodes to the extent of 75-85% by weight and vaporized in a d-c high-intensity arc operating in the range 40-60 kw. Vaporization in the arc decomposes the manganese silicate content of the rhodonite to MnO and SiO_2. The product is collected as a mixture of the respective oxides in finely particulated form. The manganese, now readily soluble, is leached from this mixture. The effects of significant process variables are discussed.

This paper describes the design and operation of a developmental pilot plant for the arc decomposition of Colorado rhodonite by means of a new process known as the Sheer-Korman "Hierarc Process" (1, 2). The primary purposes of this program were to demonstrate the technical feasibility of treating rhodonite and to obtain process design and evaluation data.

Rhodonite, a manganese silicate, is found in several sections of the United States and abounds in the southwestern area of Colorado. While deposits represent a significant quantity of Mn, the material is of such a refractory and stable nature that it has never been used as a major Mn source; instead it has been described as worthless gangue material in lead and zinc mining operations. Theoretically, pure rhodonite contains 42% Mn. Mined and milled in conjunction with lead-zinc operations, concentrates ranging up to 33, or perhaps 36% Mn, might be expected.

The Hierarc Process, utilizing the high-intensity arc, serves to decompose the manganese silicate into a mixture of two discreet, finely particulated materials, manganous oxide and silica. In this form, the Mn is readily dissolved by leaching. For example, over 95% of the Mn in samples of arc product dissolved in dilute HCl at room temperature.

Using an anode consisting of an homogeneous mixture of ore and carbon—the ore content may be as high as 80-85%—the high-intensity arc provides an effective means of heating the material to temperatures of decomposition without the necessity of heating crucibles or other containing vessels.

Elements of the Process

The rhodonite, ground to 100% minus 50 mesh, is mixed with carbon source materials, in this case coal and pitch. This mixture, with the addition of an extrusion aid material, is placed in an hydraulic press and ore-bearing electrodes are extruded. These are baked with a controlled schedule rising to a maximum temperature of 900°-1000°C. Electrodes of ⅝-in. diameter are completely baked within 2-3 hr, while 2-in. electrodes are baked 12-20 hr, depending on the desired characteristics.

The pilot plant was operated using electrodes 2 in. in diameter and 44 in. long. A direct current arc was used. Therefore, only the anode is ore-bearing; the cathode is a 1-in. diameter graphite rod. The baked electrode is placed in the arc chamber and the arc current applied. For this application the arc is operated in air at atmospheric pressure. Air, swept into the system, provides excess oxygen to the reaction, rapid quenching of the arc product gases, and arc product transport to the product collector. The arc chamber and product collector are shown schematically in Fig. 1. The simplicity of the system is evident.

Since in this application this process serves only as a means of decomposition, the Mn content of the product will usually be essentially the same as that of the feed material. Generally speaking, the values of recoveries, yields, and processing costs will remain about the same independent of the Mn concentrations in the feed. Over-all process economics, of course, are affected importantly by the Mn content of the feed material.

The arc chamber, 36 in. in diameter and 5 ft high, is ⅛-in. boiler plate; ducts are of 18-gauge galvanized iron. Air is swept into the chamber and circulated in such a way that the chamber wall temperatures do not exceed 200°F when operating at the normal level of around 50 kw.

The homogeneous electrode, being made largely of nonconductive material, has a relatively high electrical resistance, as much as two orders of magnitude greater than a pure carbon electrode. Therefore, to minimize power losses it is necessary to in-

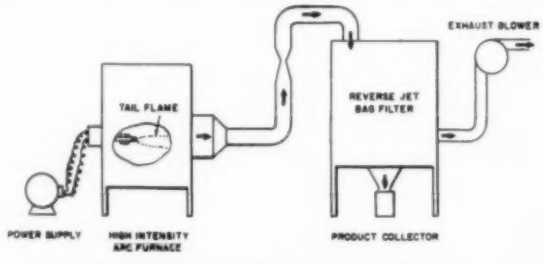

Fig. 1. Arc chamber and product collector

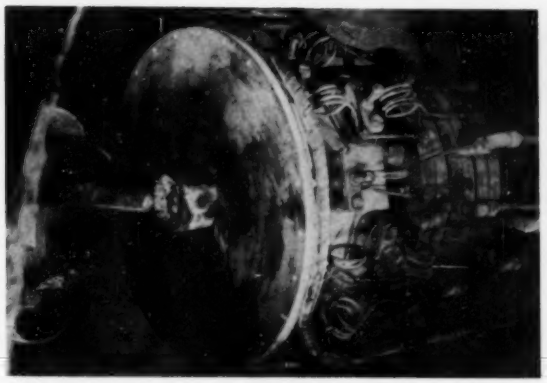

Fig. 2. Anode brush assembly showing anode crater. Graphite cathode can be seen as the smaller diameter electrode.

troduce the arc current as near to the arc crater as possible. A system of sliding brushes is used. Figure 2 shows the brush assembly and also provides a good illustration of the arc crater after the arc is extinguished. The brushes are water-cooled and spring loaded and in this case provided with replaceable graphite shoes. The round plate through which the 2-in. anode projects is water-cooled and electrically neutral, to shield the brush assembly from damage by the arc. The 1-in. cathode in its normal operating position can also be seen.

Operating Data

There are three dependent process variables of primary importance. These are: unit power consumption (in kwhr/lb of anode vaporized), erosion rate (in lb/hr of anode vaporized) and per cent slag (the ratio of the weight of spalled and melted material to the total weight loss of the electrode). These are affected most importantly by the following four independent process variables: anode carbon content (in per cent), arc current (in amperes), anode resistivity (ohm/cm^3), and anode apparent density (g/cc). A comprehensive investigation of the relations of these variables was carried out based on statistical analysis of the results of over 300 test runs. Some typical data are illustrated. Figure 3a shows the effect on unit power consumption of varying arc current and carbon content. This is for electrodes having a specific resistivity in the region of 0.05 ohm/cm^3 and density in the region of 1.75 (g/cc). The heavily inked portions of the curves represent the regions in which experimental data are available. The light portions represent the regions of statistical extrapolation. Curves which are entirely in light ink represent extrapolation of the results obtained with other carbon percentages.

Caution is necessary in viewing the extrapolated data, especially toward the extremes of their extension. They are useful primarily for indicating trends. Referring again to Fig. 3a, it cannot be said, for example, that a 10% carbon electrode can be processed at 300 amp with a unit power consumption of 1 kwhr/lb. However, it can be said that at lower currents the 10% carbon electrode will probably give better results than the higher carbon electrodes, while at higher currents the converse will be true.

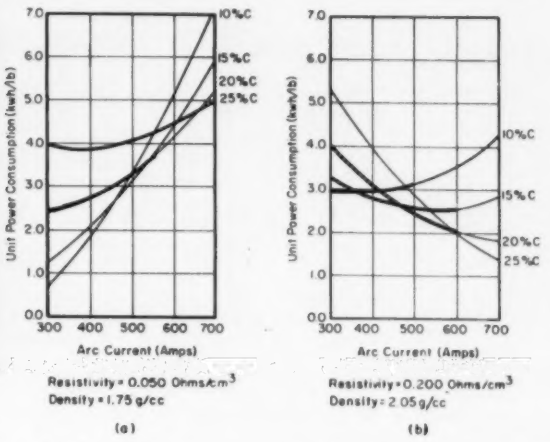

Fig. 3. Effect of arc current and carbon content on unit power consumption.

Figure 3b provides a comparison of the same factors for electrodes having a resistivity of about 0.2 ohm/cm^3 and a density of about 2 g/cc. The considerable difference in character of these curves is apparent. Improved performance is evident. Performance generally improves with current, and under these conditions a 20% carbon electrode provides better operation at higher currents than any of the electrodes in the previous figure.

A comparison of erosion rates can also be made in the same manner. Figure 4a shows the erosion rate for the low resistivity, low density type of electrode in terms of pounds of electrode vaporized per hour. It will be noted that at 600 amp the curves fall in the area below 10 lb/hr. In contrast Fig. 4b shows the same information for the high resistivity, high density anode. In this case it can be seen that at 600 amp operation is in the region of 20 lb/hr.

A similar comparison of per cent "slag" shows that the same conditions which tend to improve unit power consumption and erosion rate tend also to increase per cent slag. This material is not slag in the usual sense. It is material which either spalls from the electrode or melts and drips from the crater without being vaporized. Figure 5a shows the per

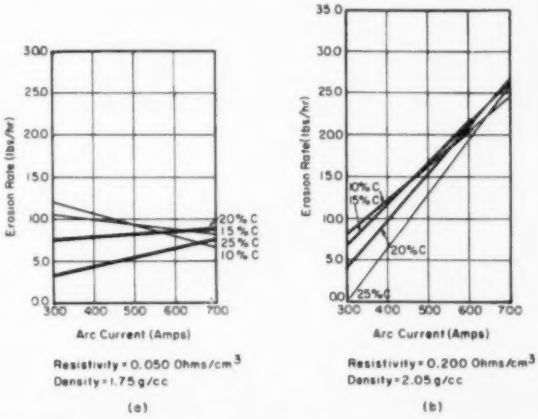

Fig. 4. Effect of arc current and carbon content on erosion rate.

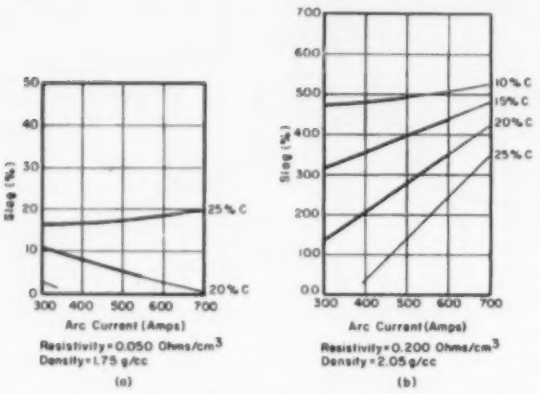

Fig. 5. Effect of arc current and carbon content on "slag" per cent.

cent slag for the low resistivity, low density electrode. The 20% carbon electrode, for example, falls entirely in the region below 10%. In Fig. 5b it is seen that, with the conditions that give better unit power consumption and erosion rate, slag is above 10%.

On the basis of these and other similar data a group of electrode characteristics were evolved as follows: apparent density in the region of 2, specific electrical resistivity in the range of 0.25 to 0.3 ohm/cm³, and carbon content in the range of from 16 to 18% after baking.

Electrodes of these characteristics were subjected to a series of runs extending over half-shift periods of about 4 hr. Typical results are shown in Table I.

Note that the slag per cent is lower than might have been expected from the statistical test results just discussed. This is because those test runs were short, involving considerable on-off operation and corresponding heating and cooling of the system. The sustained runs always exhibit better results and, of course, are more representative of production conditions.

Operations were not carried to the point of actually recycling this slag. However, with its recycling, Mn recovery in the process would be expected to approach 100%, since there is little true loss anywhere in the system. The ore used in these operations contained approximately 25% Mn. Before treatment, on the basis of analysis, over 90% of the Mn in the ore was in insoluble form. After treatment over 90% of the insoluble Mn was found to be converted to soluble form in the arc product.

Table I. Typical operational data

Current	700 amp
Power	50 kw
Anode feed	103 in./hr 24 lb/hr
Slag	16.5 % (wt)
Anode vaporized	20 lb/hr
Unit power consumption (d-c side of generator)	2.5 kwhr/lb of electrode vaporized
Production rate	13 lb/hr of arc product
Cathode consumption	0.5 lb/hr of graphite

It should be emphasized that these results represent a certain stage of development in process application. Further improvement can be expected. Development in the techniques of electrode fabrication for higher strength will permit reduction in slag per cent and operation at higher currents with higher production rates. The use of larger diameter electrodes can be expected to provide some additional improvements in unit power consumption and, of course, also higher production rates. Many other aspects of this development system are subject to engineering refinement. Work in refining the high-intensity arc in process applications is continuing.

Conclusion

This work demonstrates the technical feasibility of applying the Hierarc Process to the decomposition of Colorado rhodonite ore to provide manganese in a readily soluble form. Most importantly, this was done with rapid baked electrodes and over-all values of unit power consumption in the region of 2.5 kwhr/lb.

Acknowledgment

This work was done under contract with the Government by the West Orange Laboratory, Vitro Laboratories Division of the Vitro Corporation of America.

Manuscript received April 1, 1959. This paper was prepared for delivery before the Ottawa Meeting, Sept. 28-Oct. 2, 1958.

Any discussion of this paper will appear in a Discussion Section to be published in the June 1960 JOURNAL.

REFERENCES

1. C. Sheer and S. Korman, "The High Intensity in Process Chemistry," chapter in "Arcs in Inert Atmospheres and Vacuum," W. E. Kuhn, Editor, John Wiley & Sons, Inc., New York (1956).
2. L. Mead, M. A. Marquis, C. Sheer, and S. Korman, "Energy Transfer in the High Intensity Arc, Parts I and II," op. cit.

On the Measurement of the Temperatures of Unenclosed Objects by Radiation Methods

A. G. Emslie and H. H. Blau, Jr.

Arthur D. Little, Inc., Cambridge, Massachusetts

ABSTRACT

The functional relationships between apparent temperature and true temperature for the total radiation pyrometer, the optical pyrometer, the two-color pyrometer, and the two-temperature pyrometer are developed and discussed. It is shown that it is impossible to measure the temperature of an unenclosed object in the range 2000°-4000°K with accuracy greater than about 10% without prior knowledge of the emissivity. If the emissivity is known within 20%, the temperature can be determined within 1 or 2% by means of an optical pyrometer, particularly if the instrument is operated at the blue end of the spectrum. The accuracy obtainable with the other instruments under equivalent conditions is significantly lower.

Since the last war there has been a growing need to operate various devices at higher and higher temperatures in order, for example, to obtain more efficient rocket motors or faster airplanes. As a result a rapid increase is now taking place in research on the properties of all conceivable kinds of materials at higher temperatures. Such tools as the solar furnace, the plasma jet, the pulsed electric discharge, and the shock tube are used in these furnace techniques in several important respects.

An ordinary furnace usually has a fairly uniform internal temperature distribution, including the sample under test, and so the sample temperature can be found quite readily by means of a thermocouple inserted anywhere in the furnace or by an optical pyrometer applied to a sighting hole which emits essentially black-body radiation. With the new methods, on the contrary, there is generally no enclosure at the temperature of the sample, and the sample itself usually has sizeable temperature gradients. Under these conditions it cannot be assumed that the sample acts as a black-body radiator. Also, because of the gradients, it is very difficult to produce an artificial black-body cavity, for example, by drilling a hole in the sample. Thus the optical pyrometer cannot be used routinely to determine the temperature. Furthermore, in many cases of interest the sample temperature is above the limits of measurement by thermocouples.

How, then, can one measure the temperature of a sample under these conditions? The purpose of this paper is to evaluate the various radiometric methods under the assumption that the sample is completely unenclosed and that there is no prior knowledge about the emissivity of the sample.

Total Radiation Pyrometer

In the total radiation pyrometer the radiation from a given area of the sample is integrated over all wave lengths by a thermopile that has been calibrated against a black-body radiator.

The relation between the apparent absolute temperature T_A corresponding to an assumed average emissivity of ½ and the true temperature T corresponding to the real average emissivity $\bar{\epsilon}$ is given by

$$\frac{1}{2}\sigma T_A^4 = \bar{\epsilon}\sigma T^4 \qquad [1]$$

where σ is the Stefan-Boltzmann constant. The fractional error in the absolute temperature is

$$\frac{T_A - T}{T} = (2\bar{\epsilon})^{1/4} - 1 \qquad [2]$$

The graph of this relation, shown in Fig. 1, indicates that an error of about 20% is made when the true emissivity is 0.2 rather than the assumed value of 0.5.

The Optical Pyrometer

In the case of the optical pyrometer, radiation from the sample in a narrow band of wave lengths centered at 0.65 μ is compared with the radiation from a calibrated glowing filament. Assuming as before that nothing is known about the emissivity of the sample and that a value of ½ is guessed, we

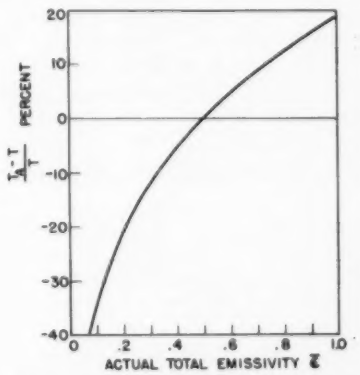

Fig. 1. Error of total radiation pyrometer vs. actual total emissivity for an assumed total emissivity of ½.

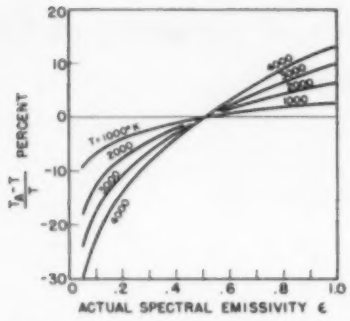

Fig. 2. Error of optical pyrometer vs. actual spectral emissivity at $\lambda = 0.65\ \mu$ for an assumed spectral emissivity of ½.

find from Wien's law the following relation between the apparent and true temperatures:

$$\frac{1}{2}\, e^{-c_2/\lambda T_A} = \epsilon\, e^{-c_2/\lambda T} \qquad [3]$$

where λ is the wave length at the center of the transmission band of the instrument, ϵ is the spectral emissivity of the sample, and $c_2 = 1.44 \times 10^4$ micron degrees.

From Eq. [3] we obtain for the relative error in the temperature

$$\frac{T_A - T}{T} = \frac{(\lambda T/c_2)\ln 2\epsilon}{1 - (\lambda T/c_2)\ln 2\epsilon} \qquad [4]$$

Figure 2 shows how the error depends on the true spectral emissivity ϵ for various fixed values of the true temperature T. For example, if the true emissivity is 0.2 instead of the guessed value of 0.5, the error is 7.5% at 2000°K and 14% at 4000°K.

Since, according to Eq. [4], the error is approximately proportional to λ, better results would be obtained by operating an optical pyrometer at as short a wave length as possible. At temperatures above 2000°K there should be enough short wavelength radiation to permit the construction of an electronic instrument with a filter in the neighborhood of 0.4 μ.

The Two-Color Pyrometer

The basis of the two-color pyrometer is that the unknown emissivity can be eliminated by taking the ratio of the radiant intensities from the sample at two different wave lengths. Unfortunately, this can only be done if the emissivity is the same at the two wave lengths. If ϵ_1 and ϵ_2 are the actual emissivities at the wave lengths λ_1 and λ_2, the radiated intensities in wave-length bands $\Delta\lambda_1$ and $\Delta\lambda_2$ are

$$\left.\begin{aligned} W_1 &= \epsilon_1 c_1 \lambda_1^{-5} \Delta\lambda_1 e^{-c_2/\lambda_1 T} \\ W_2 &= \epsilon_2 c_1 \lambda_2^{-5} \Delta\lambda_2 e^{-c_2/\lambda_2 T} \end{aligned}\right\} \qquad [5]$$

assuming that λ_1 and λ_2 are both in the region where Wien's law applies. The ratio of the intensities is

$$\frac{W_1}{W_2} = \frac{\epsilon_1}{\epsilon_2}\,\frac{\lambda_1^{-5}\Delta\lambda_1}{\lambda_2^{-5}\Delta\lambda_2}\, e^{(c_2/T)[(1/\lambda_2) - (1/\lambda_1)]} \qquad [6]$$

The apparent temperature T_A is the value derived from the instrument on the assumption that $\epsilon_1 = \epsilon_2$ and is therefore given by

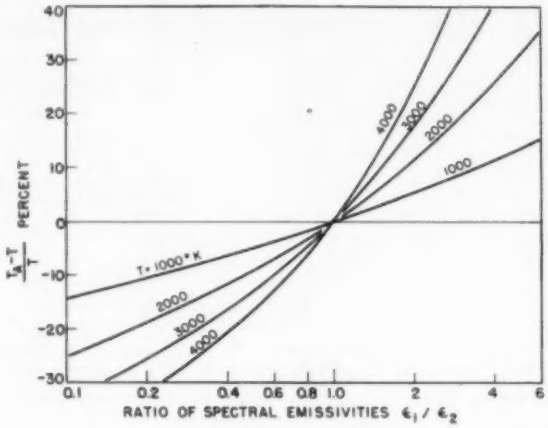

Fig. 3. Error of two-color pyrometer vs. ratio of spectral emissivities at wave lengths of 0.40 and 0.65 μ.

$$\frac{W_1}{W_2} = \frac{\lambda_1^{-5}\Delta\lambda_1}{\lambda_2^{-5}\Delta\lambda_2}\, e^{(c_2/T_A)[(1/\lambda_2) - (1/\lambda_1)]} \qquad [7]$$

The relation between the true and apparent temperature is found by equating [6] and [7]:

$$\frac{1}{T_A} - \frac{1}{T} = \frac{\ln(\epsilon_2/\epsilon_1)}{c_2\left(\dfrac{1}{\lambda_1} - \dfrac{1}{\lambda_2}\right)} \qquad [8]$$

The error $(T_A - T)/T$ calculated from this expression is shown in Fig. 3 as a function of the ratio of the spectral emissivities for different values of T, with $\lambda_1 = 0.40\ \mu$ and $\lambda_2 = 0.65\ \mu$.

The error is zero when the underlying assumption that the emissivities are the same is valid. In practice, the ratio of the emissivities at the two wave lengths can differ considerably from unity. If the ratio is 2, for example, the error is 11% at 2000°K and 25% at 4000°K.

It may be thought that the effect of the variation of emissivity with wave length may be evaded by taking the two wave lengths λ_1 and λ_2 very close together. Equation [8] shows that this idea is fallacious. The difference $1/T_A - 1/T$ is clearly proportional to the slope of the chord of the ln ϵ vs. $1/\lambda$ curve. This quantity merely becomes the slope of the tangent to the curve when $\lambda_1 \to \lambda_2$ and there is no *a priori* reason why the tangent should have a smaller slope than the chord.

The idea of the two-color pyrometer can be extended, in principle, to a multi-color pyrometer. A three-color pyrometer, for example, will give the correct temperature if the emissivity varies linearly with wave length. But in general the curvature of the emissivity vs. wave length characteristic is not zero and will produce as large an error in temperature as the slope does with the two-color pyrometer.

Two-Temperature Pyrometer

A new type of pyrometer that we have investigated, and which has also been considered by K. C. Vul'fson (1), depends on the idea that if the spectral distribution of intensity from the sample is measured at two temperatures, the spectral emissivity can be eliminated by dividing one spectral distribu-

tion by the other. Let T and T' be two temperatures. Then the two spectral distributions are given by Planck's law:

$$W = \frac{c_1 \epsilon(\lambda) \lambda^{-5} \Delta\lambda}{e^{c_2/\lambda T} - 1} \qquad [9]$$

$$W' = \frac{c_1 \epsilon(\lambda) \lambda^{-5} \Delta\lambda}{e^{c_2/\lambda T'} - 1} \qquad [10]$$

The ratio of the distributions is

$$\frac{W'}{W} = \frac{e^{c_2/\lambda T} - 1}{e^{c_2/\lambda T'} - 1} \qquad [11]$$

It will be noted that the spectral emissivity has cancelled out.

In Eq. [11] the ratio W'/W can be determined experimentally as a function of wave length λ. Since only two unknown quantities, namely, T and T', appear in the equation, it is sufficient in principle to make measurements at only two wave lengths in order to determine both T and T'. However, more accurate results should be obtainable by using data over the whole spectrum. This can be done by preparing a set of master graphs of the function

$$\frac{W'}{W} = \frac{e^{xT'/T} - 1}{e^x - 1} \qquad [12]$$

which is obtained from Eq. [11] by the substitution

$$x = c_2/\lambda T'$$

Figure 4 shows the master graphs of W'/W vs. x for various values of T/T' with x plotted on a logarithmic scale.

To determine T and T' from the experimental data, the experimental values of W'/W are plotted against λ with the same scales as in Fig. 4. The experimental graph is now moved horizontally over the master chart until the best fit with one of the master curves is obtained. By reading any pair of corresponding points on the two abscissas, one finds a value of λ and a value of $c_2/\lambda T'$. Thus T' is found. The matched master curve gives T/T', so T is also determined.

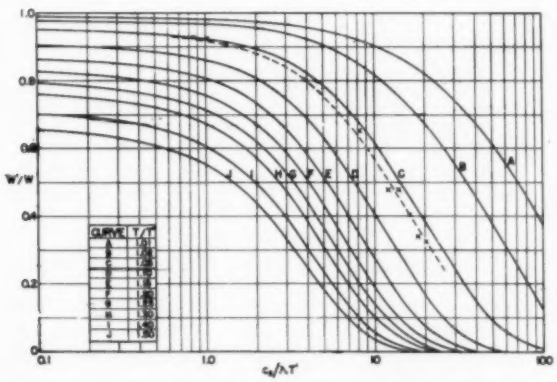

Fig. 4. Master graphs for the two-temperature pyrometer showing intensity ratio for two temperatures vs. $c_2/\lambda T'$. The crosses represent the best fit of experimental data for a hot Globar source.

The crosses on Fig. 4 represent the best fit of experimental data for a hot silicon carbide source taken with a Perkin Elmer infrared spectrometer. The position of the crosses indicates that $T'/T = 1.052$, and the horizontal position of the experimental wave-length scale (not shown in Fig. 4) gives $T' = 1126°K$. The actual temperature determined by a thermocouple embedded in the silicon carbide gave a reading of $T' = 1320°K$. The error is therefore about 15% which is comparable with the errors of the other radiometer methods.

The error in the temperature determination appears to be due to the assumption that the spectral emissivity is independent of temperature. If $\epsilon(\lambda)$ is a function of temperature, then it cannot be divided out by taking the ratio of Eq. [9] and [10].

The effect of the temperature coefficient of emissivity can be calculated most easily for the case of a two-temperature pyrometer that measures the radiation from the sample at only two wave lengths λ_1 and λ_2. For precision in fitting the two-point experimental graph to the master graphs of Fig. 4 the two wave lengths should be on opposite sides of the black-body peak.

The intensity radiated at the shorter wave length λ_1 is given by Wien's law:

$$W = c_1 \epsilon \lambda_1^{-5} \Delta\lambda_1 e^{-c_2/\lambda_1 T} \qquad [13]$$

The rate of change with temperature is

$$\left(\frac{1}{W}\frac{dW}{dT}\right)_{\lambda_1} = \left(\frac{1}{\epsilon}\frac{d\epsilon}{dT}\right)_{\lambda_1} + \frac{c_2}{\lambda_1 T^2} \qquad [14]$$

The intensity at the longer wave length λ_2 follows Rayleigh's law:

$$W = \frac{c_1}{c_2} \epsilon T \lambda_2^{-4} \Delta\lambda_2 \qquad [15]$$

and the rate of change is

$$\left(\frac{1}{W}\frac{dW}{dT}\right)_{\lambda_2} = \left(\frac{1}{\epsilon}\frac{d\epsilon}{dT}\right)_{\lambda_2} + \frac{1}{T} \qquad [16]$$

An equation for the true temperature T is obtained by eliminating dT from Eq. [14] and [16]:

$$\frac{\left(\frac{dW}{W}\right)_{\lambda_1}}{\left(\frac{dW}{W}\right)_{\lambda_2}} = \frac{\left(\frac{1}{\epsilon}\frac{d\epsilon}{dT}\right)_{\lambda_1} + \frac{c_2}{\lambda_1 T^2}}{\left(\frac{1}{\epsilon}\frac{d\epsilon}{dT}\right)_{\lambda_2} + \frac{1}{T}} \qquad [17]$$

The apparent temperature T_A that would be obtained from the master graphs is found by assuming that the temperature coefficient of emissivity is zero in Eq. [17]. Thus

$$\frac{\left(\frac{dW}{W}\right)_{\lambda_1}}{\left(\frac{dW}{W}\right)_{\lambda_2}} = \frac{\frac{c_2}{\lambda_1 T_A^2}}{\frac{1}{T_A}} \qquad [18]$$

On combining Eq. [17] and [18] we find:

$$T_A = T \cdot \left[1 + T \left(\frac{1}{\epsilon} \frac{d\epsilon}{dT} \right)_{\lambda_2} \right] \Big/ \left[1 + \frac{\lambda_1 T^2}{c_2} \left(\frac{1}{\epsilon} \frac{d\epsilon}{dT} \right)_{\lambda_1} \right] \quad [19]$$

The error in temperature is therefore, approximately,

$$\frac{T_A - T}{T} = T \left(\frac{1}{\epsilon} \frac{d\epsilon}{dT} \right)_{\lambda_2} - \frac{\lambda_1 T^2}{c_2} \left(\frac{1}{\epsilon} \frac{d\epsilon}{dT} \right)_{\lambda_1} \quad [20]$$

If $\lambda_1 = 0.4\ \mu$ and $T = 2000°K$, then $\lambda_1 T/c_2 = 0.06$. Thus the short wave-length contribution to the error is negligible compared with the long wave-length contribution and Eq. [20] reduces to

$$\frac{T_A - T}{T} = T \left(\frac{1}{\epsilon} \frac{d\epsilon}{dT} \right)_{\lambda_2} \quad [21]$$

Figure 5 shows a plot of the error vs. $(1/\epsilon)(d\epsilon/dT)$ for various values of T. The circles on the 2000°K line give the errors obtained from published values (2-4) of the temperature coefficients for tungsten, rhenium, and molybdenum. The errors are quite large enough to explain the discrepancy observed in the case of silicon carbide and are of the same order of magnitude as the errors involved in the other radiometer methods.

Conclusions

The general conclusion to be drawn from our analysis is that it is impossible to measure the temperature of an unenclosed sample in the range 2000°-4000°K with an accuracy greater than about 10% by observing only the radiation emitted by the sample and without any prior knowledge of the emissivity. On the other hand, even a 20% measurement of the emissivity at a single wave length will allow determination of temperature to 1 or 2% by means of the optical pyrometer, especially if the instrument is operated at the blue end of the spectrum.

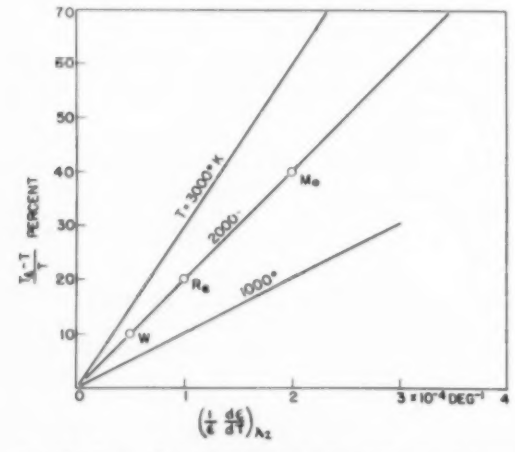

Fig. 5. Error of two-temperature pyrometer vs. temperature coefficient of emissivity. The circles indicate the calculated errors for tungsten, rhenium, and molybdenum at 2000°K.

The problem of measuring the temperature of an unenclosed object therefore hinges on being able to determine the emissivity. Since the emissivity varies quite markedly with temperature it is unsafe to extrapolate low-temperature values to the high-temperature range. Thus the emissivity has to be measured at the high temperature and, since the temperature is unknown, this can only be accomplished by finding the reflection coefficient of the sample at the operating wave length of the pyrometer. If it is assumed that the pyrometer views the surface of the sample at normal incidence, then the reflection coefficient of interest is $\rho_\lambda = I_r/I_o$ where I_o is the intensity of a beam of light at normal incidence and I_r is the intensity of the reflected light integrated over the whole hemisphere. An equivalent arrangement, using the principle of reversibility, is to flood the sample with light uniformly from all directions and measure the reflected light in a small solid angle at normal incidence. In both methods care has to be taken that any specularly reflected light is included in the measurement. Since the hot sample itself emits light in all directions, the reflection experiment requires chopped radiation. The normal emissivity is easily determined from the reflection coefficient by means of Kirchhoff's law $\epsilon_\lambda = 1 - \rho_\lambda$.

In the case of a sample heated in a solar furnace, Laszlo (5) has suggested using reflected sunlight to determine the emissivity. A total radiation pyrometer designed by Gardon is used to determine the incident and reflected radiation fluxes, the ratio of which gives the total reflectivity and hence the total emissivity ϵ_t. The temperature may then be found from the energy balance

$$P = \epsilon_t T^4$$

where P is the incident flux. This equation assumes, however, that the sample loses energy by re-radiation only.

Another method mentioned by Laszlo is use of an optical pyrometer in conjunction with a value of the spectral emissivity ϵ_λ calculated from a measured value of the total reflectivity. It is not clear how a unique value of ϵ_λ can be obtained in this way, except for the case of a gray body.

Manuscript received Sept. 8, 1958. This paper was prepared for presentation before the New York Meeting, April 27-May 1, 1958.

Any discussion of this paper will appear in a Discussion Section to be published in the June 1960 JOURNAL.

REFERENCES

1. K. C. Vul'fson, *Zhur. Eksptl. i. Teort. Fiz.*, **21**, 507 (1951).
2. D. T. F. Marple, *J. Opt. Soc. Amer.*, **46**, 490 (1956) (Rhenium).
3. W. W. Coblentz, *Int. Crit. Tables*, **5**, 242-245 (1929) (Tungsten).
4. W. W. Coblentz, *ibid.*, **5**, 242-245 (1929) (Molybdenum).
5. T. S. Laszlo, *J. Solar Energy Science and Engineering*, **1**, 78 (1957).

The Behavior of Rhenium in Electron Tube Environments

Gordon B. Gaines, Chester T. Sims,[1] and Robert I. Jaffee

Battelle Memorial Institute, Columbus, Ohio

ABSTRACT

Rhenium, tungsten, and rhenium-coated tungsten have been exposed to carburizing atmospheres and to water-cycle attack, rhenium and tungsten to aluminum oxide at 1750°C for 7000 hr, and rhenium to boron-containing atmospheres. It was confirmed that rhenium, unlike most other refractory metals, does not form a carbide. Rhenium forms a boride, which forms a eutectic with another boride or with rhenium, and melts under 2250°C. Thoriated rhenium maintains microstructural and mechanical integrity after long exposure in vacuum at 1750°C in contact with alumina. Rhenium and rhenium-coated tungsten are highly resistant to water-cycle effects.

Extensive work has been reported recently on the metal rhenium, both in this country and abroad (1, 2). Rhenium is a strong, ductile, refractory metal which melts at 3180°C and possesses chemical and metallurgical properties which are in some respects characteristic of the precious metals and in others characteristic of the refractory transition metals. Rhenium is potentially useful in vacuum tubes and other electronic devices. The behavior of Re exposed to reactive environments that might be encountered in such devices at high temperatures is of considerable interest. In this work, Re, W, and Re-coated W have been exposed to carburizing atmospheres and to water-cycle attack; Re and W were heated in contact with aluminum oxide (in commercial vacuum), and Re was heated in boron-containing atmospheres. Following exposure, the materials were evaluated to determine chemical and mechanical stability.

Carburizing Environment

The possibility that Re does not form a carbide was first suggested by Tzyrbiatowski (3). This was confirmed by Hughes (4) who studied arc-melted Re-C alloys and found that the terminal α Re solid solution was in equilibrium with graphite. A eutectic reaction occurs at 2480°C and 16.9 at. % C (1.3 wt %). Rhenium dissolves up to 11.7 at. % C at 2480°C. The solubility of C in Re decreases rapidly with decreasing temperature to about 4.5 at. % at 2000°C. The absence of a compound in the Re-C system is unique among refractory transition metals; W, Ta, Mo, and Nb, all form carbides. In this respect, Re behaves similarly to the Pt-group metals.

In this study, unalloyed Re and W filaments and a Re-coated W wire were heated in the presence of a C-bearing atmosphere to study high-temperature reactivity. The materials used were 0.020-in. annealed Re wire fabricated by conventional techniques, 0.014-in. wrought commercial W wire, and Re-coated W wire prepared by deposition of an 0.007-in. Re coating on the 0.014-in. wrought W by halide decomposition. The deposition process consisted of first preparing rhenium pentachloride by the direct action of chlorine on Re metal at 750°-850°C The rhenium pentachloride then was vaporized in vacuum in the presence of the resistance-heated W wire. The pentachloride was decomposed thermally, depositing Re metal on the hot W wire. During this process, the 0.014-in. W-wire core was resistance heated to a temperature of 900°-1000°C for a period of about 2 hr. The final Re deposit was 0.007 ± 0.001 in. thick, adherent, bright, and quite uniform in thickness along the length of the wire. Some surface roughness was apparent, which is not unusual for coatings prepared by the halide vapor decomposition process.

For carburization, the three different filaments first were heated by self-resistance to 1982°C in flowing hydrogen. Dry hydrogen at the rate of 4.2 l/min and hydrogen-toluene vapor at 0.84 l/min then were passed through the chamber for 2 min. The hydrogen-toluene vapor flow was terminated, and dry hydrogen then was allowed to flow through for an additional 30 sec before cooldown. Thus, the filaments were at temperature somewhat longer than 2 min. Portions of the filaments were mounted for metallographic inspection, and the appearance and the results of Knoop microhardness traverses for unalloyed W and Re, together with a typical wrought structure for unexposed W, are shown in Fig. 1. Uncontaminated, annealed Re wire would have an equiaxed grain structure and an average hardness of about 400-500 Knoop across the diameter.

Upon exposure to the carburizing atmosphere, the W wire recrystallized, and carbide formed at the surface. Recrystallization resulted in a hardness drop to about 400 Knoop throughout the core. The layer on the surface of the W is tungsten carbide, confirmed by the hardness values of about 1900 Knoop. The carbonized W filaments were extremely brittle and fractured at the slightest touch.

The carburized rhenium shown in Fig. 1c retained a single-phase structure. This is supporting evidence that Re does not form a carbide. However, the entire cross section of the wire exhibits rather high hardness for an annealed Re wire of this diameter, and the hardness values are rather scattered. It is believed that C has diffused completely through the Re wire and the structure shown is that of a Re-

[1] Present address: General Electric Co., Knolls Atomic Power Lab., Schenectady, N. Y.

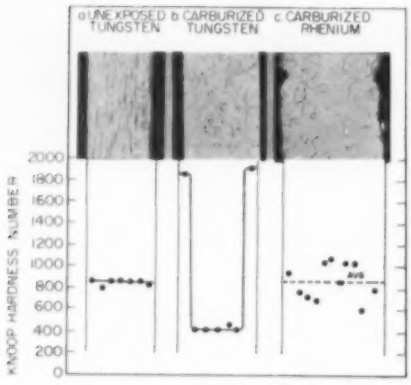

Fig. 1. Appearance and hardness traverses for unexposed and carburized W and carburized Re filaments. Magnification 100X before reduction for publication.

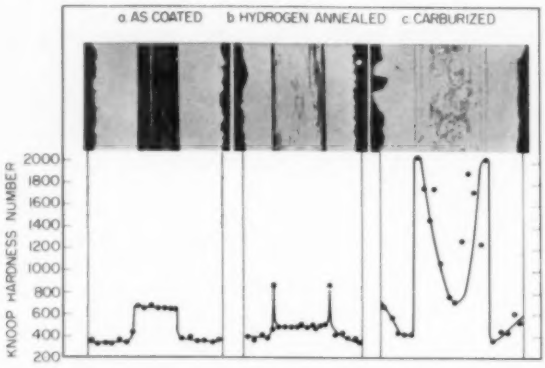

Fig. 2. Appearance and hardness traverses for unexposed, heat-treated, and carburized Re-coated W wire. Magnification 100X before reduction for publication.

base, interstitial-carbon solid solution. The rapid diffusion rate of C through Re is verified by results of the studies of Re-coated W, where W_2C formed underneath a Re layer in a short time period. Thus, although Re does not form a carbide, diffusion of C into Re occurs rapidly with considerable hardening. Although insufficient material was available for quantitative bend tests, the wire showed ductility when bent by hand. This suggests that Re metal is not hardened to the point of embrittlement when heated in carbonaceous atmospheres. This should enhance the usefulness of Re considerably.

A longitudinal section of Re-coated W wire in the as-deposited condition is shown in Fig. 2a. The large-grain, high-purity Re deposited from decomposition of the pentachloride has a somewhat lower hardness (350 Knoop) than fabricated Re filaments (400-500 Knoop). The wrought W core is slightly softer than the W of Fig. 1a, possibly because of stress relief at 900°C during preparation of the Re coating. A portion of the composite wire was exposed in pure hydrogen for 2 min at 1980°C with no C present. The resulting structure and hardness are shown in Fig. 2b. The W core has largely recrystallized, and hardness reduced to about 450 Knoop. The Re cladding is essentially unchanged. A small amount of interdiffusion has commenced between the W core and the Re cladding, causing a narrow, dark layer of a new phase to form at the interface. This phase has a relatively high hardness which may be considerably higher than that shown by measurements as the phase layer is too narrow to yield accurate readings. This new layer probably is either σ-phase (W_2Re_3) or an α-Mn-type W-Re intermetallic, or both (5). Exposure to C, as previously described, results in the structure shown in Fig. 2c. The Re coating hardened from about 350 to 700 Knoop at the surface as a result of C diffusion. This increase is similar to that noted for unalloyed Re wire which hardened from 450 to an average of 850 Knoop. Two new zones were found in the W-Re interface. Using filtered Fe radiation, x-ray diffraction measurement on the new zones showed two major phases, α—W_2C and W_2Re_3 (σ-phase). Weak diffraction lines also observed might have been due to the Re-W-Mn-type phase.

The outer interfacial zone, which has a hardness of over 2000 Knoop, is undoubtedly the W_2C formed from reactions between W and C which diffused through the Re coating. The inner zone, with a hardness of 1500 Knoop, is the diffusion product, W_2Re_3. Thus, Re coatings do not protect underlying W from reactions with ambient C-containing atmospheres, even with thick coatings, as in the present case. Reaction with the underlying W is slowed down, however, and there is no doubt that the carburized Re-coated W filament is not affected so severely by C as unalloyed W, and may be capable of some mechanical service. For instance, the wire was capable of being handled without fracture following carbonization. Although it possessed no measurable ductility, the wire exhibited a room-temperature ultimate tensile strength of 45,000 psi.

Boron-containing Atmospheres

Since Re does not form a carbide, it was thought that it might have somewhat lower reactivity with B than most other refractory metals which form borides. Boron-containing materials are potentially useful in electron-tube technology. If Re does not form a boride, it might be useful for supporting B-containing substances which are good thermionic emitters.

Three individual 0.01-in. Re filaments were heated by self-resistance to different temperatures in an atmosphere of flowing gas, which consisted of a mixture of dry hydrogen and boron trichloride. One filament was heated to 1330°C (black-body temperature), one to 1750°C, and one to 2250°C. During the adjustment of the voltage of the filaments to get the desired temperature, the filaments were in an atmosphere of flowing dry hydrogen. The filaments then were allowed to cool, and boron trichloride was introduced to give a hydrogen:boron trichloride ratio of 7:1. Filament power then was applied for a period of 2 min, following which the filaments were allowed to cool in the B-containing atmosphere.

About 10 to 15 sec after exposure commenced, the filament at 2250°C burned in half. The remaining two filaments lasted for the entire 2-min period.

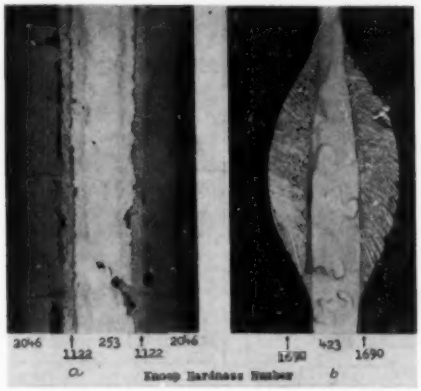

Fig. 3. Longitudinal sections and hardness of unalloyed Re wire exposed to a boron-containing atmosphere under the conditions designated. a, Exposed 2 min at 1750°C; b, exposed 15 sec at 2250°C. Magnification 100X before reduction for publication.

The filaments heated to 1330° and 1750°C appeared to have developed a coated or scaled appearance, while the burned-out filament appeared beaded. A longitudinal section of the filament exposed at 1750°C is shown in Fig. 3a and a similar section of the filament exposed at 2250°C is shown in Fig. 3b, each with pertinent hardness information.

The specimen exposed at 1750°C developed an extremely hard outer crust which readily cracked. A hard intermediate zone also was apparent. An appreciable fraction of the Re core remained unreacted. It is assumed from the appearance and hardness data for the exposed filament that the outer layer shown is a rhenium boride. The intermediate layer may be a solid solution of B in Re or a lower boride, and the inner core is essentially unreacted Re. Thus, Re is not resistant to B at high temperature and undoubtedly forms a boride or borides.

Exposure of the Re wire to B at 2250°C caused melting and burnout. The molten product froze as small beads on the filament, one of which is shown in Fig. 3b. Since the central Re core has a higher hardness than normal, it appears probable that B diffused through the 0.010-in. section at 2250°C. The bead probably is an eutectic mixture of the boride and the phase shown in the intermediate zone of Fig. 3a, which melts below 2250°C.

Life Tests on Thoriated Rhenium and Tungsten Filaments in Contact with Solid Alumina

A 0.020-in. Re-0.85ThO_2 (wt %) wire and 0.015-in. commercial W wire of the type described previously were wrapped on small high-purity (Degussa) Al_2O_3 cylinders and the assemblies were placed in a U-tube container evacuated to a pressure of about 10^{-7} mm Hg. The tube was not gettered. The temperature of the wires was held at approximately 1750°C black-body temperature for 7000 hr. The alumina cylinders were supported by the filaments. The appearance of the test device and the filaments and cylinder surfaces following exposure for 7000 hr are shown in Fig. 4.

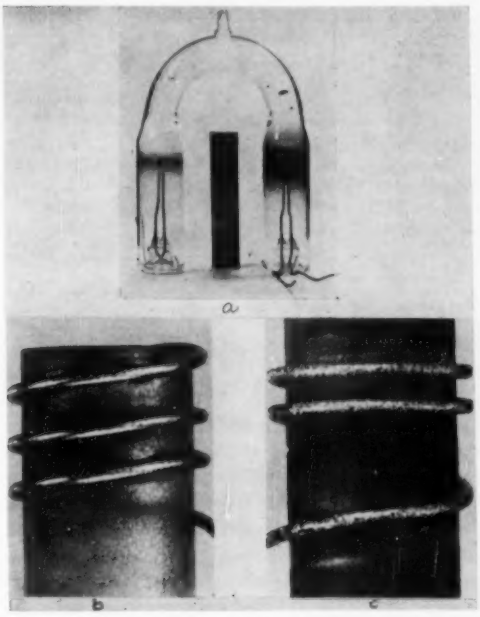

Fig. 4. Appearance of evacuated U-type and of Re and W filaments on alumina sleeves following life testing for 7000 hr at 1750°C. a, Evacuated U-tube; b, Re filament; c, W filament.

The 7000-hr life test resulted in no major changes in geometry or in mechanical or electrical failure. However, a certain amount of local reaction took place, as shown in Fig. 4. At places on the alumina cylinders where physical contact with the filaments was maintained for a long time, eroding of the alumina is evident. The surface appearances of the two filaments had been affected. The W wire possessed a much rougher surface than the Re-ThO_2 wire, although neither was as smooth as drawn wire.

The surface roughing and the black deposits on the glass walls probably are due almost wholly to the water-cycle mechanism. It is known that this mechanism affects Re much less than it does W, and this certainly is suggested by the much larger deposits around the W filament. The water-cycle attack would not be expected to be substantial at a pressure of 10^{-7} mm Hg.[1] However, the tube was ungettered and unbaked, and it is highly probable that the pressure during much of the 7000 hr was of the order of 10^{-5}—10^{-4} mm Hg and that the tube atmosphere contained a substantial amount of water vapor. Another mechanism for explaining the deposits on the tube walls and the grooves in the alumina is a reaction between alumina and tungsten, giving aluminum and tungsten oxide gases. Using published thermodynamic data (6), a simple calculation indicates that, at a pressure of the order of 10^{-6} mm Hg and a temperature of 1750°C, this possibility cannot be ruled out. Unfortunately, an analysis of the deposits was not made, so as to settle this point. It is possible, also, that atomic hydrogen and oxygen, present as a

[1] The authors are grateful to a reviewer for pointing this out.

Table I. Properties of thoriated Re and W filaments

Property	Thoriated Re		W	
	Wrought and recrystallized	Heated 1750°C for 7000 hr[a]	Wrought and recrystallized	Heated 1750°C for 7000 hr[a]
Filament diameter, in.	0.015	0.020	0.010	0.015
Ultimate tensile strength, psi	124,000	115,000	250,000	[c]
Elongation, %	8.5	4	1-4	[c]
Hardness, VHN or KHN	204	277	450	416
Bend ductility, T value[b]	0.0	0.8	1.0	200

[a] Alumina cylinder life test.
[b] T value obtained by dividing smallest successful bend radius by the thickness of the wire; thus, smaller T values mean higher ductility.
[c] Too brittle to be measured.

result of the water-cycle reaction, contributed to the attack of alumina.

The Re-alloy filament did not fracture during its removal from the tube or its handling prior to mechanical testing. The 7000-hr test produced only moderate changes in its over-all mechanical properties as compared to unexposed metal. As shown by the data in Table I, this alloy, which is somewhat less strong and ductile than unalloyed Re, showed only slightly reduced tensile strength as a result of the test. Ductility, as measured by elongation and bend tests, also dropped slightly. As expected, the recrystallized W filament possessed little mechanical integrity compared to Re or to fibered W.

Subsequent microstructure examination showed that the thoria in the Re filament has shown some tendency to agglomerate into larger particles, see Fig. 5. In addition, the W filament developed a heavy concentration of voids scattered uniformly throughout the grain structure, while no voids were found in the Re. No reason for the voids is apparent. Analyses[a] of the W revealed no unexpected or excessive impurities. However, tungsten and alumina are not compatible over about 1400°C (7), and contact with the alumina cylinder may have contributed to the void formation

[a] Impurities in the W by spectrographic analysis were as follows (wt %): Fe, 0.01-0.1; Si, 0.005-0.05; Mg, 0.005-0.05; Mo, 0.001-0.01; Ca, 0.001-0.01; Cu, Ni, K, Mn, <0.001; Th, Na, <0.05; Cr,

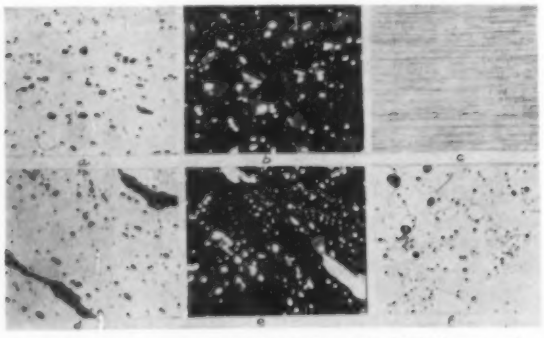

Fig. 5. Appearance of thoriated Re and of W filaments before and after life testing in alumina for 7000 hr at 1750°C. a, Unexposed recrystallized thoriated Re, lightly etched; b, unexposed recrystallized thoriated Re; polarized light; c, unexposed wrought W, etched; d, exposed thoriated Re, lightly etched, e, exposed thoriated Re, polarized light; f, exposed W, etched. Magnifications 500X before reduction for publication.

Water-Cycle Life Tests for Tungsten, Rhenium, and Rhenium-Coated Tungsten

Rhenium is considerably more resistant to the water-cycle effect at elevated temperatures than tungsten, as has been shown previously (8, 9). Accordingly, the possibility of protecting W from this phenomena by Re coatings has been suggested. In the present work, 0.005-in. wrought commercial W, 0.005-in. unalloyed Re, and Re-coated W wires were exposed to water vapor at a pressure of approximately 4×10^{-4} mm Hg[a] at two temperatures, 1300° and 1750°C. The Re coating was applied by the halide-decomposition process, as described previously in the study of attack by carburizing atmosphere. The coating was approximately 0.007-in. thick and was applied to an 0.014-in. W wire. Exposure of all specimens was for 7800 hr, each filament being heated individually by its self-resistance, and all were exposed to the same atmosphere.

Data from the life test are given in Table II. The data confirm that Re is less susceptible to water-cycle attack at all temperatures than W, and the differences is most marked at 1750°C where all of the materials react more severely. Least attack occurs on the Re-coated W, which possessed better water-cycle resistance than unalloyed Re. This is somewhat surprising, particularly since the surface of the Re-coated W was slightly rougher than that of the unalloyed Re wire. The as-deposited Re cladding is probably of higher purity than the unalloyed Re wire, which may account for the difference in rates of attack.

For the conditions of moderate water-vapor attack studied, rather heavy coatings were used in

[a] Vapor pressure over ice at −80°C.

Table II. Weight-loss data for W, Re, and Re-coated W exposed to water-cycle attack for 7800 hr

Material	Exposure temperature, °C		Total wt loss, mg	Attack in 7800 hr, mg/cm²
	Initial	Final		
W	1300	1275	0.5	1.50
	1750	1660	2.6	8.25
Re	1300	1200	0.2	0.65
	1750	1660	0.3	0.98
Re-clad W	1300	1310	0.8	0.48
	1750	1700	1.0	0.57

the present studies. With attack so light, much thinner coatings, such as those applied by electroplating, would probably be adequate protection.

Conclusions

1. It is confirmed that Re metal, unlike most other refractory metals, does not form a carbide. Although C diffuses rather rapidly through Re, causing hardening and some deterioration of mechanical properties, Re maintains dimensional stability and some mechanical integrity. Rhenium coatings on tungsten wire do not prevent carbon from diffusing to the tungsten core and reacting to form tungsten carbide, but the reaction is much slower than that when uncoated tungsten is exposed.

2. Rhenium forms a boride, which forms a eutectic between another boride, or rhenium. The eutectic melts under 2250°C.

3. Thoriated rhenium maintains structural, microstructural, and mechanical integrity after long-time (7000 hr) exposure in vacuum at 1750°C in contact with solid aluminum oxide.

4. Unalloyed rhenium has been shown again to have excellent resistance against the water cycle up to 1750°C, particularly when compared with tungsten. Rhenium coatings protect tungsten from attack by the water cycle.

Acknowledgments

The authors wish to acknowledge with thanks the help given by J. B. Baker, W. W. Kleinschmidt, and W. E. Nexsen, Jr., in carrying out the experiments and by D. F. Rosenbaum in providing rhenium-coated tungsten samples.

The work was supported by the Air Force Cambridge Research Center.

Manuscript received March 19, 1959. This paper was prepared for delivery before the Columbus Meeting, Oct. 18-22, 1959.

Any discussion of this paper will appear in a Discussion Section to be published in the June 1960 JOURNAL.

REFERENCES

1. C. T. Sims, C. M. Craighead, and R. I. Jaffee, *Trans. AIME*, **203**, 168 (1955).
2. C. Agte, M. Alterthum, K. Becker, G. Heyne, and K. Moers, Z. *anorg. u. allgem. Chemie*, **196**, 129 (1931).
3. W. Tzyrbiatowski, *ibid.*, **193**, 311 (1930).
4. J. Hughes, "The Alloy System Rhenium-Carbon," Associated Electrical Industries Report No. A497 (November 1955).
5. P. Greenfield and P. Beck, *Trans. AIME*, **206**, 265 (1956).
6. J. P. Coughlin, "Heat and Free Energies of Formation of Inorganic Oxides," Bulletin 542, U. S. Bureau of Mines, 1954, Supt. of Documents, Washington, D. C.
7. W. Kohl, "Materials Technology for Electron Tubes," Rheinhold Publishing Co., New York (1951).
8. C. T. Sims, *et al.*, "Investigations of Rhenium," WADC TR 54-371 (June 1954).
9. C. Ludington and C. T. Sims, "Rhenium—A High-Temperature Metal," AGET News Bulletin (January 1, 1958).

Oxides on the Silver Electrode

Charles P. Wales and Jeanne Burbank

U. S. Naval Research Laboratory, Washington, D. C.

ABSTRACT

Silver electrodes were studied by means of potentials and x-ray diffraction patterns. The silver was charged anodically in 35% KOH by means of either constant current or constant potential, and discharged at a low or high rate. Attempts were made to form an oxide higher than AgO by means of anodization. The products of anodization of silver in 2*N* H_2SO_4 were determined. The basis for the theory that the oxides of silver are formed by the introduction of oxygen into the octants of the face-centered cubic silver lattice was examined.

Alkaline storage and primary batteries containing positive silver electrodes have been used, in recent years, for special purposes requiring light weight or the ability to discharge at high rates. There is considerable confusion in the literature, however, as to the reactions taking place on these electrodes. In addition the potential distribution and eletcron transfer may be complex on oxide surfaces with different conducting or semiconducting properties.

A typical charge of a silver electrode in alkaline solutions shows three potential plateaus. There is general agreement with the work reported by Luther and Pokorny (1) in 1908 that the first plateau corresponds to the formation of Ag_2O. A possible subsidiary step of short duration was noted by Hickling and Taylor (2) at the beginning of this first plateau, which they suggested may represent some adsorption of oxygen prior to the production of Ag_2O, or may be the formation of a silver suboxide.

The results of Luther and Pokorny further indicate that at the second potential plateau Ag_2O is changed quantitatively and reversibly to AgO. On the other hand, Hickling and Taylor report that an oxide of Ag containing more oxygen than AgO is formed at this second plateau, and that this unstable higher oxide, perhaps Ag_2O_3, decomposes to give AgO; i.e., the AgO forms purely as a secondary product. The results of Jones, Thirsk, and

Wynne-Jones (3) are not in accord with those of Hickling and Taylor but agree partially with those of Luther and Pokorny in that they show the direct oxidation of Ag_2O to AgO. However, Jones, *et al.* claim that only 30% of the current is used to form AgO at this potential, the remaining 70% going to O_2 evolution, and they conclude that the statement about the oxidation of Ag_2O proceeding quantitatively and reversibly (1) is without foundation.

At the third potential plateau the electrode reaction is almost entirely the evolution of O_2. It has been concluded (3, 4) that an oxide higher than AgO is formed at this step, and this Ag_2O_3 potential has been reported by others (5, 6). The present investigation was undertaken to clarify these conflicting statements regarding silver electrodes in alkali. During this work it also became desirable to examine the anodization of silver in sulfuric acid.

Experimental Procedure

The positive (test) electrodes were made by cutting in half silver plates taken from a commercial Ag-Zn storage battery. The test electrodes measured about 28.5 x 66.5 x 0.7 mm and had a capacity of 1.8-2.0 amp-hr. A 3-mm-thick U-shaped plastic frame, with inside dimensions slightly larger than the positive electrode, was wrapped with several layers of separator material of the type used in Ag-Zn batteries. The electrode was then inserted into the frame. This arrangement allowed the electrode to be removed for examination and then to be replaced readily, without unwrapping or tearing the separator. X-ray diffraction patterns were obtained with a General Electric XRD-5 spectrogoniometer using Cu Kα radiation after the electrode was rinsed briefly in distilled water and blotted dry with tissue paper. The x-ray examination of the electrode surface could begin within 5 min after anodic or cathodic treatments and would characterize the deposit within a layer 0.01 mm thick.

The Ag, Ag_2O/OH^- reference electrode used for all of the potential measurements was made by packing Ag_2O into a glass tube which had a Pt wire sealed through its wall, adding a KOH solution as the electrolyte, and, after 24 hr, cathodically reducing part of the Ag_2O onto the Pt, using another Pt wire as the second electrode. This reference half-cell gives a stable potential, after being allowed to stand a few days to establish equilibrium, and electrodes of this type have been used continuously for over two years at this laboratory. The stability of a Ag/Ag_2O electrode was shown recently by Hamer and Craig (7).

A silver screen, wrapped with separator material, served as the negative electrode. The electrodes were assembled in a closed plastic container in an electrolyte of 35% KOH. The instrumentation and techniques previously described (8) were used to measure and record the potential as well as to control the cell current or potential. On a few occasions silver sheet, 0.13 mm thick, was used as the positive electrode in either 35 or 5% KOH, and in addition both types of electrode were anodized in

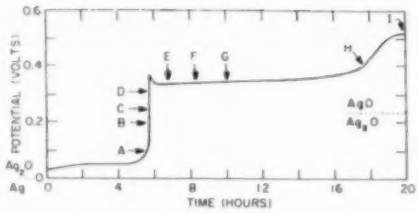

Fig. 1. Typical 100-ma charge of the Ag electrode. Letters refer to points at which x-ray diffraction patterns have been obtained. Potentials are given with respect to a Ag/Ag_2O reference electrode.

2*N* H_2SO_4. All work was carried out in a controlled temperature of 26°-27°C.

Results and Discussion

The three potential plateaus occurred at 0.03 to 0.05 v, 0.33 to 0.37 v, and 0.51 to 0.52 v, positive with respect to the Ag/Ag_2O reference electrode, during a typical 20-hr charge at 100 ma (Fig. 1). The reversible Ag_2O/AgO potential is 0.23 v,[1] and the AgO/Ag_2O_3 potential is 0.39 or 0.40 v, with respect to the reference electrode used here (1, 2).

A discharged silver electrode was charged anodically at 100 ma until its potential was 100 mv above the reference electrode potential (point A, Fig. 1), and the potential then was held at 100 mv. When the charge was interrupted after 21 hr the current had fallen to 0.47 ma, and the electrode was 20% charged (based on the discharge capacity). An x-ray diffraction pattern showed strong Ag lines with weaker Ag_2O lines, but no lines were found which could be attributed to a suboxide. When the potential was held at 200 mv for 6.5 hr, the x-ray diffraction pattern of this anode (point B, Fig. 1) was still strong in Ag, although the amount of Ag_2O had increased. This confirmed the statements that the reaction at the lower potential plateau consists only of the oxidation of Ag to Ag_2O. The same diffraction pattern was obtained when the potential was held at 250 mv for 6.7 hr (C, Fig. 1), 20 mv above what has been believed to be the reversible Ag_2O/AgO potential. It should be noted, however, that in this investigation the Ag_2O/AgO equilibrium potential was normally found to be about 267 mv (measured by charging the electrode to AgO and allowing it to stand until its potential became constant). This is 0.03-0.04 v higher than the value which is usually given (1,2) (see however, Bonk and Garrett, footnote 1).

The potential of the silver electrode then was increased to 308 mv (D, Fig. 1)and held there for 22 hr, but only 0.043 additional amp-hr of charge (2% of the total capacity) could be added. Diffraction patterns, however, showed that some AgO had formed, that the amount of Ag_2O had increased, and that there was now only half as much Ag present on the surface. AgO could not be detected by x-ray diffraction on an electrode held at 275 mv for 175 hr, although the open-circuit potential of 180 mv did indicate the presence of AgO. The fact that AgO

[1] Recent work by J. F. Bonk and A. B. Garrett (7a) indicates that this value should be 0.26 v instead of 0.23 v.

can be formed at a potential well below the Ag_2O_3 potential supports the belief (1,3) that AgO is the primary anodic oxidation product at the second plateau of a charge, but this same fact opposes the theory (2) that the primary product is Ag_2O_3, which then decomposes to AgO.

The concentration of AgO increased rapidly during a charge at the upper potential (E and F, Fig. 1) and at the same time the amount of Ag_2O decreased. It could not be determined from the x-ray patterns whether or not any Ag_2O remained by the time the electrode was half charged (G, Fig. 1), although metallic Ag was still fairly strong. X-ray patterns showed only AgO and metallic silver, both at the end of this potential plateau (H, Fig. 1) and after gassing (I, Fig. 1). When a charge was ended after 5% of the electrode capacity had been added at the second potential plateau (E, Fig. 1), comparison of x-ray patterns before and after the electrode was allowed to stand on open circuit for 24 hr indicated that Ag_2O had increased and the Ag had decreased, while only traces of AgO remained. Similar results required a 7-day stand, after 13% of the charge took place at the second step (F, Fig. 1). This confirms the report (9) that Ag and AgO react during a stand.

The first reaction at the second potential plateau appears to be Ag_2O oxidizing to AgO, since Ag_2O seems to anodize more rapidly than Ag. Then, or perhaps simultaneously, much of the remaining Ag goes to AgO, with any Ag_2O which may be formed in this process being preferentially oxidized to AgO. The reaction $Ag + AgO \rightarrow Ag_2O$ probably does not occur appreciably during a charge, since it appears to be very slow under the conditions of the experiment.

Although trickle charges lasting several days did convert more of the remaining Ag to AgO, overcharges at the normal or even higher rates were more effective in oxidizing the Ag and gave the sharpest diffraction patterns. Strong oxygen gassing appeared to perfect crystallinity. For example, the AgO lines were very sharp after a 200% charge at 100 ma, with only a very small amount of metallic Ag remaining visible in the x-ray diffraction patterns, perhaps arising from the grid mesh. Similar results were obtained by anodizing the charged electrode for 20 hr at 750 ma, at a potential of 0.68-0.71 v. No lines were ever found in the x-ray patterns which could be attributed to a higher oxide, such as Ag_2O_3, despite any of these lengthy treatments well above the equilibrium potential reported for AgO/Ag_2O_3. The transient high open-circuit potentials noted by Jones, *et al.* (3) at the end of a lengthy charge need not be attributed to higher oxides. It seems likely that the transient potentials on silver were probably potentials of the HO_2^--OH^- system. This potential would continue until enough Ag_2O was formed to establish the Ag_2O/AgO equilibrium potential. It was reported by Pleskov (4) that monovalent Ag oxidized to trivalent Ag at high potentials. His results could be interpreted in other ways. This matter is being given further consideration.

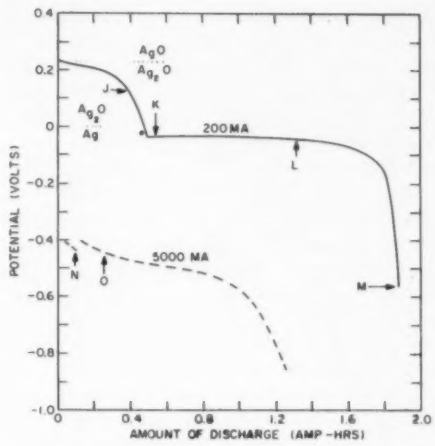

Fig. 2. Discharges of the Ag electrode at the 15-min and 9-hr rates. Letters refer to points at which x-ray diffraction patterns have been obtained. Potentials are given with respect to a Ag/Ag_2O reference electrode.

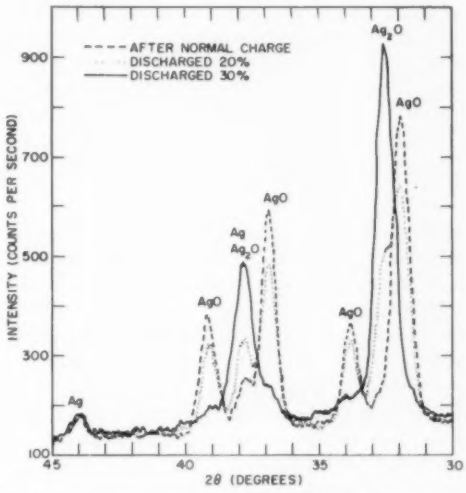

Fig. 3. Spectrogoniometer x-ray diffraction patterns of a charged and partially discharged Ag electrode.

A typical low-rate discharge (Fig. 2) showed the two steps which are associated with silver electrodes. Ag_2O had appeared on the electrode after it was partially discharged at the upper step (J, Fig. 2). The amount of AgO had decreased and metallic Ag remained constant, compared with a charged electrode. The electrode was discharged an additional 10%, reaching the lower potential plateau (K, Fig. 2). X-ray diffraction showed that practically no AgO remained on the surface at this point, and the x-ray pattern of Ag_2O was very strong, with Ag unchanged. The diffraction patterns for this marked change in surface composition are shown in Fig. 3. There is no doubt that the interior of the electrode still contained much AgO, but the x-ray diffraction patterns and the electrode potential only showed what was present near the surface. An electrode discharged 70% showed more Ag than Ag_2O (L, Fig. 2), and at the end of the discharge Ag alone was detected (M, Fig. 2). The only reaction detected

at the upper potential plateau was $AgO \rightarrow Ag_2O$. After the surface is covered with Ag_2O, the surface reaction (which determines the potential) appears to be $Ag_2O \rightarrow Ag$, although there probably is a large amount of AgO in the interior of the electrode which is discharging at this lower potential.

When the electrode was discharged for 7% at a high rate, x-ray diffraction patterns showed that Ag_2O had formed (N, Fig. 2), and after a 20% discharge the amount of Ag_2O had increased (O, Fig. 2). A comparison of the diffraction patterns showed that metallic Ag increased very little if at all during the first 20% of this discharge, despite the fact that the potential of the electrode was more than 0.4 v below the reversible Ag/Ag_2O potential.

Comparison of charge and discharge capacity showed a very high efficiency, in contrast to the report (3) that only 30% of the current charged the electrode at the second potential level. Gas evolution of a commercial 100-amp-hr Ag-Zn storage battery was measured during a 5-amp charge (Fig. 4). The potential changes shown represent changes in the silver plate, since the positive plate became fully charged before the negative one. No oxygen evolution was detected until near the end of a charge. This confirms the earlier report (1) that the oxidation is quantitative and reversible. The contradictory results obtained by Jones, *et al.* (3) may be due to their rapid charging rate.

Structure of Silver Oxides

The structure of Ag_2O had already been established as being a face-centered cube with a side a_o of 4.72Å when Jones and Thirsk (10) described a material thought to be AgO with a similar face-centered cubic structure ($a_o = 4.96$Å), and also gave evidence for a silver suboxide with a cubic structure ($a_o = 4.56$Å). However in 1924 Levi and Quilico (11) had prepared supposed suboxides by several methods, but examination by x-ray diffraction had shown only the patterns of Ag and Ag_2O. Jones, Thirsk, and Wynne-Jones (3) proposed, on the basis of the report of Jones and Thirsk, and of their own work, that the oxides of Ag are formed by the introduction of oxygen into the octants of the face-centered cubic silver lattice, and in order to complete this series they proposed Ag_2O_3 as an intermediate between AgO with half-filled octants and the hypothetical AgO_2 with completely filled octants. The data on which these investigators have based their conclusions may be interpreted otherwise.

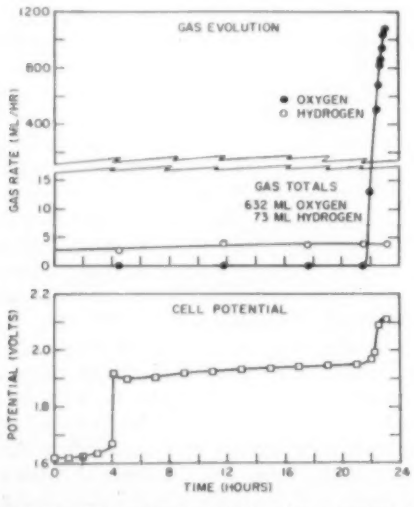

Fig. 4. Potential and gas evolution for a typical low-rate charge of a Ag-Zn storage battery.

There were no diffraction data for AgO in the literature at the time that Jones and Thirsk (10) anodized Ag in H_2SO_4. They assumed that their final product was AgO. In order to check this, they prepared silver peroxynitrate (and presumably boiled it to decompose it), and reacted a silver salt with a persulfate. They reported that all three preparations showed the same x-ray pattern, which they published as AgO. The results of Mulder (12), and Skanavi-Grigor'eva and Shimanovich (13), however, showed that the so-called silver peroxysulfate Ag_2SO_{12} is the product of electrolysis of a Ag_2SO_4 solution. Since the first anodic reaction of Jones and Thirsk was the formation of Ag_2SO_4, it is seen that their second anodic reaction should be formation of silver peroxysulfate.

The two preparations used by Jones and Thirsk for the check of their "AgO" are rather similar. Depending on reaction conditions, a silver salt solution with a persulfate may give either AgO or a compound with a formula like Ag_7SO_{12} (14). The close relationship between silver peroxysulfate and silver peroxynitrate has been noted for many years. Luther and Pokorny (1) prepared these compounds in three ways: by anodizing Ag in dilute H_2SO_4, by electrolysis of a $AgNO_3$ solution, and by electrolysis of a Ag_2SO_4 solution. They used these compounds for the "Ag_2O_3" potential measurements which are so often cited in the literature. It was concluded by Luther and Pokorny that neither the sulfate nor the nitrate was an integral part of these peroxy compounds, since both of the compounds gave the same potential and decomposed cathodically in KOH to AgO, then to Ag_2O, and finally to Ag. Therefore they reported the potential of these compounds with respect to AgO as the Ag_2O_3/AgO potential. However, Sulc (15), Mulder and Heringa (16), Tanatar (17), Watson (18), and Brown (19) all found that the compound, which they obtained by electrolysis of a $AgNO_3$ solution under various conditions, always had the empirical formula Ag_7NO_{11}. In 1954 this was confirmed again by Skanavi-Grigor'eva and Shimanovich (20), and they also reported the similarity in composition and valency of the compounds obtained by anodizing $AgNO_3$ or AgF solutions. This has recently been denied by Graff and Stadelmaier (21), but only on the grounds that a compound with the same structure was obtained by anodizing either AgF or $AgNO_3$ solutions, although they did not report analyses of their products. Yet in 1935 similar x-ray patterns had been found by Brækken (22) for what he considered to be Ag_2O_3 stabilized by either Cl, F, N, or S, with the best results from the compound with N (i.e., Ag_7NO_{11}). The same diffraction pattern for Ag_7NO_{11} has been reported more recently (23, 24), and a similar pattern has been obtained by

Table I. Diffraction data for silver anodized in H_2SO_4 and in $AgNO_3$

"AgO" from H_2SO_4[a]		Ag_7NO_{11}[b]	
d[c]	I/I_o[d]	d	I
2.85	s	2.839	95
2.48	ms	2.459	56
		2.262	15
1.75	s	1.745	98
		1.669	17
1.49	s	1.486	122
1.45	vw	1.422	30
		1.233	28
1.136	ms	1.133	75
1.106	ms		
1.104	ms	1.103	60
		1.006	63
0.953	ms	0.950	86
0.871	vw	0.873	33
0.839	m	0.835	126
0.828	m	0.823	81
0.783	w		

[a] From Jones and Thirsk (10).
[b] From Zvonkova and Zhdanov (23), omitting lines with photometric intensity of 10 or less.
[c] Interplanar spacing in A.
[d] Relative intensity: s = strong, m = medium, w = weak, v = very.

allowing O_3 to react with Ag and Ag_2O (25). Apparently all of the diffraction patterns reported for silver peroxy compounds are practically identical. Table I shows that the anodic product which Jones and Thirsk (10) reported as AgO has the same lines as Ag_7NO_{11} and probably was in reality the so-called silver peroxysulfate.

In order to check these conclusions a silver electrode was charged at 100 ma in 2*N* H_2SO_4. The initial reaction was $Ag \rightarrow Ag_2SO_4$, as reported (10). Then the potential rose sharply (by 1.3 v), and black spots appeared on the plate. This black material decomposed readily in the acid with vigorous evolution of gas. An electrode which was partially covered with this black material was examined. The diffraction pattern, which was started within 10 min after the end of electrolysis, showed the lines of four substances: Ag, Ag_2SO_4, a compound with lines like those shown in Table I, and traces of AgO. After being allowed to stand in dry air for 8 days, this electrode showed only Ag, Ag_2SO_4, and a strong diffraction pattern for AgO. Obviously the peroxysulfate had decomposed to AgO.

It had been stated by Jones and Thirsk (10) that a minimum of 3 hr elapsed between electrolysis and examination of the specimen. This would allow formation of some AgO before their x-ray diffraction examination. Their patterns may have been similar to those observed in this study: a mixture of Ag, Ag_2SO_4, AgO, and the peroxysulfate. If the lines of the patterns they attributed to "AgO" and those of Ag and Ag_2SO_4 are subtracted from the pattern of the suggested mixture, the lines remaining belong to the true pattern of AgO. Jones and Thirsk appear to have subtracted the lines of Ag_2O from such a remaining pattern, since they stated that Ag_2O was present (although none was found under these conditions in this present study). The lines which then remained were attributed to traces of a face-centered cubic substance having $a_o = 4.56$Å, which was suggested as belonging to a suboxide of silver. Table II shows that the pattern of AgO, by an unfortunate coincidence, contains many of the lines of Ag_2O, and that the remaining lines, none of which are strong, could be indexed as belonging to a cube with $a_o = 4.56$Å. Jones, Thirsk, and Wynne-Jones (3), probably relying on this earlier work, reported only Ag, silver suboxide, and Ag_2O on their fully charged electrode from alkaline solution. It is likely that they actually had Ag and AgO.

The weak Ag_2O line for $d = 3.35$, which is listed in Table II, was never observed at this laboratory. The AgO values given in this table agree closely with those previously reported (21, 25, 26) except that the weak line reported at $d = 2.95$ (21, 26) was not observed on silver anodized in 35% KOH despite repeated attempts with both the sintered silver electrode and a silver sheet, nor was the peak at $d = 2.78$ resolved into the two lines which have been reported (21, 26). When sheet silver was charged in 5% KOH this peak could be resolved into two lines, and often the weak peak at $d = 2.95$ could be observed.

The lack of resolution of the $d = 2.78$ doublet on specimens anodized in 35% KOH may be attributed to limited perfection in the crystal lattice, or it may be caused by particle-size broadening of the x-ray lines. A third possible cause of this effect, and of the lack of line $d = 2.95$, may be variation in the positions taken up by the oxygen atoms within the electrochemically formed lattices. Scatturin, Bellon, and Zannetti (26) used the line $d = 2.95$ corresponding to (hkl) of (110) to assign the distribution of the oxygen atoms. The lack of this line on specimens anodized in 35% KOH may denote a particular distribution of oxygen in the lattice positions, leading

Table II. Diffraction data for AgO, Ag_2O, and "silver suboxide"

AgO[a]		Ag_2O[b]		"Silver Suboxide"[c]
d	I/I_o	d	I/I_o	d
		3.35	1	
2.78	vs	2.72	100	
2.63	m			2.63
2.42	s	2.36	40	
2.29	m			2.28
1.74	w			
1.701	m			
1.678	w	1.67	24	
1.621	m			1.61
1.478	w			
1.451	mB[d]			
1.409	wB	1.42	16	
1.395	mB			
1.375	m	1.36	3	1.375
1.308	vw			1.316
1.208	vw			
		1.18	1	1.185
1.143	vw			
1.125	vw			
1.104	w			
1.099	w	1.08	2	
1.067	w	1.05	2	1.046

[a] Values observed for Ag specimen anodized in 35% KOH.
[b] From x-ray diffraction data cards ASTM 1950 card No. 1-1041.
[c] Calculated for a face-centered cube with $a_o = 4.56$A
[d] B indicates a broad diffuse diffraction peak.

to sufficient change in parameter to bring the doublet at $d = 2.78$ into coincidence. The resolution of these questions and their possible relation to the electrochemical activity and utilization of the battery oxide merit further study.

Summary

X-ray diffraction patterns of a silver electrode showed only the lines of Ag and Ag_2O when the electrode was charged anodically at potentials up to 250 mv above the Ag/Ag_2O potential. AgO could be formed at a potential as low as 308 mv, which indicates that the primary product at the second potential plateau is not a higher oxide which then decomposes to AgO. After the Ag_2O on the surface of the electrode oxidizes to AgO, much of the Ag deeper in the electrode then oxidizes. The silver electrode charges efficiently at the first two potential plateaus. Since the reaction $Ag + AgO \rightarrow Ag_2O$ takes place very slowly, it probably has little effect on charges of a silver electrode under normal conditions. At the end of a normal charge, the electrode contained only AgO and a little Ag. The AgO crystallinity was perfected by holding the electrode at potentials well above the gassing potential. No higher oxide was detected, even with lengthy anodization 0.3 v above the reported $AgO/"Ag_2O_3"$ potential.

The surface of a AgO electrode becomes covered with Ag_2O at the time when its potential reaches the lower plateau during low-rate discharges. Even though a high-rate discharge failed to show the first potential level and discharged at least 0.4 v below the Ag/Ag_2O potential, metallic Ag did not form in appreciable amounts during the early parts of this discharge.

The charge of a silver electrode in $2N$ H_2SO_4 goes first to Ag_2SO_4 and then to the so-called peroxysulfate. The latter compound decomposes on standing in dry air to give AgO. Neither Ag_2O nor a silver suboxide was found in acid. The existence of a suboxide on anodized silver is doubtful.

Manuscript received Feb. 27, 1959. This paper was prepared for delivery before the Columbus Meeting. Oct. 18-22, 1959.

Any discussion of this paper will appear in a Discussion Section to be published in the June 1960 JOURNAL.

REFERENCES

1. R. Luther and F. Pokorny, *Z. anorg. Chem.*, **57**, 290 (1908).
2. A. Hickling and D. Taylor, *Discussions Faraday Soc.*, **1**, 277 (1947).
3. P. Jones, H. R. Thirsk, and W. F. K. Wynne-Jones, *Trans. Faraday Soc.*, **52**, 1003 (1956).
4. Yu. V. Pleskov, *Doklady Akad. Nauk S.S.S.R.*, **117**, 645 (1957).
5. G. Rädlein, *Z. Elektrochem.*, **61**, 727 (1957).
6. K. Nagel, R. Ohse, and E. Lange, *Z. Elektrochem.*, **61**, 795 (1957).
7. W. J. Hamer and D. N. Craig, *This Journal*, **104**, 206 (1957).

7a. J. F. Bonk and A. B. Garrett, *ibid.*, **106**, 612 (1959).

8. G. W. Work and C. P. Wales, *ibid.*, **104**, 67 (1957).
9. I. A. Denison, *Trans. Electrochem. Soc.*, **90**, 387 (1946).
10. F. Jones and H. R. Thirsk, *Trans. Faraday Soc.*, **50**, 732 (1954).
11. G. R. Levi and A. Quilico, *Gazz. chim. ital.*, **54**, 598 (1924).
12. E. Mulder, *Rec. Trav. Chim.*, **18**, 91 (1899); **19**, 115 (1900).
13. M. S. Skanavi-Grigor'eva and I. L. Shimanovich, *Zhur. Obshchei Khim.*, **26**, 1540 (1956).
14. J. H. de Boer and J. Van Ormondt, *Proc. Intern. Symposium on the Reactivity of Solids*, Gothenberg 1952, Part I, 557 (1954).
15. O. Sulc, *Z. anorg. Chem.*, **12**, 89, 190 (1896).
16. E. Mulder and J. Heringa, *Rec. Trav. Chim.*, **15**, 1, 235 (1896); E. Mulder, *ibid.*, **16**, 57 (1897).
17. S. L. Tanatar, *Z. anorg. Chem.*, **28**, 331 (1901).
18. E. R. Watson, *J. Chem. Soc.*, **89**, 578 (1906).
19. M. J. Brown, *Trans. Am. Electrochem. Soc.*, **30**, 327 (1916).
20. M. S. Skanavi-Grigor'eva and I. L. Shimanovich, *Zhur. Obshchei Khim.*, **24**, 1490 (1954).
21. W. S. Graff and H. S. Stadelmaier, *This Journal*, **105**, 446 (1958).
22. H. Brækken, *Kgl. Norske Videnskab. Selskab Forh.*, **7**, 143 (1935).
23. Z. V. Zvonkova and G. S. Zhdanov, *Zhur. Fiz. Khim.*, **22**, 1284 (1948).
24. H. E. Swanson, R. K. Fuyat, and G. M. Ugrinic, *Nat. Bur. Stds. Circ. 539*, Vol. IV, 61 (1955).
25. G-M. Schwab and G. Hartman, *Z. anorg. u. allgem. Chem.*, **281**, 183 (1955).
26. V. Scatturin, P. Bellon, and R. Zannetti, *Ricerca sci.*, **27**, 2163 (1957).

Brief Communications

The JOURNAL accepts short technical reports having unusual importance or timely interest, where speed of publication is a consideration. The communication may summarize results of important research justifying announcement before such time as a more detailed manuscript can be published. Consideration also will be given to reports of significant unfinished research which the author cannot pursue further, but the results of which are of potential use to others. Comments on papers already published in the JOURNAL should be reserved for the Discussion Section published biannually.

Submit communications in triplicate, typewritten double-spaced, to the Editor, Journal of The Electrochemical Society, 1860 Broadway, New York 23, N. Y.

Hydrogen Overvoltage on Bright Platinum

III. Effect of Hydrogen Pressure

Sigmund Schuldiner

U. S. Naval Research Laboratory, Washington, D. C.

ABSTRACT

The effect of hydrogen pressure on the hydrogen overvoltage of bright platinum was determined in acid. From the anodic and cathodic overvoltages, kinetic parameters were determined. A mechanism controlled by slow combination of hydrogen atoms adsorbed on the platinum surface fits the experimental data. From the Langmuir adsorption isotherm it is shown that the surface of the active platinum electrode at equilibrium is sparsely covered with hydrogen atoms.

Several investigators (1-6) have established that hydrogen overvoltage η at a given current density in the Tafel region on a cathode evolving hydrogen is related to the hydrogen pressure by the expression $\eta = \eta_\circ + (RT/2\mathbf{F}) \ln P_{H_2}$, where η is the potential difference between the working electrode and a reversible hydrogen reference electrode in the same solution, $\eta_\circ$ is the overvoltage at 1 atm of hydrogen, P_{H_2} is the partial pressure of hydrogen above the solution, and R, T, and $\mathbf{F}$ have their usual significance. Vetter and Otto (6) in an investigation of the effect of pressure on anodic and cathodic overvoltage of an inactive platinum electrode in acid solution were able to determine the kinetic parameters and to establish reaction mechanisms that fitted their experimental findings. This investigation is a continuation of previous work (7, 8) on hydrogen overvoltage on an active, smooth platinum electrode.

Experimental

The general experimental techniques were the same as before (7, 8). The cell was constructed of Teflon and was a simplified version of the one shown in Fig. 1 of reference (8). The platinum (99.99%) cathode was a small sphere at the end of a very short length of exposed wire (apparent area 0.084 cm^2). The solution was in all cases 1M H_2SO_4. Purified gases consisting of either pure hydrogen, a prepared mixture of 5% hydrogen in nitrogen, or mixtures of hydrogen and helium were bubbled through the acid solution in the cell. The hydrogen-helium mixtures were prepared by mixing hydrogen and helium directly from their cylinders through rotameters into the gas purification train. This gave a composition of the two gases which remained constant for any given setting of the flow rates. The pressure of the gas introduced into the cell was always 1 atm. The partial pressure of hydrogen was determined by measuring the potential difference between a reversible hydrogen electrode and a saturated α Pd-H electrode in the cell. Since it was established (9) that the potential-determining reaction on the saturated α Pd-H electrode is independent of hydrogen pressure, the potential difference, E, between it and the reversible hydrogen electrode in the same solution obeyed the Nernst relation $E = 0.05 + (RT/2\mathbf{F}) \ln P_{H_2}$. From this potential the partial pressure of hydrogen flowing through the cell was determined.

After the solution was pre-electrolyzed and the Pt electrode was further cleaned by anodic polarization, the pseudo-capacitance test (7) was used to determine surface cleanliness and also the IR drop between it and the reference electrode (a Pt gauze electrode in the same solution). Repeated measurements were taken at each partial pressure of hydrogen under both anodic and cathodic polarization. Overvoltages at each current density were time independent. The data given are average values of individual runs. The precision of an individual reading was better than 0.5 mv. The spread of each particular reading for a given experiment was ±1 mv. The temperature was 25° ± 1°C.

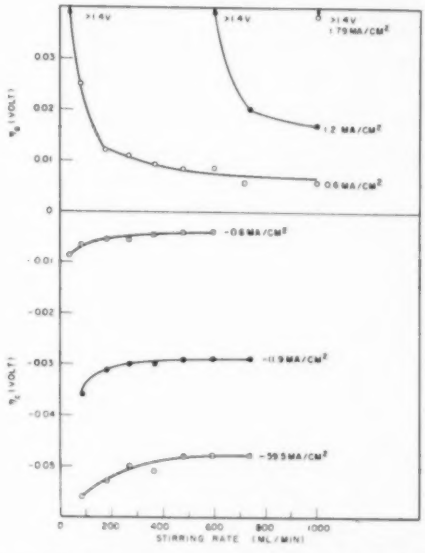

Fig. 1. Effect of stirring rate on η_a and η_c at 1 atm of hydrogen.

Experimental Results

Concentration polarization effects were minimized by stirring the solution with gas at rates for which a further increase in stirring rate would not affect the measured overvoltage. Figure 1 shows the effect of stirring rate on overvoltage for pure hydrogen flowing through the solution. The data show that at the higher current densities flow rates of at least 500 ml/min are required. It should be noted also that the dependence on stirring rate is much more pronounced for anodic than cathodic polarization. This is because for anodic polarization molecular hydrogen must diffuse to the surface at a sufficiently fast rate to maintain a given concentration of atomic hydrogen on the surface. This would be similar to the case described by Frumkin and Aikasjan (10). In the case of cathodic polarization the difference between the hydrogen pressure in the bulk of the solution and at the electrode surface is not as pronounced.

Plots of cathodic overvoltage η_c, vs. logarithm of apparent negative current density at different hydrogen pressures are shown in Fig. 2. It should be noted that the Tafel b slopes are 0.025-0.026 v rather than 0.0295 v expected at 25°C. This confirmed previous results (8). Figure 3 shows plots of anodic overvoltage η_a vs. logarithm of current density. At low currents there is a linear relationship between anodic and cathodic overvoltages and current density (Fig. 4). From experimental data shown in Fig. 2-4, kinetic parameters can be determined and a reaction mechanism suggested.

Derivation of Kinetic Equations

Cathodic overvoltage.—It is assumed that the cathode overvoltage mechanism is primarily a discharge of hydronium ions in the double layer followed by a slow combination of hydrogen atoms to molecules, that is

$$H^+ + e = H \qquad \text{(discharge step)} \qquad [1a]$$

$$2H = H_2 \qquad \text{(combination step)} \qquad [1b]$$

Assuming a Langmuir isotherm, kinetic equations for the discharge step can be written

$$\vec{i}_d = \vec{k}_d(H^+)(1-\theta)\exp(-\alpha\eta_c\mathbf{F}/RT) \qquad [2a]$$

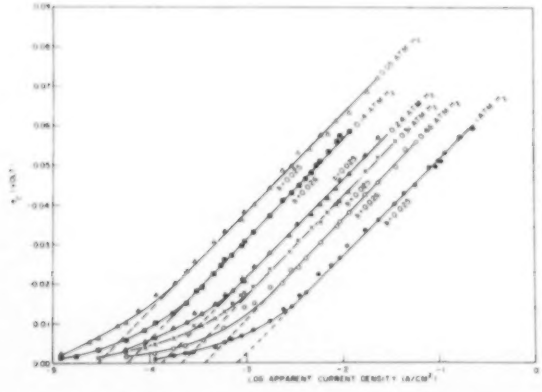

Fig. 2. Relations for η_c vs. log $(-i_c)$ at different partial pressures of hydrogen.

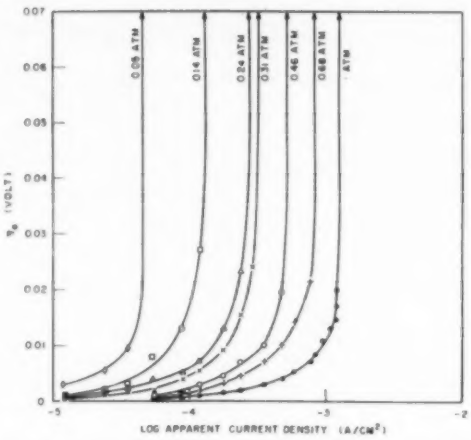

Fig. 3. Relations for η_a vs. log i_a at different partial pressures of hydrogen.

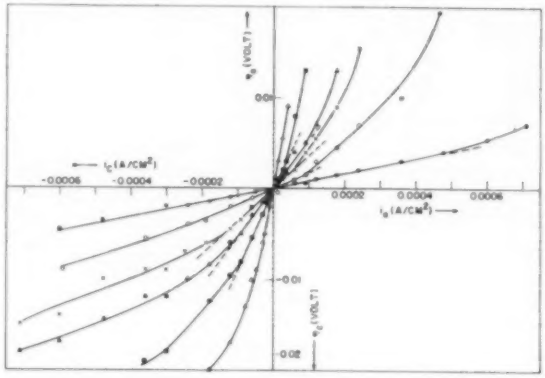

Fig. 4. Low current density relations for η vs. i. Partial pressures of hydrogen as in Fig. 2.

$$\overleftarrow{i}_d = \overleftarrow{k}_d\theta\exp[(1-\alpha)\eta_c\mathbf{F}/RT] \qquad [2b]$$

where $\vec{i}_d$, $\overleftarrow{i}_d$ represent forward and reverse current densities, respectively. The convention that cathodic current is negative and anodic current is positive is used; $\vec{k}_d$, $\overleftarrow{k}_d$ are forward and reverse rate constants which are negative and positive, respectively. (H^+) is the hydronium ion concentration in the double layer which in 1M H_2SO_4 remains virtually constant in the current density range investigated, θ is the fraction of available surface covered with atomic hydrogen, and α is the transfer coefficient. The discharge step is assumed virtually at equilibrium, hence $\vec{i}_d = -\overleftarrow{i}_d$. Therefore

$$\theta/(1-\theta) = -\mathbf{K}'\exp(-\eta_c\mathbf{F}/RT) \qquad [3]$$

where $\mathbf{K}'$ is a constant. For the slow combination step

$$\vec{i}_c = \vec{k}_c\theta^2 \qquad [4a]$$

$$\overleftarrow{i}_c = \overleftarrow{k}_c P_{H_2}(1-\theta)^2 \qquad [4b]$$

Here the partial pressure of hydrogen at the metal solution interface is considered independent of i_c. This is based on the proposition that the diffusion

of molecular hydrogen is not rate-determining. Hence the net cathodic current density i_c is the algebraic sum $i_c = \vec{i}_c + \overleftarrow{i}_c$, where the magnitude of $\vec{i}_c$ is not less than the magnitude of $\overleftarrow{i}_c$. At equilibrium, i_c is zero, and $\vec{i}_c = -\overleftarrow{i}_c = i_{o,c}$, where $i_{o,c}$ is the cathodic exchange current density (negative). Hence

$$\vec{k}_c\theta_o^2 = -\overleftarrow{k}_c P_{H_2}(1-\theta_o)^2 = i_{o,c} \qquad [5]$$

where θ_o is the fraction of available surface covered with atomic hydrogen at equilibrium. Therefore, from [4] and [5]

$$i_c = i_{o,c}[(1-\theta)^2/\theta_o^2]\{\theta^2/(1-\theta)^2 - \theta_o^2/(1-\theta_o)^2\} \qquad [6]$$

Substituting for $\theta/(1-\theta)$ from Eq. [3], and noting that at equilibrium $\eta_c = 0$ so that $K'^2 = \theta_o^2/(1-\theta_o)^2$, we obtain

$$i_c = i_{o,c}[(1-\theta)^2/(1-\theta_o)^2]\cdot\{\exp(-2\eta_c\mathbf{F}/RT) - 1\} \qquad [7a]$$

At low coverages, the factor involving the θ's reduces to unity. Equation [7a] can be expressed in logarithmic form at 25°C and at low coverages as

$$\eta_c = -0.0295 \log[(i_c/i_{o,c}) + 1] \qquad [7b]$$

This is in effect the equation first derived by Hammett (11).

Anodic overvoltage.—Here the reaction can be written as the inverse of the cathodic case, i.e., a slow dissociation of H_2 followed by ionization of H. The kinetic equations for the ionization step are

$$\vec{i}_i = \vec{k}_i\,\theta\exp(\alpha\eta_a\mathbf{F}/RT) \qquad [8]$$

$$\overleftarrow{i}_i = \overleftarrow{k}_i\,(H^+)(1-\theta)\exp[-(1-\alpha)\eta_a\mathbf{F}/RT] \qquad [9]$$

where $\vec{i}_i$, $\overleftarrow{i}_i$ are forward and reverse current densities for ionization; $\vec{k}_i$, $\overleftarrow{k}_i$ are forward and reverse rate constants and are positive and negative, respectively. The α used here is not the same as before. The ionization step is considered at equilibrium, hence $\vec{i}_i = -\overleftarrow{i}_i$. Therefore

$$\theta/(1-\theta) = -K_i'\exp(-\eta_a\mathbf{F}/RT) \qquad [10]$$

For the slow dissociation step

$$\vec{i}_a = \vec{k}_a P_{H_2}(1-\theta)^2 \qquad [11a]$$

$$\overleftarrow{i}_a = \overleftarrow{k}_a\theta^2 \qquad [11b]$$

The net anodic current density i_a is the algebraic sum $i_a = \vec{i}_a + \overleftarrow{i}_a$, where the magnitude of $\vec{i}_a$ is not less than the magnitude of $\overleftarrow{i}_a$. At equilibrium, i_a is zero, and $\vec{i}_a = -\overleftarrow{i}_a = i_{o,a}$ where $i_{o,a}$ is the anodic exchange current (positive).

Therefore

$$i_{o,a} = \vec{k}_a P_{H_2}(1-\theta_o)^2 = -\overleftarrow{k}_a\theta_o^2 \qquad [12]$$

Following the same analysis as above, one obtains

$$i_a = i_{o,a}[(1-\theta)^2/(1-\theta_o)^2]\{1 - \exp(-2\eta_a\mathbf{F}/RT)\} \qquad [13]$$

At 25°C and low coverages, Eq. [13] reduces to the logarithmic form

$$\eta_a = -0.0295 \log[1 - i_a/i_{o,a}] \qquad [14]$$

Calculation of Kinetic Parameters

The value of $i_{o,c} = -i_{o,a}$ was determined from Eq. [7a] in its limiting low coverage form. The graphs of i_c vs. $[\exp(-2\eta_c\mathbf{F}/RT) - 1]$ for various values of P_{H_2} are shown in Fig. 5. The relationship given by Vetter and Otto (6), which can be derived from Eqs. [4], [5], [11], and [12] when $\theta_o << 1$, is $\theta_o^2 = -i_{a,L}/i_{c,L}$, where $i_{a,L}$ and $i_{c,L}$, the limiting anodic and cathodic current densities, can be used to determine θ_o. It was assumed that $i_{c,L}$ is not algebraically greater than -10 amp/cm^2. This is a reasonable assumption since the Tafel slope in Fig. 2 for pure hydrogen is maintained down to negative currents approaching -1 amp/cm^2. In addition, a calculation by Salzberg and Schuldiner (12) indicated that on a Pt electrode the maximum coverage of the surface with adsorbed atomic hydrogen at -1 amp/cm^2 would be about 2%. Hence using the arbitrary value of -10 amp/cm^2 for $i_{c,L}$ and obtaining $i_{a,L}$ for various hydrogen pressures from Fig. 3, θ_o^2 can be calculated for each pressure. It should be mentioned that $i_{c,L}$ is independent of hydrogen pressure; in other words, $i_{c,L}$ is only dependent on the rate of hydrogen evolution at the cathode. Using θ_o^2 values, which indicate a low coverage with atomic hydrogen, obtained in this way, the rate constant $\vec{k}_c = \overleftarrow{k}_a = -12.08$ was calculated from Fig. 6 using Eq. [5]. The rate constant $\overleftarrow{k}_c = \vec{k}_a = 0.00143$ was calculated using Eq. [5] also. Figure 7 shows the linear relation between P_{H_2} and $i_{o,c}$ which was used to determine this rate constant.

The rate constant $k = \pm(di/d\eta)_{\eta\to 0}$ (negative for cathodic, positive for anodic directions) for the over-all reaction near equilibrium, where there is a linear relation between η and i, was determined from Fig. 4 for various hydrogen pressures. These values

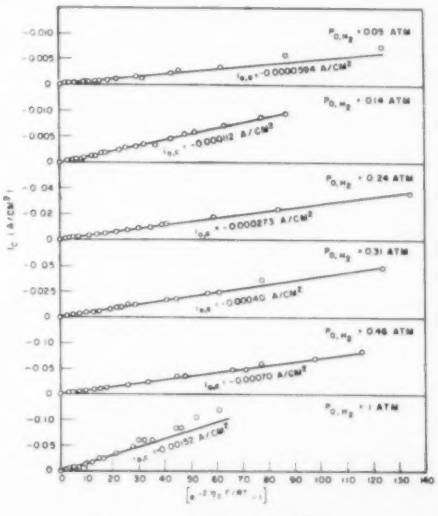

Fig. 5. i_c vs. $[\exp(-2\,\eta_c\mathbf{F}/RT - 1]$

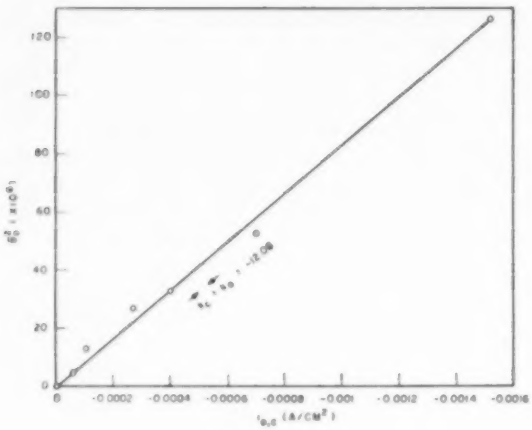

Fig. 6. θ_o^2 vs. $i_{o,c}$

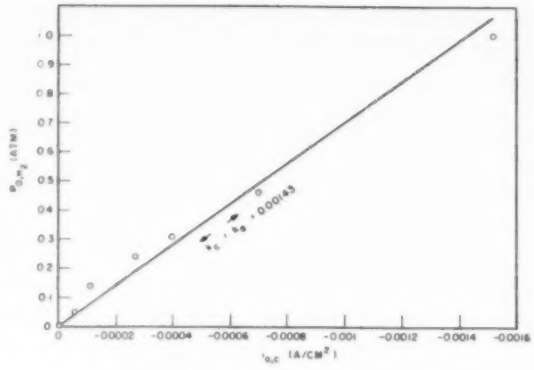

Fig. 7. P_{H_2} vs. $i_{o,c}$

are shown in Table I. Also shown are stoichiometric numbers μ calculated from the Horiuti relationship (13) $\mu = 2i_{o,c}\mathbf{F}/kRT$.

Discussion

The assumption that the surface of the active smooth Pt electrode used in this investigation was sparsely covered with atomic hydrogen at equilibrium can be verified by determining the Langmuir adsorption isotherm. This isotherm is $\theta_o^2/(1-\theta_o)^2 = KP_{H_2}$. At low coverages $\theta_o^2 = KP_{H_2}$. The linear data of Fig. 6 and 7 can be combined to give a reasonably good linear isotherm with a K value of 116×10^{-6}. The fact that this isotherm holds throughout the range of hydrogen pressures investigated, with a zero intercept, virtually proves that the surface of the platinum at zero current is only sparsely covered with atomic hydrogen. If one changes $i_{c,t}$ from -10 amp/cm^2 to a value smaller by one to two orders of magnitude, or to any larger value, this still would not affect the linearity of the isotherm, but would merely change K.

The linear relations shown in Fig. 5 confirm the mechanisms assumed, namely, that the hydronium ion discharge is followed by a rate-determining slow combination step. Another way of showing this is to plot anodic and cathodic overvoltages vs. the logarithmic relationships given in Eqs. [7b] and [14]. This should give a straight line with a slope of 0.0295 v. Figure 8 shows this relation for all partial pressures of hydrogen and confirms that the mechanism assumed is a reasonable one. Additional proof is given by the fact that the stoichiometric numbers

Table I. Cathodic kinetic parameters

P_{H_2} atm	$-k$, mho/cm^2	$-i_{o,c}$ amp/cm^2	μ
1.0	0.13	0.00152	0.92
0.46	0.053	0.00070	1.03
0.31	0.027	0.00040	1.15
0.24	0.019	0.000273	1.12
0.14	0.011	0.000112	0.79
0.05	0.0046	0.0000594	1.01
		Av =	1.00

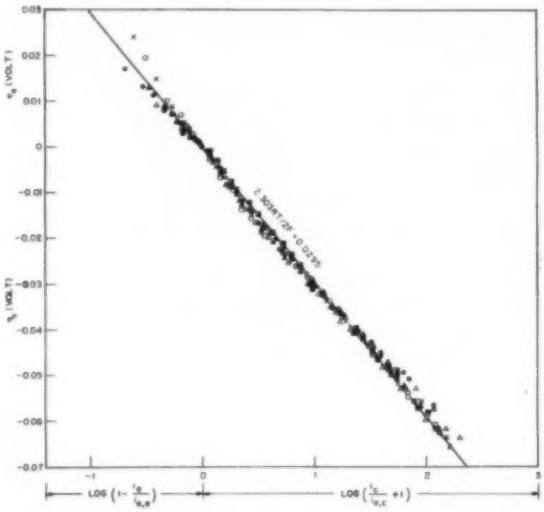

Fig. 8. Hammett relations for η vs. i. Partial pressures of hydrogen as in Fig. 2.

μ for the series of hydrogen pressures shown in Table I are all approximately equal to one.

The Tafel relation derived from the curves in Fig. 2 is only an empirical equation which proves to be compatible with theoretical Eq. [7b]. However at higher current densities one would expect a definite upward curvature from the straight lines shown in Fig. 2. At log $(-i_c) = 0$, the curvature would be such that η_c for 1 atm would be -0.083 v rather than -0.076 v as obtained by extrapolating the linear portion in Fig. 2. Similarly for the other hydrogen pressures there will be an increasing curvature as the pressure is decreased. Experimentally there was an indication of such a deviation at high current densities. However, there exists also a significant concentration overvoltage effect which is undoubtedly owing to the diffusion away of molecular hydrogen from the metal solution interface (14), and it is experimentally difficult to eliminate this effect at higher overvoltages. It should also be noted that an extrapolation of the Tafel lines in Fig. 2 to zero overvoltages give current density values which are much lower than the $i_{o,c}$ values obtained from Eq. [7b].

Acknowledgment

The author is indebted to Drs. J. C. White and G. W. Castellan for their comments and suggestions.

Manuscript received Feb. 5, 1959.

Any discussion of this paper will appear in a Discussion Section to be published in the June 1960 JOURNAL.

REFERENCES

1. S. J. Bircher and W. D. Harkins, *J. Am. Chem. Soc.*, **45**, 2890 (1923).
2. M. Knobel, *ibid.*, **46**, 2751 (1924).
3. H. M. Cassel and E. Krumbein, *Z. physik., Chem.*, **A171**, 70 (1934).
4. G. Schmid and E. K. Stoll, *Z. Elektrochem.*, **47**, 360 (1941).
5. J. O'M. Bockris and R. Parsons, *Trans. Faraday Soc.*, **45**, 916 (1949).
6. K. J. Vetter and D. Otto, *Z. Electrochem.*, **60**, 1072 (1956).
7. S. Schuldiner, *This Journal*, **99**, 488 (1952).
8. S. Schuldiner, *ibid.*, **101**, 426 (1954).
9. S. Schuldiner, G. W. Castellan, and J. P. Hoare, *J. Chem. Phys.*, **28**, 16 (1958).
10. A. N. Frumkin and E. A. Aikazan, *Doklady Ak. Nauk, USSR*, **100**, 315 (1955).
11. L. P. Hammett, *J. Am. Chem. Soc.*, **46**, 7 (1924).
12. H. W. Salzberg and S. Schuldiner, *This Journal*, **104**, 319 (1957).
13. J. Horiuti, *J. Research Inst. Catalysis, Hokkaido*, **1**, 8 (1948).
14. C. A. Knorr, *Z. Elektrochem.*, **59**, 647 (1955).

A Porcelain Reference Electrode Conductive to Sodium Ions for Use in Molten Salt Systems

Roger J. Labrie and Vernon A. Lamb

Chemistry Division, National Bureau of Standards, Washington, D. C.

ABSTRACT

A reference electrode for use in molten salt systems is described. It consists of a porcelain capsule conductive to sodium ions, containing a silver electrode immersed in a melt of silver chloride and sodium chloride. The electrode is reversible to sodium ions. It is stable, reproducible, and temperature-reversible and can be used at temperatures 400° to 500° higher than can similar electrodes made of glass. The capsule-type construction prevents the salt inside the electrode from contaminating the melt under study. Electrodes made from specially prepared porcelains and also from a commercial porcelain were used. Data are presented on the resistivity of the specially prepared porcelains and on the mechanism of conduction by the porcelain.

Accurate data on electrode potentials in molten electrolytes are of importance in electrodeposition from molten salts, corrosion by molten salts, and in studies of the thermodynamic properties of molten salt systems. The amount of research in these fields has increased in recent years because of interest in the production of refractory metals by electrodeposition from molten salt solutions, in the development of molten salt batteries, and in the various applications of molten salt processes in the atomic energy program.

Several types of reference electrodes have been used in previous researches in these fields, such as the Ag/AgCl electrode with a liquid junction (1, 2); the Pt electrode (3, 4); an Ag/AgCl electrode in a graphite sheath for use in fluoride melts (5); the Cl^-/Cl_2 (graphite) electrode (6); and electrodes in glass capsules with the internal electrode in the glass capsule consisting of Na (7, 8), Na-Hg (9), Na-Sn (10, 11), and Ag in a mixture of AgCl-LiCl-KCl (12).

A reference electrode has been developed in this laboratory which is similar to that described by Bockris, *et al.* (12), but differs in that the glass capsule used by them is replaced by a porcelain capsule conductive to sodium ions. The main advantage of the porcelain electrode is that it can be used at much higher temperatures than can glass. In common with the glass capsule electrodes, it also has the advantage that salts in the capsule cannot intermix with those outside the capsule. The porcelain is reversible to sodium ions in the melt under study, and since the inner Ag/AgCl electrode is reversible, the entire electrode system is reversible. Electrodes of the design described below have been used at temperatures up to about 900°C. They should be capable of use at temperatures up to the melting point of silver. If the design were modified to make possible the retention of molten silver, the electrodes might be serviceable at temperatures approaching the softening point of the porcelain.

Preparation of Electrodes

Preparation of porcelain.—The composition of the porcelain from which most of the capsules were made was approximately: Na_2O, 2.5%; SiO_2, 73.1%; Al_2O_3, 24.4%, by weight. The objective in preparing this porcelain was to obtain a material that was nearly free of alkali metals other than sodium and of alkaline-earth metals, with the thought that such porcelain might be conductive only to sodium ions. The sodium content was chosen arbitrarily. In later work, a commercial porcelain and a porcelain containing a higher proportion of sodium were used.

The porcelain containing 2.5% Na_2O was prepared as follows: A glass of the composition $Na_2Al_2Si_2O_8$

was made by dry-milling together in a jar mill with flint pebbles an equimolar mixture of Na_2SiO_3, Al_2O_3, and SiO_2, followed by firing of the mixture at 1100°C, after which the fired mass was reground. A portion of the glass (186 g) then was milled in a 1-gal jar mill with flint pebbles for 10 to 12 hr, together with 388 g of Kentucky ball clay, 520 g of Georgia kaolin, 696 g of flint, 820 ml of water, and 0.5 g of sodium silicate or sodium carbonate. The sodium silicate (or carbonate) was added to effect deflocculation of the slip.

Construction of electrodes.—The construction of the porcelain electrode is shown in Fig. 1. The slip was formed into electrode tubes by slip-casting in a split mold of plaster of Paris, which had been formed over a glass pattern of the electrode tube. The slip-casts were dried in the mold, removed, and usually were fired to 1285°C, but some were fired as high as 1400°C. Although the higher firing temperature caused blisters to form, the tubes still were serviceable.

A T-tube of Nonex glass was sealed to the porcelain tube. At its working temperature, the glass wets the porcelain readily to form a good seal. (The porcelain that contains 10% Na_2O, described in the section on Electrical resistivity of porcelain, was joined to a T-tube of Kovar sealing glass, Corning No. 7052.)

The inner Ag electrode was made as follows: A length of 1 mm W wire, the tip of which had been cleaned by filing, was inserted into a ceramic tube of 1 mm i.d. (McDanel high-temperature porcelain) to within about 1-in. of the end of the tube. The tube was supported vertically in a clamp with the open end upward. A short length of 1 mm Ag wire was inserted into the tube and melted by applying a torch flame, first where the Ag wire touched the W and then higher as the Ag melted, so that the Ag flowed into intimate contact with the W wire and completely filled the tube. Electrical continuity between the Ag and W was checked with an ohmmeter. All of the Ag electrodes used in the cells described in this paper were constructed in this manner, so that the W-Ag thermoelectric potentials cancel. The W wire was then beaded with U glass (Corning No. 3320) and sealed into the T-tube at a position such that the tip of the Ag electrode extended nearly to the bottom of the porcelain bulb. Care must be taken in making this seal to insure that the inner electrode does not touch the inner surface of the porcelain tube. The porcelain is sufficiently translucent so that the location of the inner electrode can be checked by viewing it against a strong light.

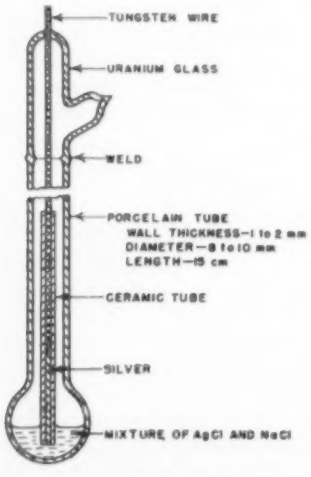

Fig. 1. Construction of porcelain electrode

The assembled electrode was filled with the desired mixture of AgCl and NaCl through the sidearm of the T-tube, which then was sealed off while evacuating the electrode through it. Evacuation and sealing are not essential, but this procedure was preferred. Various proportions of AgCl and NaCl have been used, but a mixture high in AgCl is preferred because of its lower melting point and because fewer capsules break when re-used if they contain such a mixture. Complete cells usually were assembled with two porcelain electrodes and one or two electrodes of some other type, dipped into a melt in a short cylindrical container.

Characteristics of Porcelain Electrodes

Reproducibility and stability.—Reproducibility of the porcelain electrodes was checked by measuring the potentials of cells in which identical electrodes were opposed. In the following cell, P represents the porcelain membrane; the numbers are the mole per cents of each component.

Ag/AgCl 40, NaCl 60/P/AgCl 4.76, NaCl 47.6,

KCl 47.6/P/AgCl 40, NaCl 60/Ag (I)

The results of measurements of the emf of cell (I) are shown in Table I for five replicate electrodes, represented as a to e.

It is seen that there was a difference of 5-7 mv betwen electrodes a and b, which was probably caused by a small difference in the concentrations of the electrode solutions. These were prepared separately, and an error of about one percentage unit in concentration would account for the discrepancy. The temperature of cells c/d and d/e was varied irregularly over long periods. The results show that the emf of the porcelain electrodes was stable and reproducible to within a few millivolts under temperature cycling over a period of nearly six days. These experiments also showed that the

Table I. Electromotive force of cells(I)

Cell a/b			Cell c/d			Cell d/e		
Time, hr	Temp, °C	Emf, mv	Time, hr	Temp, °C	Emf, mv	Time, hr	Temp, °C	Emf, mv
0	720	5.3	0.2	760	1.1	0	760	0.7
0.4	720	6.6	0.5	760	0.4	5	850	0.3
0.7	720	7.1	2.0	760	1.2	22	760	0.3
2.7	720	6.4	4.0	760	0.1	26	850	0.3
3.7	720	6.5	20.0	760	−2.5	27	900	0.4
			21.0	760	0.2	28	850	0.2
			26.0	828	−1.3	29	800	0.2
			29.0	760	1.4	118	770	3.0
						141	800	0.0

porcelain electrode is re-usable since electrode d was used in two separate experiments. This is a distinct advantage for a reference electrode.

The period of time required for the porcelain electrode to reach equilibrium, following a shift in temperature or other disturbance, usually ranged from a few minutes to about 30 min. Occasionally a cell potential did not become stabilized until after several hours. The cause for the variation is not known.

Temperature reversibility.—Temperature reversibility is indicated by the results shown in Table I. Additional experiments bearing on the variation of the emf of the porcelain electrode with temperature are described in this section.

Electromotive forces of the following concentration cell were measured over a range of temperature from 646° to 850°C (numbers are mole per cents).

Ag/AgCl 40, NaCl 60/P/AgCl 9.6, NaCl 45.2,

KCl 45.2/P/AgCl 78, NaCl 22/Ag (II)

The temperature was cycled within this range in a random manner over a period of several days. Repeat readings at the same temperature agreed within about 1 mv. Data are plotted in Fig. 2. The temperature at the break in the curve corresponds reasonably well with the liquidus temperature given in International Critical Tables (ICT) for the AgCl-NaCl system at a mole ratio of 40/60 (from ICT, 675°C; from Fig. 2, 688°C).

The emf of cell (II) may be written

$$E = (2.303\,RT/F)\log(0.78 \times 0.60/0.40 \times 0.22) \quad [1]$$

where mole fractions are used in the log term and activity coefficients are taken as unity. This equation is obtained by combining the equation for the emf of a concentration cell without transference with the equations for the two membrane potentials. The latter are based on the assumption that only sodium ions are transferred through the membranes. With this assumption, the over-all cell (II) process for one faraday is

AgCl (78 mole %) + NaCl (60) =

AgCl (40) + NaCl (22) [2]

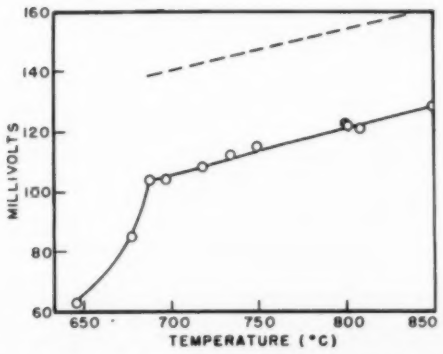

Fig. 2 Emf of cell (II) as a function of temperature. The dashed curve is calculated from Eq. [1].

Equation [1] gives the emf of this process and yields a value of E/T of 0.000144 v/deg. The slope of the curve in Fig. 2 beyond the break, i.e., in the range of temperature at which the salt phase in the left-hand electrode of cell (II) is completely molten, is 0.000148 v/deg. The agreement indicates that the porcelain electrodes behave normally with respect to temperature change.

Theoretically, the curve in Fig. 2 should extrapolate to zero emf at absolute zero. The dashed line shows the position of the theoretical curve calculated from Eq. [1]. It lies about 34 mv above the experimental curve. The difference may be due to deviations of the activity coefficients from unity, or to an effect of the potassium ions in the melt on the membrane potential (see section on Effect of potassium ions in the melt on the potential of the porcelain electrode).

Membrane asymmetry.—Theoretically, the potential of a half-cell including a sodium ion-conductive membrane in contact with a given external melt should be independent of the composition of the membrane. However, it is conceivable that unsymmetrical surface effects might result in an asymmetry potential. To check this point, cells were set up in which two capsule-type electrodes were dipped into the same melt contained in a small crucible. Melts in the two half-cells were identical, but the membranes were different, as shown in cell (III) (numbers are mole per cents).

Ag/AgCl 50, NaCl 50/P/Na-K-Sr

chloride/G/AgCl 50, NaCl 50/Ag (III)

In this cell, the membrane P was a porcelain capsule made from porcelain containing 2.5% Na_2O, fired at 1350°C, and G was a capsule of Pyrex glass. Measurements were made on two additional cells, like cell (III), except that in one cell, capsule G was replaced by a porcelain capsule that had been fired at 1400°C, and in the other by a capsule made from a commercial porcelain. (McDanel high-temperature porcelain in the form of a thermocouple protective tube, 1/2 in. OD, 1/16 in. wall; composition by weight: Al_2O_3, 56.2%; SiO_2, 43.0%; K_2O + Na_2O, 0.32%; C, Mg, and Fe oxides, 0.62%.) Temperatures ranged from about 550° to 750°C, depending on the material of the capsule. The potential of each of these three cells was less than 1 mv.

Since no significant membrane asymmetry potential was found in comparing these unlike membranes, it is unlikely that an asymmetry potential will be a complicating factor in the use of the porcelain-type electrode. The result with the commercial porcelain is especially significant, since the use of commercially available porcelain makes the rather tedious preparation of a special porcelain unnecessary. However, further work on the relationships between the composition of a porcelain and its selective permeability to specific ions might be fruitful.

Effect of the concentration of sodium chloride within the porcelain capsule.—Porcelain electrodes represented as Ag/AgCl(x), NaCl ($1-x$) porce-

lain, in which $1-x$, the mole fraction of sodium chloride, varied from 0.05 to 0.40, have shown reproducible, stable potentials. It is probable that both higher and lower proportions of sodium chloride could be used.

Effect of potassium ions in the melt on the potential of the porcelain electrode.—The effect of potassium ions on the potential of the porcelain electrode was studied by comparing cells having different ratios of sodium chloride to potassium chloride. Data for the following two cells are illustrative (numbers are in mole per cents).

Ag/AgCl 25, KCl 70, NaCl 5/P/

AgCl 50, KCl 45, NaCl 5/Ag (IV)

and

Porcelain electrode/AgCl 75,KCl 20, NaCl 5/Ag (V)

where "Porcelain electrode" designates the left electrode of cell (IV) up to and including the P membrane. The emf values for cells (IV) and (V) at 750°C, were 0.111 and 0.201 v, respectively. By use of assumptions analogous to those employed for calculating the emf of cell (II), the following theoretical values are obtained

	Cell IV v	Cell V v
Porcelain reversible to Na^+ only	0.061	0.097
Porcelain reversible to both Na^+ and K^+	0.097	0.194

The emf values calculated on the assumption that the porcelain membrane is reversible to both Na and K ions are much closer to the experimental values than those calculated from the assumption that only Na ions determine the membrane potential. It must be concluded that the porcelain electrode does not act solely as a Na electrode. However, in view of its stability and reproducibility, this result does not affect its potential usefulness as a reference electrode in any given system.

Current reversibility of the porcelain electrode.—An important property of an electrode is its ability to return to equilibrium after accidental passage of current. To check this property, cell (II) was polarized by passing a current of about 0.1 amp for 20 sec at 800°C. A polarization of 6 mv was measured immediately after passage of current. The polarization decayed to about 1 mv within 5 min. Reversal of the polarizing current gave an equal but opposite polarization, which decayed within 5 min to about 0.3 mv. Within 20 min the residual polarization was less than 0.1 mv. It is concluded that the porcelain electrode is reversible to passage of current.

Electrical resistivity of the porcelain.—Approximate measurements were made of the resistivity of porcelains of two compositions. One of the porcelains had the composition described in the section on Preparation of Electrodes; the other had a higher content of Na_2O. The composition of the latter was Na_2O, 10%; SiO_2, 54%; Al_2O_3, 36% by weight. Sodium was introduced into this porcelain as before in the form of a glass, but in this case the glass was prepared from Na_2SiO_3, SiO_2, and Al_2O_3, plus about one-third of the clays, followed by firing. The clays were added to render the glass less soluble in the slip mixture. The slip-casts were fired at 1170°C. Resistivity was estimated by measuring the voltage drop across the porcelain for a known direct current. The porcelain conductor was an electrode capsule in the case of the low-sodium porcelain. The resistivity of the porcelain containing 10% of Na_2O was so low that a conductor in the form of a U-shaped bar was used. In both cases the porcelain was in contact with a molten mixture of sodium salts having an appropriate melting point. Resistivity data are given in Table II. Even though the results are only approximate, it is believed they are of interest.

The low resistivity of the porcelain containing 10% Na_2O is noteworthy. It is of the order of 100 times that of molten alkali halides and is much lower than that of glasses. For example, the resistivity of soda-glass at 400°C is about 80,000 ohm-cm.

Mechanism of conduction by the porcelain.—Since application of the porcelain membranes to some experiments on conductivity and transference was planned, information on the mechanism of conduction through the porcelain was desired. The cell consisted of a porcelain capsule and a Ag anode dipped into a crucible that contained molten NaCl. The capsule contained a melt of AgCl-NaCl and a Ag cathode. Separate experiments were carried out with the low- and high-Na porcelains. Results are shown in Table III.

The gain in weight shown in the last column was calculated from Faraday's law on the assumption that only sodium ions pass through the porcelain. The agreement is within the limits of experimental error. In the experiment with the low-Na porcelain, examination of the inside of the bulb after the electrolysis showed blackening, probably due to reduction by the Na deposited on the cathode after complete deposition of the silver ion present in the melt. In the experiment with the high-Na capsule, Na was not deposited, and the porcelain was not

Table II. Resistivity of porcelains

Temperature, °C	Resistivity, ohm-cm	
	2.5% Na_2O	10% Na_2O
400		730
450		420
550		140
650		64
700		42
860		25
900	430	20
940	380	
1000	300	

Table III. Ion conductance of porcelain

Porcelain composition	Current, ma	Time, min	Temp, °C	Wt gain, g	Calc wt gain, g
Low-Na	50	300	850	0.215	0.215
High-Na	85	240	850	0.295	0.292

visibly changed, even though the amount of sodium ion transferred was sufficient to replace all of the Na contained in the porcelain.

The above results indicate that the porcelain conducts solely by transfer of sodium ions and not by transfer of electrons or oxygen ions.

Resistance of porcelain electrodes to breakage.—The likelihood of accidental breakage of these electrodes is about the same as that of similar glass electrodes. However, electrodes made with glass capsules usually break on cooling after being used once, whereas the porcelain electrodes usually can be used at least twice. In the course of this work, 26 porcelain electrodes were used. Of this number, 20 operated satisfactorily for one or more experiments, and 6 failed during initial use. Failure was due to breakage of the bulb, breakage of the glass-porcelain seal, or contact defects associated with the Ag-W junction or the porcelain sheath over the Ag. It is probable that improvements in design and construction might make them more durable.

An Application of the Porcelain Electrode

A porcelain reference electrode has been used successfully by another group in this laboratory working on the deposition of Ti from molten salt solutions. In these experiments, changes in the potential of Ti cathodes were followed during electrolyses of solutions of $TiCl_2$ or $TiCl_3$ in a eutectic melt of LiCl-KCl-NaCl at 600°C. The porcelain reference electrode, which was made from the low-Na porcelain, was used repeatedly over a period of five weeks. It was cooled, washed with water, and stored dry during intervening periods of nonuse. At both the beginning and the end of this period, its equilibrium potential against Ti in a fresh, carefully prepared melt was 1.23 v. Since a precision of one centivolt was adequate in these experiments, the data were not recorded to millivolts, but the constancy of the electrode was in fact significantly better than 1 centivolt.

Prolonged immersion of the electrode in the Ti solutions caused a film of Ti to form. A brief dip in a 25% solution of hydrofluoric acid (1 part concentrated HF to 1 part water by volume) removed the Ti film without damage to the electrode.

Acknowledgments

The authors acknowledge the contributions of Gwendolyn B. Wood and Paul A. Krasley, who carried out the work described in the section on Application of the Porcelain Electrode, and of Seymour Senderoff, now at National Carbon Research Laboratories, Parma, Ohio, who initiated this project. Acknowledgment is also made to the Atomic Energy Commission, Division of Research, Chemistry Branch, for financial support and for permission to publish this material.

Manuscript received Jan. 7, 1959. This paper was prepared for delivery before the Ottawa Meeting, Sept. 28-Oct. 2, 1958.

Any discussion of this paper will appear in a Discussion Section to be published in the June 1960 JOURNAL.

REFERENCES

1. S. Senderoff and A. Brenner, *This Journal*, **101**, 31 (1954).
2. S. N. Flengas and T. R. Ingraham, *Can. J. Chem.*, **35**, 1139 (1957).
3. R. A. Osteryoung, *Dissertation Abstr.*, **15** [1], 36 (1955).
4. Kurt H. Stern, *J. Phys. Chem.*, **60**, 1443 (1956).
5. H. Coriou, J. Dirian, and J. Hure, *J. chim. phys.*, **52**, 479 (1955).
6. S. Senderoff and G. W. Mellors, *This Journal*, **105**, 224 (1958).
7. E. M. Skobets and N. S. Kavetski, *J. Gen. Chem. (U.S.S.R.)*, **10**, 1858 (1940).
8. Yu. K. Delimarskii, *Zhur. Fiz. Khim. (U.S.S.R.)*, **24**, 875 (1950).
9. Yu. K. Delimarskii and R. S. Khaimovich, *Ukrain. Khim. Zhur.*, **15**, 340 (1949).
10. Yu. K. Delimarskii and A. A. Kolotti, *ibid.*, **16**, 438 (1950); **24**, 146 (1958).
11. A. A. Kolotti, *Zhur. Fiz. Khim.*, **30**, 508 (1956).
12. J. O'M. Bockris, G. J. Hills, D. Inman, and L. Young, *J. Sci. Instruments*, **33**, 438 (1956).

Manuscripts and Abstracts for Spring 1960 Meeting

Papers are now being solicited for the Spring Meeting of the Society, to be held at the Lasalle Hotel in Chicago, Ill., May 1, 2, 3, 4, and 5, 1960. Technical sessions probably will be scheduled on Electric Insulation (including a Symposium on "Electrolytic Capacitors"), Electronics (including Luminescence and Semiconductors), Electrothermics and Metallurgy (including a symposium on "High-Purity Vanadium" and a round table on "Methods of Reducing Iron Ores"), Industrial Electrolytics, and Theoretical Electrochemistry.

To be considered for this meeting, triplicate copies of abstracts (*not exceeding 75 words in length*) must be received at Society Headquarters, 1860 Broadway, New York 23, N. Y., *not later than January 4, 1960. Please indicate on abstract for which Division's symposium the paper is to be scheduled, and underline the name of the author who will present the paper.* Complete manuscripts should be sent in triplicate to the Managing Editor of the JOURNAL at the same address.

• • •

The Fall 1960 Meeting will be held in Houston, Texas, October 9, 10, 11, 12, and 13, 1960, at the Shamrock Hotel. Sessions will be announced in a later issue.

Galvanic Behavior in Fused Electrolytes

II. Discharge of the System Mg/LiCl-KCl-K_2CrO_4/Ni

Sidney M. Selis[1] and Laurence P. McGinnis

Diamond Ordnance Fuze Laboratories, Washington, D. C.

ABSTRACT

The discharge of the system Mg/LiCl-KCl-K_2CrO_4/Ni at current densities of several microamperes per square centimeter yields a potential-time curve with discrete potential plateaus. Two of the plateau potentials are controlled by nickel oxides formed by the oxidation of nickel by chromate ion. Another plateau potential is controlled by the reduction of hydroxide ion at the cathode.

An effect of added silicon dioxide is the stabilization of initial equilibrium potentials. Another effect of silicon dioxide, or other solid acidic oxides, is the diminution of coulombic output. These effects are attributed to a buffering of oxide ion activity and a removal of hydroxide ion from the electrolyte.

In a recent paper (1), the authors considered the galvanic system Mg/LiCl-KCl/Ni. Lithium chloride is a hygroscopic substance and, if not specially purified, it will contain small amounts of water and hydroxide ion even after it has been melted; the impurity content is on the order of 10^{-3} mole/liter (1-3). The proton of this hydroxide ion is the cathodically reducible material in the above system, and at temperatures below 450°C the cathode half-cell reaction is

$$2\,OH^- + 2e^- \rightarrow H_2 + 2\,O^= \qquad [1]$$

It is of interest to consider the effects of an oxidizing agent stronger than hydroxide ion. Potassium chromate is a convenient choice because it has reasonable thermal stability. Furthermore, it is found that magnesium is not attacked rapidly in the molten electrolyte LiCl-KCl-K_2CrO_4. The investigation of the system including chromate ion has been made by measuring potentials of cells at equilibrium and under resistive load. Relative coulombic capacities have also been determined. Data are presented for cells with and without added solid acidic oxides.

Experimental

Materials.—The chemicals used in this study were all of reagent grade and not purified further. As far as possible they were handled in an atmosphere with a relative humidity of 6% or less. The sheet magnesium and nickel, both 99.5% pure, have been described before (1). The cylindrical magnesium electrodes were machined from stock which was 99.97% pure, the impurities being small amounts of calcium and zinc. The nickel cups were prepared by electrodeposition on a chromium-clad mandrel. The nickel was over 99% pure, the major impurities being cobalt, manganese, iron, and possibly carbon. The sintered nickel, used to prepare nickel-nickel oxide electrodes, has been described by Fleischer (4).

[1] Present address: Research Laboratories, General Motors Technical Center, Warren, Mich.

Procedure.—The procedure followed in studying cells with strip or sheet electrodes has been discussed by Jennings (5) and by us (1). The silver-silver chloride glass reference electrode has already been described (1). The cylindrical cell design is shown in Fig. 1 (for clarity, the horizontal dimension has been exaggerated in Fig. 1). Spacing flanges and a nickel lead wire were welded to the top of the cup, the carefully weighed electrolyte components were added, and the cup was positioned in a Pyrex tube envelope. The latter was then placed in a furnace controlled at 300°C. The sidearms accommodating the wires were sealed, the envelope was capped, and the cup was evacuated to about 20 μ Hg for 18 hr so as to remove excess gas from the elec-

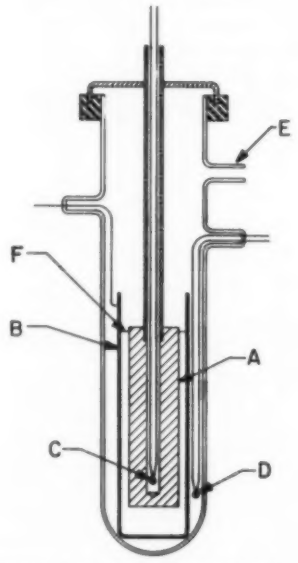

Fig. 1. Diagram of the cylindrical cell. A, magnesium electrode; B, nickel cup cathode; C, measurement thermocouple; D, control thermocouple; E, vacuum sidearm; F, electrolyte level.

trolyte. (This gas is mainly water and hydrogen chloride generated by hydrolytic reactions.) The temperature was then raised to 440°C, thereby melting the salt.

In assembling the anode, a small hole was first drilled nearly through the whole length of a magnesium cylinder of fixed diameter. The upper part of the hole was then enlarged and threaded to accept a threaded brass tube. Through this and the anode could be inserted the measurement thermocouple as distinguished from the control thermocouple located outside the cup (the thermal emf of the magnesium-brass junction was shown to be negligible). The brass tube was then screwed all the way through a threaded hole in the cap shown in the diagram.

After the pre-pumping, the system was opened, and the anode assembly was positioned and properly braced. Using a predetermined reference mark on the brass tube, the anode was lowered to the proper level, and all possible leaks were closed with a wax. The cell was evacuated to 0.5 mm Hg, and final temperature adjustments were made to 440° ± 1°C. Stable initial emf's could be recorded 24 hr later, and the resistive load could then be applied. Available equipment permitted the use of a fixed resistance, and discharge of the cells through this resistance satisfactorily provided the data needed for the discussion presented below.

Voltage-time data were obtained with a recording oscillograph having an input impedance of 9 megohms. Since discharges lasted as long as two days, periodic calibration of the oscillograph was necessary, and the apparatus was calibrated automatically every hour. Additional cell and thermocouple emf measurements were made with a student-type null-balancing potentiometer. Because the changes in cell voltage occurred exclusively at the positive electrode, as will be discussed later, the observed voltages may be considered as electrode potentials referred to the magnesium electrode.

The mixture of electrolyte salts was composed of 55.2 mole % LiCl, 40.0 mole % KCl, 4.83 mole % K_2CrO_4. For each cell, 20.0 ± 0.1 g was used. The amount of added solid oxide was 1 g, which was sufficient to saturate the electrolyte.

The interelectrode distance on the side was 4.4 ± 0.1 mm and was 14.0 ± 0.5 mm at the bottom. After certain runs, the electrolyte level was determined, and from this current densities were estimated for a given potential. Currents were calculated by dividing potential by the external load resistance (it was demonstrated that cell impedances were <1 ohm). For the maximum potential of 1.80-1.81 v, anode and cathode current densities for the 50-ohm load were 552 and 334 $\mu a/cm^2$, respectively; for the 2000-ohm load they were 13.8 and 8.34 $\mu a/cm^2$.

Results and Discussion

A typical potential-time curve for cells discharged across the 2000-ohm load at 440°C is shown in Fig. 2. It will be noted that there is a series of discrete potential plateaus corresponding to 1.80-1.81, 1.76, 1.70, and 1.67 v. A large number of these cells were studied and the plateau potentials were

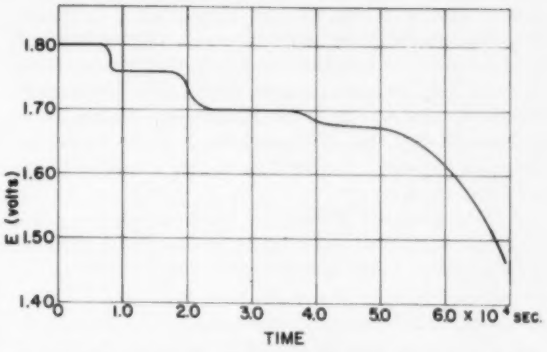

Fig. 2. Potential-time curve for discharge of a cell with SiO_2 through a 2000-ohm resistance.

reproducible to within less than 10 mv. However, as will be shown later, all of the various levels could be obtained dependably only when the electrolyte was buffered by the addition of SiO_2.

Changes in cell potential can be attributed solely to effects at the positive electrode. This was demonstrated by introducing a silver-silver chloride glass electrode in cells with electrodes of sheet magnesium. Measurements of the polarized potentials of these magnesium electrodes, corresponding to the current densities of interest, showed that polarization of magnesium was negligible.

Most of these potentials could be obtained by other means. If, for example, sintered nickel is rubbed with commercially available "black nickel oxide" and its potential is measured against magnesium in the LiCl-KCl electrolyte, the value obtained is 1.76 v. This potential persists for a while and then suddenly falls to 1.70 v. Concurrent with this potential drop, the color of the coating changes from black to green.[2] Green nickel oxide (NiO), rubbed on sintered nickel and measured against magnesium in LiCl-KCl, gives a stable potential of 1.70 v.[3] The 1.67-v potential has been considered before (1); it is obtained with the hydroxide ion-nickel electrode in LiCl-KCl at 440°C.

The following inferences can be made from this work. It is suggested that, during the 24-hr immersion in the electrolyte LiCl-KCl-K_2CrO_4, the nickel becomes coated with successive layers of oxidation products. Next to the metal there is probably a phase which includes nickel (II) ion; upon this, there is nickel in a higher state of oxidation (possibly the dark colored phase already mentioned). To account for the 1.80 v potential there may be nickel in a yet higher state of oxidation, presuming that the chromate ion is a sufficiently strong oxidizing agent so that this phase could be generated. Upon discharge, the potential for the first plateau is determined by the outer layer. As the latter is depleted there is a counter tendency for the higher oxide to be re-formed by the oxidative

[2] Hill, Porter, and Gillespie (6) prepared a "black nickel oxide" *in situ* at 658°C. This was accomplished by bubbling oxygen at unit pressure through a molten Li_2SO_4-K_2SO_4-CaO electrolyte in which was dipped a nickel wire. On decreasing the oxygen pressure, the dark-colored phase behaved in the same way as described above.

[3] The behavior of this electrode has already been measured and discussed (1).

action of the chromate ion. Apparently, however, it is discharged faster than it can be formed. When it eventually disappears, the cell voltage becomes governed by the next lower oxide. Such an explanation is offered for each solid layer. Finally, it is presumed that the cell potential is determined by reaction [1] until the hydroxide ion becomes fairly well depleted.

A few remarks should be made concerning the possible nature of such solid phases. The idea of simple oxides must be discarded. Brewer (7) states in summary that there is only one nickel oxide (nominally NiO with a NaCl-type cubic structure), although its composition range extends to nearly NiO_2. On the other hand, it is a different matter if alkali metal ions can be included in the oxide lattice. Verwey and his co-workers (8, 9) have presented strong evidence that the inclusion of lithium ion in the NiO lattice will induce the formation of Ni(III) ions. Dyer, Borie, and Smith (10) report the preparation of a stable $LiNiO_2$; here the formal valence number is three but the authors suggest that the lattice may actually include a mixture of Ni(II) and Ni(IV) ions. A compound with Ni(IV) ions, i.e., K_2NiO_3, has been characterized by Wahl, Klemm, and Wehrmeyer (11); the evidence is strong for the existence of this phase. But possibly of most pertinence is the observation of Hill, *et al.* already noted above, that a discrete phase producing a higher potential can be formed with oxygen in a fused salt electrolyte.

An explanation has been offered for the observed potential plateaus in terms of different reducible phases at the cathode. Certainly an explanation based on the direct electrochemical reduction of chromate ion would not be reasonable since, in this case, the potential would change continuously rather than in discrete steps. On the other hand, the chromate ion would function in oxidizing the nickel as indicated by reaction [2].[4] Here Cr_2O_3 is shown as a product; it has been identified by x-ray powder diffraction techniques. In any case, the matter is not highly pertinent to the present discussion. Reaction [2] would be followed by the half-cell reaction [3]

$$2xCrO_4^=(l) + 3Ni(c) \rightarrow 2xO^=(l) + xCr_2O_3(c) + 3NiO_x(c) \quad [2]$$

$$NiO_x(c) + 2(x\text{-}y)e^- \rightarrow NiO_y(c) + (x\text{-}y)O^=(l) \quad [3]$$

For reasons not pertinent to the information presented in this paper, the effects of including silicon dioxide and other solid acidic oxides were studied. One important effect is shown by the data in Table I which presents initial equilibrium voltages for a number of cells with and without SiO_2. The difference in reproducibility of emf is of immediate interest, but the difference of 40 mv in the averages is of doubtful significance.

Another interesting effect was the difference in coulombic delivery with and without added solid acidic oxides. Such comparisons are presented in Fig. 3 and in Table II. Relative coulombic deliveries were obtained to an arbitrary cutoff potential of 0.60 v by measuring the areas under the potential-time curves and dividing these by the external load resistance of 50 ohms. The data presented here were obtained from cells which had an initial potential of 1.80-1.81 v. Table II shows that the coulombic deliveries of cells with added solid oxides is from 38 to 53% of that for cells without added material.

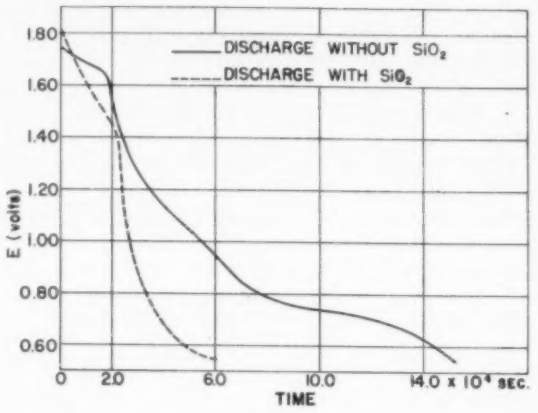

Fig. 3. Effect of added SiO_2 on discharge through a 50-ohm resistance.

To postulate an explanation for these effects of emf stabilization and differences in coulombic delivery, reference is made to reaction [2] in which it is seen that the oxide ion activity is a variable factor. Since it is at least partially governed by originally entrapped water of hygroscopicity, this quantity will depend on the specific batch of lithium chloride used, as well as on room humidity conditions and inadvertent differences in cell preparation. It is possible that, from one cell to the next, variations in oxide ion activity could determine the particular nickel oxide which governs the initial cell emf. But with added silicon dioxide a buffering effect could occur in terms of reaction [4].

$$SiO_2(c) + 2Li^+(l) + O^=(l) \rightarrow Li_2SiO_3(s, amorph) \quad [4]$$

Table I. Equilibrium potentials of nickel, with and without silicon dioxide in the melt, referred to magnesium electrode

With SiO_2		Without SiO_2	
Cell	EMF, v	Cell	EMF, v
1	1.82	8	1.70
2	1.80	9	1.80
5	1.82	10	1.85
6	1.80	13	1.80
24	1.82	14	1.77
25	1.81	17	1.79
27	1.81	18	1.76
28	1.80	21	1.72
		22	1.75
Av:	1.81 v	Av:	1.77 v
AD*:	0.010 v	AD:	0.034 v
SD*:	0.013 v	SD:	0.045 v

* AD is average deviation, SD standard deviation from the mean.

[4] Reactions [2] and [3] have been written in terms of nickel oxide phases. It is to be remembered that these would be stabilized by the presence of alkali metal ions in the oxide lattices.

Table II. Effect of acidic oxides on the relative coulombic capacities of cells with nickel oxide electrodes

Added material	Capacity (coulombs)
None	3015 ± 115
SiO_2	1145 ± 45
B_2O_3	1585 ± 45
Al_2O_3	1475 ± 55

The presence of solid lithium silicate was confirmed by chemical methods, and an equilibrium involving two solids would fix the oxide ion activity which is the one variable in reaction [2].

The present authors prefer this explanation which involves the concept of different initial potentials being based on different potential-determining couples. An alternative explanation might have been offered in terms of reaction [3] for which potential is conceivably a continuous function of oxide ion activity. However, it is observed, as stated above, that plateau potentials are always reproducible to within less than 0.01 v. If an initial equilibrium potential was less than 1.81 v, then the plateau corresponding to this latter potential was simply never observed.

Regarding the diminution of coulombic delivery due to the addition of solid acidic oxides, a decrease in capacity might be due to the removal of hydroxide ion, and a material such as SiO_2 could provide for this. Hydroxide ion participates in the equilibrium shown in reaction [5],

$$2\,OH^-(l) \rightarrow O^=(l) + H_2O(g) \qquad [5]$$

and the removal of oxide ion by SiO_2 would result in the equilibrium being shifted to the right. In fact, when SiO_2 is added to these electrolytes, the evolution of water is immediately discernible. The authors believe that the added boron oxide or aluminum oxide would behave in a manner analogous to that of silicon dioxide.

Acknowledgment

The authors wish to thank the Dow Chemical Company for the pure magnesium rod used in this work.

Manuscript received March 10, 1959. This paper was prepared for delivery before the Cincinnati Meeting, May 1-5, 1955.

Any discussion of this paper will appear in a Discussion Section to be published in the June 1960 JOURNAL.

REFERENCES

1. S. M. Selis, G. R. B. Elliott, and L. P. McGinnis, *This Journal*, **106**, 134 (1959).
2. H. A. Laitinen, W. S. Ferguson, and R. A. Osteryoung, *ibid.*, **104**, 516 (1957).
3. W. J. Burkhard and J. D. Corbett, *J. Am. Chem. Soc.*, **79**, 6361 (1957).
4. A. Fleischer, *J. (and Trans.) Electrochem. Soc.*, **94**, 289 (1948).
5. C. W. Jennings, *This Journal*, **103**, 531 (1956).
6. D. G. Hill, B. Porter, and A. S. Gillespie, Jr., *ibid.*, **105**, 408 (1958).
7. L. Brewer, *Chem. Rev.*, **52**, 1 (1953).
8. E. J. W. Verwey, *Bull. soc. chim. France*, **1949**, Mises au point D122.
9. E. J. W. Verwey, P. W. Haaijman, F. C. Romeijn, and G. W. van Oosterhout, *Philips Res. Repts.*, **5**, 173 (1950).
10. L. D. Dyer, B. S. Borie, Jr., and G. P. Smith, *J. Am. Chem. Soc.*, **76**, 1499 (1954).
11. K. Wahl, W. Klemm, and G. Wehrmeyer, *Z. anorg. u. allgem. Chem.*, **285**, 322 (1956).

Technical Notes

The Diffusion of Corrosion Hydrogen in Aluminum Alloys

W. E. Tragert

Research Laboratory, General Electric Company, Schenectady, New York

Essentially pure aluminum and many aluminum alloys corrode catastrophically in pressurized water at temperatures above say 275°C. It has been proposed (1) that the resistance of an aluminum—1% nickel alloy (X8001) to such oxidation is due to the presence in the surface of second phase Al_3Ni particles which function as cathodic sites for the evolution of corrosion product hydrogen. Such hydrogen is considered responsible for the usual accelerated oxidation by a mechanism of diffusion through the surface oxide film, discharge at internal pores or grain boundaries in the metal, and resultant blistering of the aluminum and disruption of the otherwise continuous surface oxide film. The local cathodic discharge of hydrogen at the surface thus inhibits entry of hydrogen into the aluminum and prevents catastrophic failure. The present experiment was devised to test the above described hypothesis.

Test samples were aluminum cans, 9.5 in. by 1.44 in. diameter with a wall thickness of 0.030 in. These were filled about 1/3 with distilled water and sealed with solid end plugs which were inert arc welded in place. A small nipple on each plug, pierced with an 0.030-in. hole, served as a vent during welding and was subsequently welded shut. The cans and end plugs were of two alloy compositions, Alloy 1245 (99.45% Al minimum) and Alloy X8001, mentioned above.

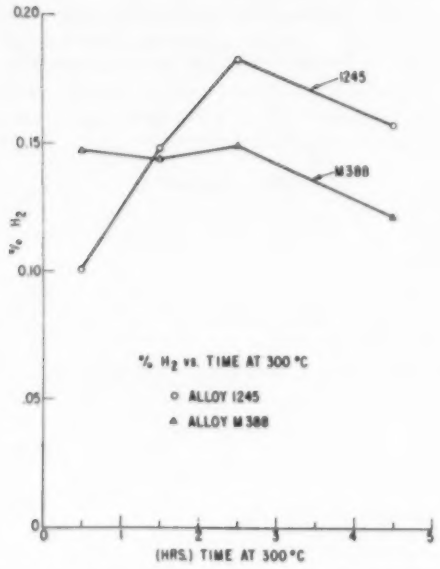

Fig. 1. Hydrogen content of the autoclave atmosphere as a function of time at 300°C.

The experimental procedure was to place a sealed aluminum alloy can in a stainless steel autoclave of internal dimensions 12 in. by 3 in. diameter, and then evacuate and purge the sealed autoclave with pure helium. The autoclave was resistance heated and the water vapor pressure within the aluminum can (inferred from temperature measurements) was compensated by valving helium into the autoclave during heating. When the system had reached 300°C, the atmosphere of the autoclave was sampled periodically, the samples being taken into evacuated 100 cc flasks. The flask contents were analyzed mass spectrographically for water and hydrogen. No water was detected in the several experiments, and data for hydrogen are presented graphically in Fig. 1 as a percentage of the total gas sample collected. The individual values are significant analytically to within 2%. That the proportion of hydrogen appears to diminish with time in these experiments can be attributed to several factors. First, the initial reaction of both aluminum alloys is quite rapid, the rate more or less diminishing as filming occurs; second, the oxide film is thinner and presumably more permeable at the outset than later in the experiment; third, hydrogen is lost from the pressure system by virtue of the samples taken and by diffusive loss through the heated walls of the autoclave.

A blank sample was run on the heated autoclave system and yielded no detectable hydrogen. A second blank was run on the system containing a can of Alloy 1245 that had been filled only with helium and sealed according to the procedure outlined above. No hydrogen was detected prior to heating, during heating, or at 300°C. At the conclusion of each of the corrosion gas sampling experiments, the can was cooled under supporting helium pressure, removed from the autoclave, and cut open. Unfortunately, no measure was made of the residual hydrogen gas pressure in the sample cans. Upon visual examination, there was noted superficial oxidation of the internal surfaces of the X8001 can and extensive oxidation of the 1245 can, although in the latter case one might have expected greater attack than was observed. It has been noted (2) that the transport of corrosion hydrogen appears from these data to be higher than would be expected from published diffusion data (3). It should be further noted, however, that the literature values for Q and D_o are unusually high and may reflect experimental difficulties as judged from the large scatter in the individual diffusion data points.

The present data and observations indicate that corrosion hydrogen diffuses through both Alloy 1245 and X8001. It must be considered, however, that the experimental configuration employed here is not typical of corroding systems; that is, corrosion hydrogen is not usually contained within the material under test. Consequently, it cannot be concluded that under normal conditions of corrosion, where the ambient hydrogen pressure may be small, hydrogen diffuses into either of these alloys to any great extent, although such may in fact be the case. The significance of these data is that, under conditions of hydrogen permeation, Alloy X8001 remained relatively uncorroded while Alloy 1245 was extensively oxidized. According to the galvanic protection hypothesis, the proton flux should have produced accelerated oxidation of both alloys in these tests.

It thus appears that rather than functioning as local cathodes, the second phase particles in Alloy X8001 serve, on oxidation, to alter the nature of the corrosion product film and to render it less permeable to the diffusing reactants. Although the concentration of hydrogen in the oxide film and basis metal may exert an influence on the reaction kinetics, this effect must be considered of secondary importance relative to the rate-controlling mechanism.

Manuscript received April 13, 1959.

Any discussion of this paper will appear in a Discussion Section to be published in the June 1960 JOURNAL.

REFERENCES

1. J. E. Draley and W. E. Ruther, *Corrosion*, **12**, 480 (1956).
2. G. J. Biefer, A.E.C.L., Chalk River, Ont., Canada, Private Communication.
3. C. E. Ransley and D. E. J. Talbot, *Zeit. Metallkunde*, **46**, 328 (1955).

On the Crystallization of Simple Rhombohedral Boron from Platinum

F. Hubbard Horn

Research Laboratory, General Electric Company, Schenectady, New York

Since the report on the preparation of a simple rhombohedral (red) allotrope of boron by pyrolysis of a boron halide or hydride on a filament below a temperature of about 1200°C (1), it has seemed of interest to determine whether this allotrope can be obtained by crystallization from a melt. Requisite to such a process is a solution of boron from which boron and not boron compounds will crystallize below about 1200°C. The boron-platinum system is known to have a low melting eutectic. The remainder of the phase diagram apparently has not been published. A compound PtB or Pt_3B_2 has been reported (2).

Boron-Platinum Alloy System

An attempt to investigate the solidus-liquidus by a normal thermal-arrest procedure was not successful. However, the eutectic was determined by thermal arrest. The crucible was hot-pressed boron nitride which is not appreciably attacked by molten boron (3). The thermocouple was calibrated at the freezing temperature for silver. The eutectic temperature was determined as 825° ± 5°C. The eutectic exists over the composition range explored, from 5 to 87.5 at. % boron. The alloys were prepared from commercial grade platinum and granular boron of 99.8% purity.

The liquidus-solidus for boron-rich alloys was determined by immersing a small boron nitride probe into a melt of predetermined composition and noting the lowest temperature at which the probe could be removed from the melt without any solid (boron) adhering to the probe. In order to assure that the boron freezing on the probe was the first boron to freeze anywhere in the system, it was necessary to approach the liquidus-solidus temperature from a temperature well above it. Once boron had frozen to the probe, the temperature that was just sufficient to melt it could also be determined. With care, it was found possible to reproduce the conditions to about ±5°C. The temperatures measured are probably somewhat higher than true equilibrium temperatures since some additional heat must be supplied to compensate for losses such as those along the probe. Temperature was measured by optical pyrometer sighted on the clean melt surface near the center of the crucible. No correction for emissivity has been made since a calibration of the temperatures obtained by optical pyrometer against those from the embedded thermocouple agreed within 10°C over the temperature range 1200°-1400°C.

Data obtained for the liquidus-solidus line for the boron-platinum alloys investigated are plotted in Fig. 1. A curve through the points indicates a eutectic composition of about 40 at. % boron in platinum. There is no suggestion of compound formation for compositions between the eutectic and pure boron.

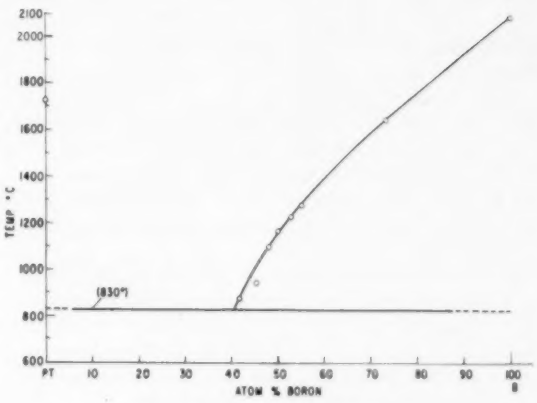

Fig. 1. Phase diagram of boron-platinum system

Attempts to use the probe method to complete the solidus-liquidus line were unsuccessful for alloys richer in platinum than the eutectic composition. The material freezing would not adhere to a boron nitride or graphite probe and probes of Ni, Fe, W, Mo, and Ta were attacked by the alloys.

Crystallization of Simple Rhombohedral (red) Boron

The simple rhombohedral form of boron is stable for a long period of time at 1200°C. It is seen from Fig. 1 that an alloy of about 50 at. % boron in platinum is molten at this temperature. Thus, from such an alloy cooled slowly to the eutectic temperature, boron will crystallize. If the simple rhombohedral form is stable at these temperatures, the boron crystallizing may be of this structure.

Typically, a 50-50 at. % alloy of boron and platinum was prepared from commercial platinum and zone-refined boron. The first melt was allowed to solidify and the surface and sides of the ingot ground away in order to remove a slag found frequently on initial melts. The alloy was transferred to a crucible of boron nitride having a conically tapered bottom. After melting the alloy in vacuum, the crucible was lowered gradually through the high-frequency heating coils. The rate of lowering has been about 0.04 mm/min. As the melt approaches the eutectic temperature it is allowed to freeze suddenly.

A cut and polished section through such a solidified melt shows crystallization of black (boron) in the bottom tip; moreover, regions of translucent red crystals are seen embedded in the remainder of the

section. The red crystals are highly reflecting and may be easily missed in the matrix if with vertical illumination the incident light is not polarized. The red crystals may be recovered by crushing the brittle platinum-boron matrix. They may be separated from the dust of the matrix by performing a gravity separation. The red crystals and some black solids float on bromoform. This fraction is skimmed and the solids allowed to settle by adding acetone. The settled material is rinsed with acetone and dried. Red crystals are readily separated visually from black solids using a microscope.

Powder x-ray diffraction analysis identifies the red crystals as entirely simple rhombohedral boron (4).

Crystals that have been recovered to date are very small, the largest being tenths of millimeters. Thus no attempt has been made to characterize their properties. There is no foreseen reason why larger crystals may not be grown.

It is of interest that the simple rhombohedral boron crystallized is translucent red; this suggests rather high purity. Either the solubility of impurities present must be very small at the low temperatures of formation or some purification may take place during the freezing of the boron in the tip of the ingot prior to crystallization of the simple structure. By x-ray diffraction the identification of the black material that separates with the red crystals or the black material crystallizing in the tip of the ingot is not positive; there is, however, some similarity to the pattern for the complex rhombohedral form of boron. Preliminary results suggest there may be a number of intermediate structures between the complex and simple rhombohedral forms.

Manuscript received May 15, 1959. This paper was prepared for delivery before the Philadelphia Meeting, May 3-7, 1959.

Any discussion of this paper will appear in a Discussion Section to be published in the June 1960 JOURNAL.

REFERENCES

1. L. V. McCarty, J. S. Kasper, F. H. Horn, B. F. Decker, and A. E. Newkirk, *J. Am. Chem. Soc.*, **80**, 2592 (1958).
2. J. H. Puddery and A. J. E. Welch, *Nature*, **167**, 362 (1951).
3. F. H. Horn, *J. Appl. Phys.*, Letter to Editor, in press.
4. B. F. Decker and J. S. Kasper, *Acta Crystallographica*, in press.

Technical Review

Report of the Chlor-Alkali Committee of the Industrial Electrolytic Division for the Year 1958

Clifford A. Hampel

Skokie, Illinois

Nelson J. Ehlers

Columbia-Southern Chemical Corporation, Pittsburgh, Pennsylvania

Chlorine-Caustic

Production and Sales

Consistent with the general chemical sales decline, U. S. chlorine production in 1958 decreased 8.8% from 1957 and was about 3,600,000 tons. For the first time in twelve years, the annual production was lower than that of the previous year. U. S. capacity at the end of 1958 is estimated at near 12,360 TPD, which means the industry operated at about 80% of capacity during the year. Apparent per capita chlorine consumption was 41.2 lb as compared to 22.2 lb in 1948 and 6.7 lb in 1938.

Concerning production in 1959, some sources predict a return to the 1957 production of about 3,950,000 tons and, of course, it is hoped that subsequent annual production tonnages will follow the traditional chlorine growth curve.

Chlorine production in Canada was 268,000 tons in 1958 as compared to 226,000 tons in 1957. Indications are that about 275,000 tons will be produced in 1959.

Caustic soda production for 1958 was at a 4,055,000-ton level, which meant a 6.7% decrease from 1957. Apparent per capita consumption was 44.2 lb compared to 29.9 in 1948 and 11.2 in 1938. Indications are that 1200 TPD lime soda caustic was produced as an average for the first eight months of 1958. This marks an increase for this period of about 260 TPD over the 1957 average and represents about 10.8% of the total caustic production in 1958 as compared to 7.9% in 1957. The Bureau of Census, after August 31, 1958, is not separating lime soda and electrolytic caustic production figures.

In general, the industry was more in balance between chlorine and caustic than in 1957. Again in

Table I. Sources of chlorine

	1957		1958 (preliminary)	
	Tons	%	Tons	%
Cl_2 equiv. of NaOH	3,548,579	89.9	3,234,813	89.9
Cl_2 equiv. of KOH	47,714	1.2	43,717	1.2
Cl_2 equiv. of Na	204,958	5.2	170,002	4.7
Cl_2 equiv. (other sources)	146,417	3.7*	151,182	4.2*
Cl_2 total gas produced	3,947,668	100.0	3,599,714	100.0

* By difference.

1958 soda ash was used to produce lime soda caustic in several plants in the U. S., and Dow Chemical Company, Freeport, Texas, continued to produce soda ash from electrolytic caustic.

Approximately 75.8% of chlorine capacity in 1958 was in diaphragm cells, 18.4% in mercury cells, 5.1% in sodium cells, and 0.7% in nonelectrolytic processes. The estimated sources of chlorine comparing 1958 with 1957 appear in Table I.

New Plants and Expansions

Approximately 640 TPD new U. S. chlorine capacity is estimated to have come on line in the U. S. in 1958, as follows: Columbia-Southern Chemical Corporation, Natrium, W. Va., 160 TPD (Uhde mercury cell); Dow Chemical Company, Plaquemine, La., 300 TPD (Dow bipolar cell); E. I. du Pont de Nemours & Company, Memphis, Tenn., 100 TPD (Downs sodium cell); and Weyerhaeuser Timber Company, Longview, Wash., 80 TPD (DeNora mercury cells).

The Arkansas Louisiana Chemical Corporation started operating the chlorine-caustic plant at Pine Bluff, which is rated at 75 TPD, in 1958, after Diamond Alkali Company terminated its lease.

Among the new plants or expansions to be completed in 1959 are: Diamond Alkali Company, Deer Park, Texas, 200 TPD (DeNora mercury cells); Jefferson Chemical Company, Port Neches, Texas, 150 TPD (Hooker S-3B cells); Stauffer Chemical Company, Niagara Falls, N. Y., 30 TPD (expand and modernize); and Wyandotte Chemical Corporation, Geismar, La., 300 TPD (Diamond diaphragm cell). Diamond Alkali Company announced early in 1959 plans to modernize chlorine cell facilities at Painesville, Ohio.

A listing of U. S. chlorine plants and estimated capacity appears in the March 7, 1959 issue of *Chemical Week*.

In Canada, the estimate of chlorine capacity by the end of 1958 was about 850 TPD. In 1958, among the new plants and expansions were: Shawinigan Chemical Company, Shawinigan Falls, Quebec, 50 TPD (mercury cell); and Western Chemicals Company, du Vernay, Alberta, 20 TPD (diaphragm cell). Dow Chemical Company in Canada has announced an integrated chemical plant at Fort Saskatchewan, Alberta. The chlorine-caustic unit will be built first and other units are to follow. Western Chemicals has announced an additional 20 TPD capacity scheduled to come on the line late in 1959. A chlorine plant for the St. John, New Brunswick area has been announced by K. C. Irving.

Table II. Chlorine—caustic soda end-use pattern

Chlorine*	%	Caustic Soda†	%
Miscellaneous chemicals	83.0	Miscellaneous chemicals	30.6
Pulp and paper	13.0	Rayon and film	16.9
Others	4.0	Pulp and paper	8.3
		Metallurgical	7.5
		Export	6.8
		Petroleum refining	6.3
		Lye and cleansers	4.5
		Textiles	3.7
		Soap	1.6
		Others	13.8
Total	100.0	Total	100.0

* Source, *Chemical Week*, March 7, 1959, p. 116 (for more detailed breakdown, see "Chemical Week," May 26, 1956.
† Source, *Chemical Week*, Jan. 18, 1958, p. 76.

Markets and End-Use Patterns

There appears to be no significant change in the end-use pattern of chlorine and caustic soda during 1958. In the production of ethylene oxide, the oxidation process continues to increase in importance relative to the chlorination process. The reduction in military requirements for titanium adversely affected the demand for chlorine. In 1958, the use of chlorine increased in the pulp and paper, and water and sewage treatment areas. The decline in general business levels reduced the other chlorine uses. Latest end-use patterns appearing in the literature are shown in Table II.

Technical Developments

Some chlorine manufacturers are now using or installing germanium and silicon rectifiers for conversion of a-c to d-c power. Diamond Alkali Company, Deer Park, Texas, is installing germanium rectifiers. Columbia-Southern Chemical Corporation, Natrium, W. Va., has used germanium rectifiers commercially for chlorine production since early 1958. Hooker Chemical Corporation has installed silicon rectifiers at its Niagara Falls, N. Y., plant.

Hooker Chemical Corporation and Diamond Alkali Company continue to offer licenses for their processes to recover blow-off chlorine. The Hooker process calls for dilute chlorine gas to be absorbed in water destined for direct-contact cooling of hot cell gas. In the Diamond process, the gas stream containing chlorine to be recovered contacts carbon tetrachloride in a packed tower under pressure. Further stripping and cooling gives liquid chlorine.

A patent by H. H. Heller (U.S. 2,836,551) discloses the advantages of forcing brine through a mercury type cell at high velocities. A German patent (1,014,080) was issued to Dow Chemical Company for a "slot" type mercury cell.

Platinized titanium anodes were publicized by Imperial Chemical Industries, Ltd., for chlorine, chlorate, and other production uses.[1]

[1] "Bright Future for ICI's Newly Developed Electrodes," *Chemical Age*, Jan. 3, 1959, and "Titanium Anodes," *Chemical Trade Journal*, Jan. 2, 1959.

Monsanto Chemical Co. is operating a cell designed by DeNora for recovery of chlorine from hydrochloric acid. The cell is believed to be economically feasible for many situations.

Among articles of interest appearing recently were: "For Cell Operators: What Price Efficiency?" *Chemical Week*, April 19, 1958, p.41-48; A debatable analysis on caustic soda was published in *Chemical Week*, Jan. 18, 1958, p. 69-76, entitled "Caustic—Plenty for Now and Future"; *Chemische Industrie*, June 1958, p. 309, cited research by VEB Farbenfabrik Wolfen to manufacture chlorine by nonelectrolytic means; "Too Much Chlorine," *Barrons*, March 24, 1958, p. 17-19; and "Thermal Data for Chlorine and HCl," *Chemical Engineering*, Feb. 10, 1958, p. 144-146.

Soda Ash

For the last two years, total production of soda ash has decreased. Production in 1958 was 4,955,200 tons, which was 7.1% below 1957. The apparent per capita consumption at 55.73 lb for 1958 was the lowest since 1941. Total domestic consumption in tons per year reached the all-time high in 1955 of 5,444,560 tons and has been on a decline since then. Natural soda ash production for both 1958 and 1957 accounted for 12.6-12.7% of the total soda ash produced. Total capacity of the soda ash plants in the U. S. is near 7,000,000 tons; therefore, it may be concluded that the industry operated at near 70% of capacity.

During 1958, Olin Mathieson Chemical Corporation completed facilities at its Saltville, Va., plant for production of dense ash. Columbia-Southern Chemical Corporation began production of soda ash and sodium sesquicarbonate at a new plant at Bartlett, Calif. The plant reportedly triples the output of an older unit there, now being scrapped. Food Machinery & Chemical Corporation has announced that a major expansion of soda ash production facilities at its Wyoming plant will be completed during the first half of 1959. Solvay Process Division of Allied Chemical Corporation is reported to be doubling dense soda ash capacity at its Baton Rouge, La., plant. Total ash capacity remains the same.

An estimated capacity for U. S. plants appears in *Chemical Week*, May 3, 1958, p. 72. The latest end-use pattern for soda ash appearing in the literature is shown in Table III.

Table III. Soda ash end-use pattern (estimate)*

	%
Chemicals	37
Glass	30
Nonferrous metal refining	10
Pulp and paper	7
Cleansers	3
Water softeners	2
Soap	1
Miscellaneous	10
Total	100

* Source, *Chemical Week*, May 3, 1958, p. 71.

Miscellaneous Chemicals

Potassium hydroxide.—Production of KOH (88-92%) decreased about 8.3%, from 83,898 tons in 1957 to a preliminary figure of 76,870 tons in 1958. Most of the newer caustic potash expansions have been by the mercury cell process. Caustic potash is making gains in the detergent field as a result of greater acceptance of some of the newer types of liquid detergents.

Chlorates.—American Potash & Chemical Corporation started operation of its sodium chlorate plant of 15,000 TPY capacity at Aberdeen, Miss., in early 1959. Reported for American Potash is a company capacity of 45,000 TPY. Hooker Chemical Corporation expanded sodium chlorate production at Columbus, Miss. Standard Chemical Limited announced the start of construction of a plant to produce sodium chlorate at Beauharnois, Que. During 1958, Electric Reduction Company of Canada claimed to be the world's largest producer of sodium chlorate as the result of expansion that doubled capacity of the firm's Buckingham, Que., plant. It has been estimated that U. S. sodium chlorate capacity will exceed 100,000 TPY in 1959 when announced new plants and expansions are on line. Production increased from 59,142 tons in 1957 to 67,247 tons in 1958, about 13.7%.

Perchlorates.—The importance of perchlorates in the production of solid fuels for missiles is highlighted by the announcements of additional plants for their preparation. HEF, Inc., jointly owned by Foote Mineral and Hooker Chemical, began construction on a 4,000,000 lb/yr ammonium perchlorate plant at Columbus, Miss. Pennsalt Chemicals Corporation announced a plant for production of ammonium perchlorate at Portland, Ore.

Two papers on the preparation and use of lead dioxide anodes in the electrolytic conversion of sodium chlorate to sodium perchlorate were published in this JOURNAL by Grigger, Miller, and Loomis of Pennsalt Chemicals Corporation and Schumacher, Stern, and Graham of American Potash & Chemical Corporation. Lead dioxide deposited on tantalum was found to be a suitable substitute for platinum in perchlorate cells.

Miscellaneous Metals

Aluminum.—Electrolysis processes are vital to the production of many of the metals, both old and new, used in this country. The aluminum industry, which consumes 5 to 6% of the total electricity generated in the U. S., continues to grow. At the end of 1957, the aluminum ingot capacity was some 1,842,000 TPY located in 18 plants of 4 companies. By 1960, this will rise to 2,604,000 tons in 23 plants of 6 companies. In Canada, the corresponding tonnages are 821,000 tons at the end of 1957 and 956,000 tons in 1960.

Magnesium.—Consumption of primary magnesium in the U. S. is expected to total about 45,000 tons in 1959. Consumption of scrap and secondary will account for another 10,000 tons or so. Consumption of this order is not a record for peacetime but does represent a resumption of the upward trend

Table IV. 1958 Sodium end-use pattern (estimated)*

	%
Tetraethyl lead	71.0
Sodium cyanide	11.2
Sodium peroxide	6.9
Metal reduction	4.7
Miscellaneous	6.2
Total	100.0

* Source, *Chemical Week*, Jan. 24, 1959, p. 78.

following the recent recession. Production in 1959 will be about 30,000 tons because of a large inventory carry-over. A large inventory was built up in 1957 when Dow Chemical Company was uncertain about the disposition of the then government-owned plant at Velasco, Texas (the plant eventually was sold to Dow, the higher of two bidders). Magnesium uses are roughly 40% structural, 60% nonstructural. Applications are divided about 50-50 between commercial and military.

Sodium.—Capacity for sodium production was reported to be 153,000 TPY as of Jan. 1, 1958. Production in 1958 was 110,298 tons as compared to 132,977 tons in 1957, a decrease of 17%. The Woodstock, Tenn., plant of du Pont for the production of sodium went on the line early in 1959. Capacity was reported as 45,000,000 lb/yr. This new installation, plus recent expansions of other producers, will increase U. S. capacity to about 400,000,000 lb/yr. The general reduction in sodium use since the peak in 1956 is attributed to loss of the fatty alcohol market and the drastic reduction in titanium metal use. The largest use of sodium continues to be in production of tetraethyl lead, and this use is increasing a small percentage each year.

The present status of the sodium industry is given in *Chemical Week*, Jan. 24, 1959, p. 76. The estimated sodium end-use pattern is given in Table IV.

Titanium.—Production of titanium sponge metal in 1958 at 4585 tons was about 27% of the 1957 output; however, the consumption of sponge metal and production and consumption of titanium ingot were, respectively, about one-half that of 1957. Total sponge held by General Services Administration at the end of 1958 was 22,400 tons.

There has been a continued increase in consumption of sponge since early 1958, and by the end of 1958 it was at least 50% of the peak rate in the brightest days of the industry. Use of titanium for its corrosion-resistant properties is increasing.

Zirconium.—The major U.S. production of zirconium metal is for the Atomic Energy Commission program. Carborundum Metals Corporation, Mallory-Sharon Metals Company, and Columbia-National Corporation are the three AEC sponge suppliers. These three producers have contracted to supply about 2,200,000 lb/yr of hafnium-free zirconium sponge.

Mallory-Sharon and Columbia-National began operations in 1958. Carborundum and Columbia-National processes involve the magnesium reduction of zirconium tetrachloride, while Mallory-Sharon uses sodium reduction. Wah Chang Corporation, Albany, Ore., has shut down its zirconium facilities and is now converting hafnium oxide to hafnium metal for the Atomic Energy Commission.

No expansion of zirconium facilities is planned at the present time.

Lithium.—Lithium, made by the electrolysis of fused lithium chloride admixed with potassium chloride, is finding increased use in such fields as the preparation of boron fuels. Olin Mathieson Chemical Corporation has installed electrolytic cells for lithium production at its Model City, N. Y., boron fuel plant, and Foote Mineral Company announced expansion of lithium production.

Manganese.—The use of manganese ore for the production of the metal in the U. S. in 1958 was over 10,000 tons. Production capacity is located in the plants of Foote Mineral Company, Knoxville, and Union Carbide Metals Company, Marietta, Ohio. The electrolytic process is the only one producing pure metal.

Chromium.—High-purity chromium metal is made by electrolysis of ammonium chromium sulfate solution in the Union Carbide Metals Company Marietta plant.

Uranium.—Most uranium metal is derived from the reduction of uranium tetrafluoride with magnesium. While the demand for uranium depends on the scope of the nuclear power plant development and the amount of uranium oxide used in fuel elements, estimates of 50,000-100,000 TPY in 1970 or 1975 have been made. Not only new metal requires magnesium for preparation, but magnesium is also used in reprocessing spent fuel elements.

Beryllium.—Pure beryllium metal is made in the U. S. from the reduction of beryllium fluoride with magnesium. New plants constructed by The Beryllium Corporation at Hazelton, Pa., and The Brush Beryllium Corporation at Elmore, Ohio, produce beryllium metal for nuclear and other applications. Each of these firms had a contract for annual delivery of 100,000 lb each of beryllium ingot to the Atomic Energy Commission, but the contracts were revised and the new production level set at 37,500 lb of ingot per year for each company.

Tantalum and columbium.—Tantalum production was estimated to be 225,000 lb in 1958 and is expected to reach 300,000 lb in 1959. Most of the metal is obtained either by electrolysis of fused potassium fluotantalate or by sodium reduction of this and other tantalum compounds. Columbium, the sister metal of tantalum, reached a production in 1958 estimated at 50,000 lb. While it is made chiefly by reaction between columbium carbide and columbium oxide, it can be made by the process used for tantalum, i.e., sodium reduction.

Stauffer Chemical Company announced construction of a $300,000 semiworks plant to make tantalum and columbium pentachlorides at its Richmond, Calif., research laboratories. National Research Corporation, Mallory-Sharon Metals Company, and Union Carbide Metals Company all had their processes for producing tantalum and/or columbium de-

scribed in articles published in 1958. Each used some form of sodium reduction of metal compounds to produce the metals. Recently, Haynes Stellite Company exhibited the largest tantalum sheet ever produced, the size being 28 x 60 x 0.030 in. The availability of large sheet should increase the use of tantalum in chemical equipment. Other producers of tantalum and/or columbium include du Pont, Fansteel Metallurgical Corporation, Wah Chang Corporation, Kawecki Chemical Company, Kennametal, Inc., and Molybdenum Corporation of America.

Manuscript received June 8, 1959. This paper was prepared for delivery before the Philadelphia Meeting, May 3-7, 1959.

Any discussion of this paper will appear in a Discussion Section to be published in the June 1960 JOURNAL.

Brief Communication

Action of Alkali on Caustic Cell Slimes

S. Wawzonek and P. D. Klimstra

Department of Chemistry, State University of Iowa, Iowa City, Iowa

Used graphite anodes have been the only source of material from which the caustic color compound has been isolated (1, 2). The report (3) that anode graphite slimes from chlorine-alkali cells contained 0.3-0.5% chloride suggested a study of various slimes from diaphragm and mercury cells to determine whether these could serve as a source of the caustic color compound.

Three samples of slimes have been treated with 50% sodium hydroxide at 100° for varying periods of time and the colors produced examined.

A sample of graphite particles removed from the bottom of one of the used anode plates after it had been used for the production of chlorine and caustic soda for approximately six months in a de Nora mercury cell gave the typical bluish-purple color associated with the caustic color compound.

A second sample consisting of graphite particles which were separated from the depleted brine stream after it had flown through the mercury cells gave under similar treatment a cherry red coloration. The possibility that this color was caused by colloidal ferric hydroxide was eliminated by the inability to discharge the color with sodium sulfide solution. This color, however, did not change to the blue on further heating with alkali.

A third sample consisting of the anode slimes from a diaphragm Tucker Windecker Cell operating with untreated anodes gave no color with 50% caustic.

Results obtained indicated that the caustic color compound or its precursor is produced in the mercury cell in the anode compartment but is effectively screened out by the circulating mercury which picks up the sodium in the mercury cell electrolyzer and subsequently releases the sodium as caustic soda in the denuder.

The absence of the caustic color compound in the anode slimes from a diaphragm cell suggests that most of the precursor may have been extracted by the caustic soda.

Acknowledgment

The authors wish to thank C. C. Silsby, Jr., of the Diamond Alkali Company, for the samples which were obtained from the Painesville and Muscle Shoals plants, and for his helpful discussion and advice.

Manuscript received June 12, 1959.

Any discussion of this paper will appear in a Discussion Section to be published in the June 1960 JOURNAL.

REFERENCES

1. H. H. Heller, *Trans. Electrochem. Soc.*, **87**, 501 (1945).
2. S. Wawzonek and D. S. P. Eftax, *This Journal*, **104**, 494 (1957).
3. S. Dahlerus and G. Wranglen, *Svensk Kem. Tidskr.*, **68**, 387 (1956).

Errata

In the September 1959 issue of the *Journal* in the paper by Barlane R. Eichbaum "The Dielectric Behavior of Solids Embedded in a Homogeneous Medium," in Fig. 1, 4, 6, 8, and 10, the tan δ graphs were omitted. Below are the dielectric constant and tan δ curves as they should have been shown.

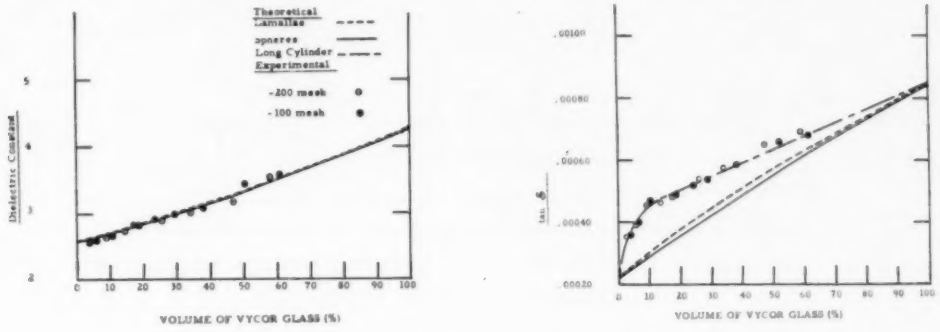

Fig. 1. Volume of vycor glass and polystyrene vs. dielectric constant and tan δ

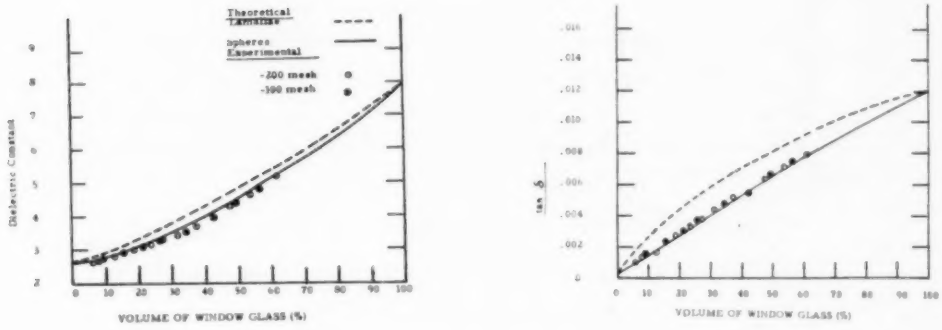

Fig. 4. Volume of window glass in polystyrene vs. dielectric constant and tan δ

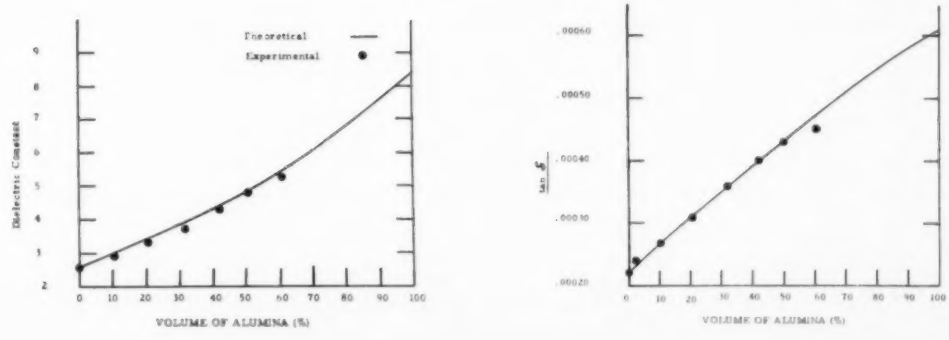

Fig. 6. Volume of alumina in polystyrene vs. dielectric constant and tan δ

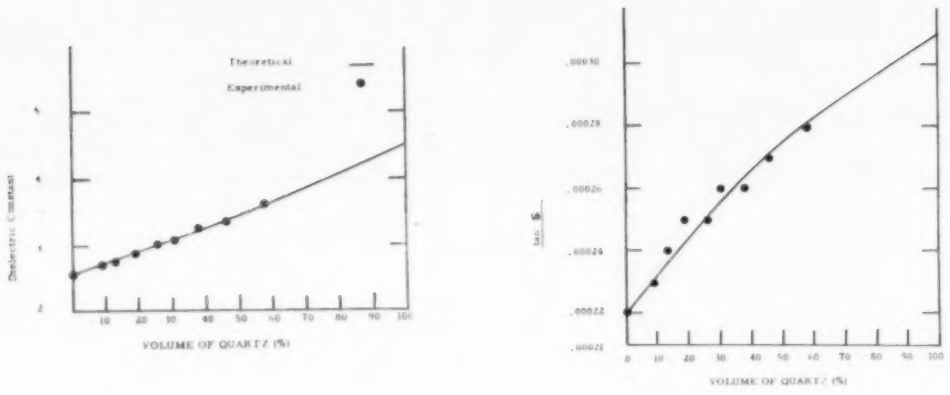

Fig. 8. Volume of quartz in polystyrene vs. dielectric constant and tan δ

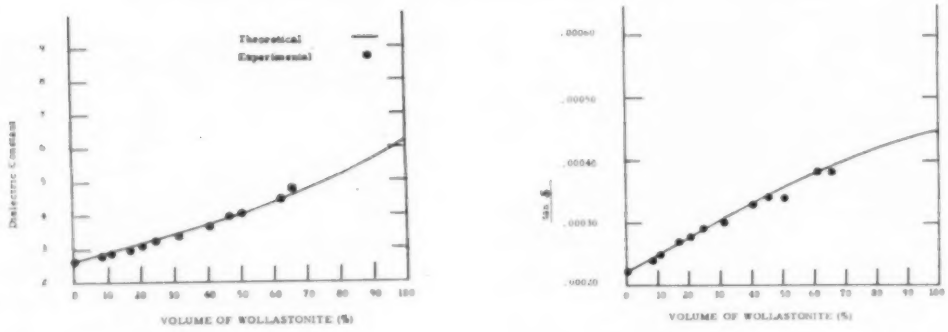

Fig. 10. Volume of wollastonite in polystyrene vs. dielectric constant and tan δ

In the paper by M. J. Pryor, "The Significance of the Flade Potential," which appeared on pp. 557-562 of the July 1959 JOURNAL, Eq. [9] on p. 561 is stated incorrectly. It should read:

$$\tfrac{1}{2}\,O_2 \longrightarrow O'' + \boxed{+\atop +} \qquad [9]$$

crystal lattice — bound positive hole

FUTURE MEETINGS OF
The Electrochemical Society

Columbus, Ohio, October 18, 19, 20, 21, and 22, 1959

Headquarters at the Deshler Hilton Hotel

Sessions will be scheduled on

Batteries, Corrosion (including a joint Corrosion–Electronics-Semiconductors session), Electrodeposition (including symposia on "Electrodeposition from Organic Solvents" and "Electro- and Chemical-Polishing"), Electronics (Semiconductors), Electro-Organics, and Electrothermics and Metallurgy

★ ★ ★

Chicago, Ill., May 1, 2, 3, 4, and 5, 1960

Headquarters at the Lasalle Hotel

Sessions probably will be scheduled on

Electric Insulation (including a symposium on "Electrolytic Capacitors"), Electronics (including Luminescence and Semiconductors), Electrothermics and Metallurgy (including a symposium on "High-Purity Vanadium" and a round table on "Methods of Reducing Iron Ores"), Industrial Electrolytics, and Theoretical Electrochemistry

★ ★ ★

Houston, Texas, October 9, 10, 11, 12, and 13, 1960

Headquarters at the Shamrock Hotel

★ ★ ★

Indianapolis, Ind., April 30, May 1, 2, 3, and 4, 1961

Headquarters at the Claypool Hotel

★ ★ ★

Detroit, Mich., October 1, 2, 3, 4, and 5, 1961

Headquarters at the Statler Hotel

Papers are now being solicited for the meeting to be held in Chicago, Ill., May 1-5, 1960. Triplicate copies of each abstract (*not exceeding 75 words in length*) are due at Society Headquarters, 1860 Broadway, New York 23, N. Y., *not later than January 4, 1960* in order to be included in the program. *Please indicate on abstract for which Division's symposium the paper is to be scheduled, and underline the name of the author who will present the paper.* Complete manuscripts should be sent in triplicate to the Managing Editor of the JOURNAL at 1860 Broadway, New York 23, N.Y.

Current Affairs

Book Reviews

The Design of Physics Research Laboratories—A Symposium held by the London and Home Counties Branch of the Institute of Physics at the Royal Institution on November 27, 1957. Edited by J. S. Forest. Published by Reinhold Publishing Corp., New York, 1959. 108 pages; $4.50.

Proceedings of the Twelfth Annual Battery Research and Development Conference. Published by Battery Conference Committee, Power Sources Division, U. S. Army Signal Research and Development Laboratory, Fort Monmouth, N. J., 1958. 134 pages; $10.00 first copy, $5.00 each additional copy on each order.

Proceedings of the Third Annual Appalachian Underground Corrosion Short Course, West Virginia Bulletin Series 59, No. 4-1, October 1958. Published by West Virginia University, Morgantown, W. Va.; 349 pages.

It usually is difficult to review the bound volume of papers presented at a symposium other than to list some of the titles and to comment on the quality of the printing. This, however, is not the case with the small volume of the symposium on Design of Physics Research Laboratories. There is a unified approach with each of the six speakers taking a separate but complementary part of the subject.

Although the emphasis was on the design of physics research laboratories in Great Britain, rather than on the construction or reconstruction of chemistry laboratories in the United States, there is much here of interest to ECS members. A good deal, of course, falls into the category of common sense, which means that it would not be thought of unless specifically mentioned by someone else. However, there is some factual information as well. For example, the paper by Hopkinson on laboratory design mentions that the results of a survey of 300 individuals at two large research institutes show that the space needs of one man are met 97% of the time by 12 feet of bench space and 5 feet of sink and drainboard. Also, a scientific officer (project leader) spends on the average about 28% of his time reading or writing and has less need for lab. space.

Extremely pertinent is a remark by T. Emmerson: "I am frequently surprised at the extent to which the design of the working accommodation particularly is influenced by the opinions of the man at the top who probably ceased to do useful experimental work ten years ago."

The book is well illustrated with sketches, designs, and pictures. There is a discussion section at the end of the volume.

* * *

The "Proceedings" of the Twelfth Annual Battery Research and Development conference, held at Fort Monmouth in May 1958, in contrast to the other two volumes reviewed here, is concerned with new material. It is the report of a symposium, or symposia, on fuel cells, nickel cadmium batteries, special purpose batteries, new primary designs, and low-temperature primary batteries. Some of the papers are reviews of basic material, but even these have been brought up to date with new material. Each article has its own bibliography and there are numerous graphs, pictures, and diagrams of high quality. It is to be regretted that there is no record of the discussions that followed each paper.

* * *

The "Proceedings" of the Third Annual Appalachian Underground Short Course differs from the other two volumes above in that it is didactic in nature. These papers were presented during a three-day study course on problems and practices of prevention of underground corrosion. The papers themselves are short, simple, and straightforward, well illustrated, and with very little elaboration of theory. Very little new work is presented, the emphasis being placed on teaching accepted practice and whatever elementary theory considered useful in the field. Sample titles are "Demonstration of the Theory of Cathodic Protection," "An Engineering Approach to the Selection of Pipe Line Coating," "Cathodic Protection Fundamentals," and Installing Graphite and Duriron Anodes."

H. W. Salzberg

Solid State Physics: Advances in Research and Applications, Vol. 8. Edited by Frederick Seitz and David Turnbull. Published by Academic Press, Inc., New York. 519 pages, 273 illustrations; $13.50.

With the continuing growth in volume and variety of research activity, there has come to be an increased need for authoritative reviews of special topics. The present volume, the eighth in an encyclopedic series on solid state physics, is one such effort. It contains five articles, ranging in length from 47 to 175 pages, on somewhat diverse subjects by an international representation of authors.

The longest article is "The Structure and Properties of Grain Boundaries," by S. Amelinckx and W. Dekeyser. It describes in detail the various dislocation models of grain boundaries in solids, first from a geometrical standpoint (as confirmed by the recent and powerful methods of observing dislocations directly), then from an energy and stability standpoint (as confirmed mostly by macroscopic measurements). Those readers who are unfamiliar with the spectacular recent progress in this field will be impressed by the direct and detailed experimental evidence shown in electron and optical micrographs. While low-angle boundaries are well understood by such models, high-angle boundaries have been treated only in special cases under rather severe simplifying assumptions. Subboundaries formed during solidification from the melt or by polygonization are less well understood. This article treats more briefly such phenomena in grain boundaries as

melting, migration, precipitation of solutes, diffusion, and electrical effects.

"The Interaction of Thermal Neutrons with Solids," by L. S. Kothari and K. S. Singwi, treats the scattering of low-energy neutrons by the thermal vibrations of crystals. In contrast to x-rays, such neutrons may suffer large relative changes in energy by inelastic collisions. The theory is well developed, but the very promising application of such neutron scattering to the investigation of crystal lattice dynamics and of liquids is just beginning.

The valence crystal germanium has proven to be an exceedingly useful material for studies of processes in solids that require very exact knowledge and control of conditions. The band structure of highly purified germanium is well understood and many properties associated with the presence of foreign atoms have been studied in detail. R. Newman and W. W. Tyler present a concise account of "Photoconductivity in Germanium" emphasizing the steady-state effects found in homogeneous material. Relevant theory is outlined and there is a short but fully referenced summary on the preparation and properties of doped crystals. Examples of experimental studies are presented and a note is appended on germanium as an infrared detector.

The article "Electronic Processes in Zinc Oxide," by G. Heiland, E. Mollwo, and F. Stöckman, is an exhaustive treatment of certain properties of a II-V compound which has been widely used commercially for many years. The study of the processes which make zinc oxide useful as a catalyst and photocatalyst has profited from the recent intensive research on semiconductors and ionic crystals on photoconductivity, luminescence, and surface properties. A brief review is given of the physical properties and of methods of preparation of single crystals, evaporated layers, and sintered specimens. The authors consider, in turn, for the various types of specimens, diffusion of defects, optical properties of pure and impure crystals, adsorption and catalysis, the equilibrium electrical conductivity of pure and impure material, slow and fast photoconductive processes, and surface conductivity. Considering the strong dependence of the various properties considered on the method of sample preparation, the authors present a coherent account of research on this substance.

D. S. McClure, in "Spectra of Molecules in Crystals," presents a brief introduction to the theory of localized excited states in molecular solids. Many additional spectral lines appear in molecular crystals as a result of intermolecular resonance and of violation of the selection rules for free molecular transitions. The comparatively recent application of group-theoretical (symmetry) considerations is the method which is leading to interpretation of such spectra.

Each article has an extensive set of references, covering work adequately through 1957 and containing a substantial number of 1958 publications. The format is neat and attractive, the illustrations and figures numerous and well reproduced, and the substantial cost about par for an American book of this nature. There are separate author and subject indexes.

R. O. Simmons

The Physics of Electricity and Magnetism, by William T. Scott. Published by John Wiley & Sons, Inc., New York, 1959. 635 pages; $8.75.

This textbook, written with emphasis on the physics of electricity and magnetism, is a very welcome addition in these times when most texts in this field are written by and for the engineering group. According to the author, it is suitable for juniors, seniors, and first-year graduate students, but surely he cannot be thinking of the C or B grade undergraduate. The book is too comprehensive and uses far too much mathematics to be satisfactory as a text in an intermediate course. It should be ideal for an honors or a seminar type of course.

The first four chapters, roughly one third of the book, are given over to electrostatics. In the chapter on dielectric materials, one finds a section on quadrupole fields; also in the same chapter is a discussion of electric D lines which are not closed, have no ends, and do not pass to infinity. This gives an idea of the author's determination to do a complete job and is indicative of the vein in which the book is written. As for the level of the mathematical background, one finds zonal and cylindrical harmonics used in the solution of Laplace's equation. In the appendix is a section on vector invariance which is needed for the discussion of special relativity in the chapter on radiation. The author states in his preface, "The book should have somewhat more material than can be covered in an average course, for different instructors will wish to cut out different sections." In this connection, he has conveniently included suggestions on the material to be used for various groups of readers.

This reviewer was pleased to find in the chapter on steady currents the general theorems relating to network analysis and the solution of problems by the loop current technique. Although often omitted in a physics text as being engineering property, these topics certainly have their place. Energy bands, the Fermi distribution function, and Fermi level are introduced but discussed only briefly in a qualitative manner for their relationship to conduction, contact potential, semiconductors, and the p-n junction. There are chapters, from 65 to 80 pages each, on The Magnetic Field, Magnetic Materials, Alternating Currents, and Electromagnetic Radiation. By and large, the material treated is traditional electricity and magnetism but the treatment has the flavor of good physics. The exposition is clear and

June 1960 Discussion Section

A Discussion Section, covering papers published in the July—December 1959 JOURNALS, is scheduled for publication in the June 1960 issue. Any discussion which did not reach the Editor in time for inclusion in the December 1959 Discussion Section will be included in the June 1960 issue.

Those who plan to contribute remarks for this Discussion Section should submit their comments or questions in triplicate to the Managing Editor of the JOURNAL, 1860 Broadway, New York 23, N. Y., *not later than March 1, 1960.* All discussion will be forwarded to the author(s) for reply before being printed in the JOURNAL.

the author has the happy facility for specifically pointing out inferences and conclusions implied in the theory but which, nevertheless, are likely to be overlooked by the reader. Generous footnotes and references are given at the bottom of the page, thus making for easy reading. Problems are placed at the end of the related section instead of being lumped together at the end of each chapter. They seem adequate in number, graded in difficulty, and chosen with an aim to illustrate the theory rather than promote proficiency in problem solving. At the end of the text is an extensive appendix dealing with various topics in mathematics and including almost enough material on vector analysis for a one-term course in this subject.

T. C. Hardy

Mechanisms of Inorganic Reactions; A Study of Metal Complexes in Solution, by Fred Basola and Ralph G. Pearson. Published by John Wiley & Sons, Inc., New York City, 1958. 426 pages: $11.75.

In this excellent book of limited application, the authors have held a huge round-up of facts and theories relating to the mechanisms and kinetics of metal complex and metal ligand reactions. Upon completion of the tally, most of the herd is scattered while the "mossy-horn" electrostatic theory and its new offspring, the crystal field theory, are driven merrily to market. This approach is not undesirable. Other current and past theories are carefully examined in the light of their usefulness and shortcomings before they are relegated to minor roles in the ensuing text. The combination of the old and new seems to answer more questions than do the valence bond and molecular obital theories.

The book opens with a short elementary treatment of the field, and defines at some length the type of compounds and reactions to be discussed. The succeeding chapters deal with the coordinate bond, octahedral and square complexes, stereochemistry, isomerization, racemization, oxidation, and reduction, and catalytic effects. A concluding omnibus chapter discusses adsorption spectra, ion pairs, acid-base properties, and exchange reactions.

While the jacket review states that the book deals exclusively with inorganic chemistry, an inordinate number of organometallics are used as illustrative compounds.

Notice to Members
Re Voting Ballot

By now you have received your official voting ballot from Society Headquarters. If you have not already done so, please return the ballot *by December 15* so that your vote can be included in the final election count.

The 400-odd pages of text and references are printed in easily read type on a glarefree off-white paper of good quality. No printing errors were discovered.

The book is an excellent collection of data and theory for the specialist in the metal-complex field. Source credits are well marked in the text and each chapter has an exhaustive bibliography. It is not recommended for the student chemist, without proper preparation, lest it discourage him unwarrantedly. The value as a text is questionable, but it is a fine source book.

Dale D. Williams

Division News

E & M Round Table on Methods of Reducing Iron Ores, Spring 1960

The Electrothermics and Metallurgy Division of the Society proposes to hold a round-table conference on the timely subject "Methods of Reducing Iron Ores" at the Spring 1960 Meeting of the Society to be held in Chicago, May 1-5. The purpose of the conference is to compare the various nonelectric methods of reducing typical iron ores with one another, and with electric smelting methods.

The conference will consist of:

1. A number of formal papers, each one by a specialist in one particular type of reduction
2. A general discussion of the subject.

R. R. Rogers, Mines Branch, Dept. of Mines & Technical Surveys, 552 Booth St., Ottawa, Ont., Canada, would be glad to receive suggestions as to the types of iron ore to be discussed, the types of reduction which should be covered in the formal papers, and specialists who would be qualified to discuss these particular types of reduction.

E & M Symposium on High-Purity Vanadium, Spring 1960

Papers on the subject "High-Purity Vanadium—Its Preparation, Properties, and Alloys" are being solicited by the Electrothermics and Metallurgy Division of the Society for a symposium, under the Co-Chairmanship of D. J. Hansen and M. Schussler of Union Carbide Metals Co., at the Spring Meeting of the Society in Chicago, May 1-5, 1960.

Topics on which contributions will be welcomed include:

- Resources of Vanadium Minerals—Domestic and Foreign
- Mining and Beneficiation of Vanadium Minerals
- Techniques for Reduction to High-Purity Metal
- Consolidation and Fabrication Techniques
- Properties of Alloys Based on High-Purity Vanadium
- Applications for Ductile Vanadium and Its Alloys.

Availability of ductile vanadium has stimulated exploratory work on its properties and potential uses in many laboratories. If enough of this information is presented at the symposium to warrant separate publication, the Division will sponsor preparation of a booklet containing the papers and discussion.

Titles, authors' names, and abstracts in triplicate (*not exceeding 75 words*) must be received at Society Headquarters, 1860 Broadway, New York 23, N. Y., *by January 4, 1960*. Abstracts should bear the notation "For Vanadium Symposium, Spring 1960," and the name of the author who will present the paper should be underlined. Complete manuscripts, ready for publication in all details, must be given to the Symposium Chairman immediately following presentation.

E & M Symposium on Rhenium, Spring 1960

The Electrothermics and Metallurgy Division is inviting papers on various aspects of rhenium technology to be combined into a symposium for the Spring Meeting in Chicago, May 1-5, 1960. Bruce W. Gonser of Battelle Memorial Institute is Chairman of this symposium.

Although emphasis may be given to the extractive and physical metallurgy of rhenium, a broader coverage is planned. In particular, papers are desired that cover recent investigations on properties, alloys, and development of applications.

Rhenium is relatively expensive, but in recent years excellent sources of supply have been developed which are far in excess of current consumption. Some excellent and unique properties indicate that more rhenium could be used advantageously if it were better known.

Titles, authors' names, and abstracts in triplicate (*not exceeding 75 words*) must be received at Society Headquarters, 1860 Broadway, New York 23, N. Y., *by January 4, 1960*. Abstracts should bear the notation "For Rhenium Symposium, Spring 1960," and the name of the author who will present the paper should be underlined. Complete manuscripts, ready for publication in all details, must be given to the Symposium Chairman immediately following presentation.

Section News

India Section News

Electroplating Journal Started in India—The first number of the journal *Electroplating*, Vol. 1, No. 1, May 1959, has been published. This new journal is devoted to the development of plating and metal finishing industries. The topics to be covered are: cleaning, plating, polishing, surface conversion treatments, testing of deposits, analytical methods, plating shop problems, theoretical aspects, abstracts. The Editorial Committee consists of T. L. Rama Char (Chairman), A. N. Kappanna, G. F. Weill, R. Grauer, V. T. Talim, A. K. Chatterjee, T. Banerjee, H. V. K. Udupa, I. Sanghi, and S. K. Panikkar (Editor). All communications should be sent to the Editor, *Electroplating*, 547 Kalbadevi Rd., Bombay 2.

Battery Study Group Meeting—The Electronic Development Panel, Ministry of Defence, Govt. of India has formed a Study Group to examine the various proposals regarding the development of new types of batteries for adoption by the Services. A meeting of the Group was held in February 1959 at the Electronics Research and Development Establishment, Bangalore. There were representatives from the Defence Services, government laboratories, research institutions, and industrial establishments. The following members of The Electrochemical Society participated in the deliberations: H. V. K. Udupa, S. Ghosh, H. G. Singh, R. C. Misra, J. Balachandra (Representative India Section), and T. L. Rama Char (Representative India Section). The discussions covered various types of batteries: dry, mercuric-oxide, lead-acid, silver-zinc, nickel-cadmium, and solar. The program was rounded off with visits to important industries in Bangalore.

New Patron, India Section—Ronuk Industries Ltd., Bombay, has joined the Section as Patron.

T. L. Rama Char,
India Correspondent

Pittsburgh Section

On May 22, the Section held its annual spring meeting. In keeping with the bicentennial year of Pittsburgh, the meeting centered around two fields in which Pittsburgh has made significant contributions, namely, corrosion and atomic power. U.S. Steel Laboratories were host for the morning. Several very interesting papers on corrosion were presented. After a luncheon and business meeting, the afternoon was spent touring the Shippingport Atomic Power Plant which is supplying part of Pittsburgh with electricity. At the business meeting, the nominating committee presented the following slate of officers who were subsequently elected for the 1959-1960 term:

Chairman—E. H. Phelps, 522 Firethorn Dr., Monroeville, Pa.

Vice-Chairman—J. W. Faust, Jr., Westinghouse Electric Corp., Beulah Rd., Churchill Boro., Pittsburgh 35, Pa.

Secretary-Treasurer—W. E. Haupin, Aluminum Research Labs., Aluminum Co. of America, New Kensington, Pa.

Local Section Councilors—A. J. Cornish and J. J. Stokes

The Treasurer gave his annual report. A. J. Cornish reported that Jan Higgenbothum won the award of 25 silver dollars presented by the Pittsburgh Section of The Electrochemical Society at the annual Science Fair held at Buhl Planetarium. Miss Higgenbothum's exhibit was "Flame Fusion Method for Growing Corundum Crystals." Plans for the coming year were briefly discussed.

J. W. Faust, Jr.,
Secretary-Treasurer, 1958-1959

San Francisco Section

The final meeting of the 1958-1959 season was held on May 27, 1959 at the University of California Men's Faculty Club. The speaker was Dr. Hakon Flood, professor of inorganic chemistry at Norwegian Institute of Technology and head of the Institute of Silicate Science. His subject was "The Exchange Reaction Approach to the Calculation of Chemical Equilibria in Liquid Salt Mixtures."

The following have been elected officers of the Section for the 1959-1960 term:

Chairman—R. A. Zimmerly, Columbia-Geneva Steel Div., U. S. Steel Corp., Pittsburg, Calif.

Vice-Chairman—R. E. De La Rue, Stanford Research Institute, Menlo Park, Calif.

Secretary—H. F. Stout, Columbia-Geneva Steel Div., U. S. Steel Corp., Pittsburg, Calif.

Treasurer—S. H. Dreisbach, 21869 Monte Court, Monta Vista, Calif.

Local Section Councilors—

(1959-1961) R. L. Bechtold, 3725 Bon Homme Way, Concord, Calif.

(1959-1960) Morris Feinleib, Varian Associates, 611 Hansen Way, Palo Alto, Calif.

R. E. De La Rue, *Vice-Chairman*

Washington-Baltimore Section

Officers for the coming year, 1959-1960, were elected at the seventh meeting of the Washington-Baltimore Section held at the National Bureau of Standards on April 30, 1959:

Chairman—David Schlain, P. O. Box 348, College Park, Md.

Vice-Chairman—Jerome Kruger, 101 N.W. Bldg., National Bureau of Standards, Washington 25, D. C.

1960 Bound Volume

Members and subscribers who wish to receive bound copies of Vol. 107 (for 1960) can receive the volume for the low, prepublication price of $6.00 if their orders are received at Society Headquarters, 1860 Broadway, New York 23, N. Y., by *December 1, 1959*. After that date, members will be charged $12.00, and nonmembers, including subscribers, $18.00, subject to prior acceptance.

Bound volumes are *not* offered independently of JOURNAL subscription.

Secretary—R. J. Brodd, National Bureau of Standards, Section 1.8, Washington 25, D. C.

Treasurer—Sigmund Schuldiner, 3101 "P" St., S. E., Washington 20, D. C.

Local Section Councilor—(to fill J. C. White's expiring term)—J. C. White, 4205 Woodberry St., University Park, Hyattsville, Md.

"The Handbook of Chemistry and Physics" was presented to winners of the Science Fair Awards sponsored by the Washington-Baltimore Section for the best electrochemical projects in five local area science fairs.

The speaker of the evening was Dr. Morris Cohen of the National Research Council of Canada who spoke on the topic "The Effect of Initial Surface Preparation on Passivity and Oxidation Reactions."

Speakers and their topics at other monthly meetings of the Section were: January 15, Robert J. Fallon of Catholic University, "Occlusion of Hydrogen by Palladium"; February 19, David Schlain of the U.S. Bureau of Mines, "Corrosion Behavior of Titanium and Its Alloys"; March 19, A. C. Simon of the Naval Research Lab., "Problems of Storage Battery Design and Performance as Investigated by Microscopy"; April 14, H. C. Savage of the Oak Ridge National Lab., "Corrosion Problems Associated with the Aqueous Homogeneous Reactor"; May 21, Ralph J. Brodd of the National Bureau of Standards, "Relaxation Effects of Electrodes."

Jerome Kruger,
Secretary, 1958-1959

New Members

In August 1959, the following were approved for membership in The Electrochemical Society by the Admissions Committee:

By action of the Board of Directors of the Society, all prospective members must include first year's dues with their application for membership.

Also, please note that, if sponsors sign the application form itself, processing can be expedited considerably.

Active Members Sponsored by a Sustaining Member

R. M. Felsenthal, Exmet Corp., 127 Marblehead Rd., Tuckahoe, N. Y. (Battery)

J. J. Root, Three Point One Four Corp., 24 Woodworth Ave., Yonkers, N. Y. (Battery)

L. B. Valdes, Rheem Semiconductor Corp., 327 Moffett Blvd., Mountain View, Calif. (Electronics)

A. K. Wright, Tung-Sol Electric Inc., 1 Summer Ave., Newark 4, N. J. (Electronics)

Active Members

W. T. Allen, Franklin & Marshall College; Mail add: 8 Girard Ave., Lancaster, Pa. (Electronics)

R. L. Batdorf, Bell Telephone Labs., Inc.; Mail add: 10 Horseshoe Rd., Berkeley Heights, N.J. (Electronics)

J. J. Banewicz, Southern Methodist University, Dallas 5, Texas (Electronics)

Marco Bono, Fiat; Mail add: Corso Matteotti O, Torino, Italy (Industrial Electrolytic)

Eugenio Bertorelle, Istituto Chimico, RHO Milan, Italy (Electrodeposition, Theoretical Electrochemistry)

W. E. Bulman, Ohio Semiconductors Inc.; Mail add: 379 Beaver Ave., Columbus 13, Ohio (Electronics)

T. S. Burkhalter, Texas Instruments Inc., 6000 Lemmon Ave., Dallas 9, Texas (Electronics)

J. J. Collins, Shieldalloy Corp.; Mail add: 617 Heston Rd., Glassboro, N. J. (Electrothermics & Metallurgy)

E. B. Cox, General Electric Co., John St., Hudson Falls, N. Y. (Electric Insulation)

M. J. Dignam, Dept. of Chemistry, University of Toronto, Toronto 5, Ont., Canada (Theoretical Electrochemistry)

Kurt Ekler, Loyola College; Mail add: 2170 Lincoln Ave., Montreal, Que., Canada (Theoretical Electrochemistry)

Sixdeniel Faria, Sylvania Electric Products Inc.; Mail add: 456 37th St., Lindenhurst, N.Y. (Electronics)

G. C. Florio, Sr., Tung-Sol Electric Co.; Mail add: 24 Euclid Place, Montclair, N.J. (Electrodeposition, Electronics)

I. R. Gillet, University of Liége, 2 rue A. Stevart, Liége, Belgium (Electro-Organic Theoretical Electrochemistry)

F. L. Gittler, Bell Telephone Labs., Inc.; Mail add: 1217 N. 16 St., Allentown, Pa. (Electronics)

R. E. Grace, School of Metallurgical Engineering, Purdue University, Lafayette, Ind. (Electrothermics & Metallurgy)

Robert Guizonnier, Faculté des Sciences, 20 Cours Pasteur, Bordeaux, France (Electric Insulation)

W. F. Hall, Hughes Products Co.; Mail add: 2332 Cornell Dr., Costa Mesa, Calif. (Electrothermics & Metallurgy)

J. F. Harvey, Drexel Institute of Technology; Mail add: Serials Dept., Library, Philadelphia 4, Pa.

Juro Horiuti, Hokkaido University; Mail add: 405 Hiragishi, Toyohira, Sapporo, Japan (Theoretical Electrochemistry)

W. F. Houlihan, Heatbath Corp., Box 78, Springfield 1, Mass. (Corrosion, Electrodeposition, Electro-Organic)

H. B. Kirkpatrick, National Bureau of Standards, Washington 25, D.C. (Corrosion)

D. E. Lundy, Sylvania Electric Products Inc., Towanda, Pa. (Electronics)

W. B. MacKenzie, Phelps Dodge Copper Products Corp., 63 St. Andrews Place, Yonkers 5, N. Y. (Electric Insulation)

K. E. McAbee, P. R. Mallory Co.; Mail add: 8804 El Rico Rd., Indianapolis 20, Ind. (Electronics)

D. A. McLean, Bell Telephone Labs., Inc.; Mail add: 78 Fairview Ave., Chatham, N. J. (Electric Insulation)

J. L. Montgomery, AVCO Electronics Research Labs., 750 Commonwealth Ave., Boston 15, Mass. (Electronics)

J. C. Myers, Dow Chemical Co.; Mail add: 704 Winding Way, Lake Jackson, Texas (Industrial Electrolytic)

R. G. Olsson, General Electric Co.; Mail add: R.D. No. 1, Jamesville, N. Y. (Electronics)

E. S. Palik, General Electric Co.; Mail add: 1747 Lyndhurst Rd., Cleveland 24, Ohio (Electronics)

J. I. Pankove, RCA Labs., Radio Corp. of America, Princeton, N.J. (Electronics)

Charles Pettus, I.B.M. Corp.; Mail add: 400 Main St., Vestal, N. Y. (Theoretical Electrochemistry)

P. V. Popat, General Electric Co.; Mail add: 2161 Daisy Lane, Schenectady, N.Y. (Battery, Theoretical Electrochemistry)

W. H. Reinmuth, Dept. of Chemistry, Columbia University, New York, N. Y. (Theoretical Electrochemistry)

E. H. Reynolds, British Insulated Callenders Cables, Ltd.; Mail add: 16 Court Lane Gardens, Dulwich, London, S.E. 21, England (Electric Insulation, Electrodeposition, Industrial Electrolytic, Theoretical Electrochemistry)

D. K. Roe, Dept. of Chemistry,

University of Illinois, Urbana, Ill. (Theoretical Electrochemistry)

W. J. H. Rogers, Industrial Testing Labs.; Mail add: 614 W. 113 St., New York 25, N. Y. (Electro-Organic)

Warren Ruderman, Isomet Corp., 433 Commercial Ave., Palisades Park, N. J. (Electronics)

Tobie Salomon, Institut Francais du Petrole, Rueil-Malmaison (S.&O.), France (Corrosion, Electric Insulation, Electro-Organic)

G. M. Schmid, Chemistry Dept., University of Texas, Austin 12, Texas (Theoretical Electrochemistry)

Irving Shain, Chemistry Dept., University of Wisconsin, Madison 6, Wis. (Theoretical Electrochemistry)

C. L. Scheirer, Jr., Sylvania Electric Products Inc., Towanda, Pa., (Electronics)

B. L. Shely, Minnesota Mining & Mfg. Co.; Mail add: 1155 Mahtomedi Ave., Mahtomedi 15, Minn. (Electronics)

H. L. Shepard, National Carbon Co.; Mail add: Route No. 1, Goode, Va. (Industrial Electrolytic)

Mark Steidlitz, International Resistance Co., 401 No. Broad St., Philadelphia, Pa. (Electronics)

C. F. Stocker, RCA Labs., Radio Corp. of America, Princeton, N.J. (Electronics)

Nancy J. Tighe, National Bureau of Standards, Connecticut Ave. & Van Ness St., Washington 25, D.C. (Corrosion)

Hans Tropper, Queen Mary College, Miles End Rd., London E. 1, England (Electric Insulation)

Issac Trachtenberg, American Oil Co.; Mail add: 5614 Borden, Galveston, Texas (Theoretical Electrochemistry)

P. G. Walker, Electro Metallurgical Co., 1425 Mountain St., Montreal, Que., Canada (Industrial Electrolytic)

E. L. Williams, Sylvania Electric Products Inc., P. O. Box 17, North Lake, Ill. (Electronics)

J. D. Winters, Incar, Inc., 1480 Lakeside Ave., Cleveland 14, Ohio (Electrodeposition)

W. V. Wright, Jr., Electro Optical Systems, Inc., 170 Daisy, Pasadena, Calif. (Electronics)

Student Associate Members

Peter Delvigs, Western Reserve University; Mail add: 1718 ½ Strathmore Ave., East Cleveland 12, Ohio—Cleveland Award Winner (Theoretical Electrochemistry)

K. J. Martin, Dept. of Chemistry, University of Wisconsin, Madison 6, Wis. (Theoretical Electrochemistry)

G. E. Walrafen, University of Chicago; Mail add: 1005 E. 60, Chicago 37, Ill. (Theoretical Electrochemistry)

Reinstatement to Active Membership

J. S. Hart, Hanson-Van Winkle-Munning Co.; Mail add: 4765 Tully Rd., Bloomfield Hills, Mich. (Electrodeposition)

Deceased Member

A. K. Huntley, Cleveland, Ohio

Personals

John R. Thomas has been appointed manager of the Battery Engineering Research Dept. of Globe-Union Inc., Milwaukee, Wis. He had been manager of the Battery Separator Research Dept. of the Dewey Almy Chemical Division of the W. R. Grace Co. at Cambridge, Mass.

Daniel Chapin, formerly with the sales staff of the Dow Chemical Co.'s Cincinnati office, has been advanced to a new post as assistant to the manager, Detroit office, specializing in the sale of products to the automobile industry. Mr. Chapin joined Dow in 1950, and was on the magnesium sales staff at the Cleveland office until 1954 when he was assigned to Cincinnati.

Justo B. Bravo has been named group leader, New Products and Processes, at the Berwyn, Pa., laboratories of the Foote Mineral Co.

Ralph E. Ramsay, former vice-president and research director, retired from the Ray-O-Vac Co., Madison, Wis., on July 1, 1959 after 34 years of service. Prior to entering battery research in 1925, he had been an associate for five years of the late Dr. Oliver P. Watts on the chemical engineering faculty of the University of Wisconsin. Mr. Ramsay's home address is: 7 Paget Rd., Madison 4, Wis.

Notice to Members and Subscribers

(Re Changes of Address)

To insure receipt of each issue of the JOURNAL, please be sure to give us your old address, as well as your new one, when you move. Our records are filed by states and cities, not by individual names. The Post Office does not forward magazines.

Everett Keith McMahon

Everett Keith McMahon, manager of the Chemical Sales Division of Tennessee Products & Chemical Corp., Nashville, Tenn., died suddenly on August 25, 1959 of a heart attack. He was 39 years old.

Dr. McMahon, widely known in the field of chemical engineering and market research, had served since 1949 with Tennessee Products & Chemical Corp., a subsidiary of Merritt-Chapman & Scott Corp.

Graduated from Georgia Institute of Technology in 1942 with a B.S. degree in chemical engineering, Dr. McMahon later earned his M.S. and Ph.D. degrees in chemical engineering at Columbia University in New York where he was a research associate on electronic heating.

When he first became associated with Tennessee Products & Chemical, Dr. McMahon served as supervisor of the Chemical Engineering and Research Section in Chattanooga, Tenn. In 1954, he was named manager of Technical Sales Development and moved to Nashville, site of the company's general offices. He was appointed manager of the Chemical Sales Division in 1958.

Active in many professional organizations, Dr. McMahon was a member of The Electrochemical Society, American Chemical Society, American Institute of Chemical Engineers, Commercial Chemical Development Association, and the Chemical Market Research Association. He was a well-known lecturer before student groups on the subject of chemical engineering and market research.

He is survived by his wife, Martha G., and three children, Kenneth G., Margaret K., and Brenda E.

News Items

New ECS Sustaining Member

General Instrument Corporation, Newark, N. J., recently became a Sustaining Member of The Electrochemical Society.

Powder Metallurgy Research May Lead to High Tensile Strength Lead

A research grant has been awarded to Dr. Fritz V. Lenel, professor of metallurgical engineering at Rensselaer Polytechnic Institute, to investigate powder metallurgy techniques with lead and lead alloys. The project is part of the over-all research program of the Lead Industries Association.

Earlier studies of lead and lead alloys produced by powder metallurgy indicate that it may be possible to effect dramatic increases in tensile strength and other physical properties of the metal. Tensile strength has already been increased to twice the usual values via this powder technique. Some researchers have reported that lead test specimens prepared by powder metallurgy have shown six times the tensile strength of unalloyed lead.

Journal of ECS Microfilmed

The Electrochemical Society announces that an agreement has been entered into with University Microfilms, Inc., Ann Arbor, Mich., for the microfilming of all volumes of the TRANSACTIONS and JOURNAL of the Society.

This consists of 15 reels and covers Vol. 1-104 (1902-1957), and positive microfilm copies of all these volumes sell for $375.00. When reels are sold separately for any of these volumes, the price is $25.00 each.

Subsequent volumes of the JOURNAL will be on separate reels. Vol. 105 (1958) is now available for $3.10.

One of the most pressing problems faced by libraries is that of providing adequate space for their publications. Microfilm editions are one solution to this problem.

Inquiries concerning purchase should be addressed to University Microfilms, Inc., 313 N. First St., Ann Arbor, Mich.

Developments in the Field of Molecular Electronics

Halex, Inc., of El Segundo, Calif., a new corporation pioneering in the field of molecular electronics, is specializing in the process of depositing thin films of conductive, semiconductive, and resistive substances to form electronic circuits, according to an announcement made by Harold R. Larsen, president.

Halex engineers utilize high-vacuum techniques to build up thin films with controlled properties, molecule by molecule, on secondary substances. Thicknesses are readily produced in ranges from less than one millionth of an inch to one hundred millionths of an inch, thereby reducing bulk materials more efficiently and economically than by conventional methods such as cutting, etching, drawing, rolling, or other fabrications. Through critically controlled processes, specified properties and geometry of almost any material can be achieved.

Developments in the field of molecular electronics by Halex, Inc., include experimentations with micro-resistors, -capacitors, -semiconductors, -transducers and microsensing devices. Eventually, the firm will concentrate on complete replacement circuits to be used in virtually every kind of electronic device.

Engelhard and Imperial Chemical Join in Production of Pt-Ti Electrodes

Engelhard Industries, Inc., and Imperial Chemical Industries, Ltd., two of the largest international companies in their fields, have concluded agreements covering the production and sale of platinum-titanium electrodes, it was announced recently in New York and London.

Following the established production of platinized titanium electrodes by the Metals Division of Imperial Chemical Industries, Ltd., Englehard Industries will produce similar electrodes which will replace present materials in industrial use, such as graphite, silicon-iron, and lead alloys.

Since 1861
AMES has been making these
SILVER SALTS
to YOUR specifications

Silver Nitrate
Silver Cyanide
Silver Chloride
Silver Sulfate
Monovalent Silver Oxide
Divalent Silver Oxide

And now for your Battery
Silver Flour
and
for powder metallurgy
Nodular Silver

M. AMES CHEMICAL WORKS, INC.
17-19 Rogers Street
Glen Falls, New York
Phone 2-4394

Engineers or Scientists

The fast expanding Research and Development Department of The Rauland Corporation, Chicago (a subsidiary of Zenith Radio Corp.), has openings for engineers or scientists with creative ability and bent for experimental work in the field of

photoemissive surfaces and their application to display devices.

B.S. or more advanced degree and at least one year experience in the photoemissive field are desired.

For those qualified, there are also openings in the field of photoconductors and solid state display panels.

Write to: Personnel Director

The Rauland Corporation
4245 North Knox Avenue
Chicago 41, Illinois

Advantages of the new electrode for the production of chemicals, such as chlorine, will lead to increased operating efficiency and consequent lower costs, together with substantial savings in servicing and maintenance.

The electrodes are also used as anodes in the cathodic protection of the steel hulls of ships, from the largest tankers, freighters, and naval vessels down to the smallest pleasure boats, as well as for bridges, metal piers, and industrial plants.

Dow Opens New Office in Johannesburg

Opening of a new sales office in Johannesburg, Union of South Africa, has been announced by Dow Chemical International Ltd. S. A. The office will serve the entire continent south of the Sahara.

John R. Myers, area supervisor for Europe and Africa, has been named sales supervisor of the office. He has been located at the Midland, Mich., headquarters.

Announcements from Publishers

"Radioactivity Measuring Instruments." Edited by M. C. Nokes. Published by Philosophical Library, Inc., New York City, 1958. vii + 75 pages; $4.75.

This is a small do-it-yourself manual for use mainly by secondary school teachers interested either in having students learn to build apparatus or in saving money on demonstration equipment. The emphasis is on making instruments of fair accuracy with a minimum expenditure of time and money. Some basic theory is given, together with simple circuit diagrams and directions. Cost and sources of parts are included.

"Encyclopedia of Chemical Reactions, Vol. VIII." Edited by C. A. Hampel and C. A. Jacobson. Published by Reinhold Publishing Corp., New York City, 1959. 531 pages; $14.00.

This is the final volume of the "Encyclopedia of Chemical Reactions." It includes the reactions of tungsten, uranium, vanadium, ytterbium, yttrium, zinc, and zirconium; 200 pages of addenda covering entries received subsequent to the publication of the volume with which they were concerned, an index of reagents mentioned, and an index of substances obtained, both indexes covering the entire set of eight volumes. Each entry contains a description of the reaction, the equations, and the literature reference.

"Control in Electroplating." Published by Robert Draper Ltd., Teddington, Middlesex, England, 1959. ix + 92 pages; $2.50 plus 15 cents postage.

This book contains four talks presented in a one-day symposium organized by the London Branch of the Institute of Finishing, held in London, November 1958. The aim of the symposium, and therefore of the book, was to present to an audience of plating chemists and practical platers well-established facts on a number of practical aspects of technical control. The talks were entitled "Chemical Control of Plating Electrolytes," "Control of Electrodeposition Processes by Examination of the Deposits," "Trouble Shooting in the Plating Shop," and "Requirements and Inspection of Metallic Finishes for (Armed) Services' Equipment." The discussions also are reported.

"The Atom and the Energy Revolution," by Norman Lansdell. Published by Philosophical Library, Inc., New York City, 1958. XIV + 200 pages; $6.00.

Features of special attention are: the introductory section on world energy resources and demand, giving a country-by-country breakdown; a discussion of sources of natural materials for atomic energy development; and a chapter on radiation risks and insurance against them.

The author believes that the fuel cell using alcohol probably will be the most important energy source for transport except for the very largest ocean-going ships and special-purpose vessels, such as submarines. An interesting statement, in light of current events, is that the Tsangpo River, in Tibet, has a horseshoe-bend enabling a short-circuiting tunnel to provide a water head of a mile and a quarter, capable of supplying 150-330 billion kwhr/yr, one eighth to one fourth that of the present total world electricity output.

"Diffusion of Beryllium in Beryllium Oxide," Dec. 1958. AEC Report NAA-SR-3170,* 22 pages; 75 cents.

"A Preliminary Study of High-Strength Zirconium-Base Alloys," Aug. 1958. AEC Report NMI-1205,* 36 pages; $1.00.

"Refractory Metals and Their Alloys: A Literature Search," Jan. 1959. AEC Report TID-3524,* 10 pages; 50 cents.

"The Colorimetric Determination of Titanium in Uranium," Oct. 1955. AEC Report LA-1967,* 16 pages; 50 cents.

* Order from Office of Technical Services, U. S. Dept. of Commerce, Washington 25, D. C.

Notice to Subscribers

Your subscription to the JOURNAL of The Electrochemical Society will expire on *December 31, 1959*. Avoid missing any issue. Send us your remittance now in the amount of $18.00 for your 1960 subscription. (Subscribers located outside the United States must add $1.00 to the subscription price for postage, and payment must be made by Money Order or New York draft, not local check.) An expiration notice has been mailed to all subscribers.

A bound volume of the 1960 JOURNALS can be obtained at the prepublication price of $6.00 by adding this amount to your remittance. However, no orders will be accepted at this rate after *December 1, 1959*, when the price will be increased to $18.00 subject to prior acceptance. Bound volumes are *not* offered independently of your JOURNAL subscription.

Advertiser's Index

American Brass Company 268C
M. Ames Chemical Works, Inc. 276C
E. I. du Pont de Nemours & Company (Inc.) 267C
Enthone, Incorporated ..... Cover 4
Great Lakes Carbon Corp., Electrode Division ..... Cover 2
Perkin Engineering Corporation 262C-263C
The Rauland Corporation 276C
E. H. Sargent & Company 266C
Stackpole Carbon Company 265C

The Electrochemical Society

Patron Members

Aluminum Co. of Canada, Ltd.,
Montreal, Que., Canada
International Nickel Co., Inc.,
New York, N. Y.
Olin Mathieson Chemical Corp.,
Niagara Falls, N. Y.
Industrial Chemicals Div., Research
and Development Dept.
Union Carbide Corp.
Divisions:
Union Carbide Metals Co.,
New York, N. Y.
National Carbon Co., New York, N. Y.
Westinghouse Electric Corp., Pittsburgh, Pa.

Sustaining Members

Air Reduction Co., Inc.,
New York, N. Y.
Ajax Electro Metallurgical Corp.,
Philadelphia, Pa.
Allen-Bradley Co., Milwaukee, Wis.
Allied Chemical & Dye Corp.
General Chemical Div., Morristown, N. J.
Solvay Process Div., Syracuse, N. Y.
(3 memberships)
Allied Research Products, Inc.,
Detroit, Mich.
Alloy Steel Products Co., Inc., Linden, N. J.
Aluminum Co. of America,
New Kensington, Pa.
American Machine & Foundry Co.,
Raleigh, N. C.
American Metal Climax, Inc.,
New York, N. Y.
American Potash & Chemical Corp.,
Los Angeles, Calif. (2 memberships)
American Zinc Co. of Illinois,
East St. Louis, Ill.
American Zinc, Lead & Smelting Co.,
St. Louis, Mo.
American Zinc Oxide Co., Columbus, Ohio
M. Ames Chemical Works, Inc.,
Glens Falls, N. Y.
Auto City Plating Company Foundation,
Detroit, Mich.
Basic Inc., Maple Grove, Ohio
Bell Telephone Laboratories, Inc.,
New York, N. Y. (2 memberships)
Bethlehem Steel Co., Bethlehem, Pa.
(2 memberships)
Boeing Airplane Co., Seattle, Wash.
Burgess Battery Co., Freeport, Ill.
(4 memberships)
C & D Batteries, Inc., Conshohocken, Pa.
Canadian Industries Ltd., Montreal, Que.,
Canada
Carborundum Co., Niagara Falls, N. Y.
Catalyst Research Corp., Baltimore, Md.
Chrysler Corp., Detroit, Mich.
Ciba Pharmaceutical Products, Inc., Summit,
N. J.
Columbian Carbon Co., New York, N. Y.
Columbia-Southern Chemical Corp.,
Pittsburgh, Pa.
Consolidated Mining & Smelting Co. of
Canada, Ltd., Trail, B. C., Canada
(2 memberships)
Continental Can Co., Inc., Chicago, Ill.
Cooper Metallurgical Associates, Cleveland,
Ohio
Corning Glass Works, Corning, N. Y.
Crane Co., Chicago, Ill.
Diamond Alkali Co., Painesville, Ohio
(2 memberships)
Dow Chemical Co., Midland, Mich.
Wilbur B. Driver Co., Newark, N. J.
(2 memberships)
E. I. du Pont de Nemours & Co., Inc.,
Wilmington, Del.
Eagle-Picher Co., Chemical Div., Joplin, Mo.
Eastman Kodak Co., Rochester, N. Y.
Electric Auto-Lite Co., Toledo, Ohio
Electric Storage Battery Co.,
Philadelphia, Pa.
Englehard Industries, Inc., Newark, N. J.
(2 memberships)
The Eppley Laboratory, Inc., Newport, R. I.
(2 memberships)
Erie Resistor Corp., Erie, Pa.
Exmet Corp., Tuckahoe, N.Y.
Fairchild Semiconductor Corp., Palo Alto,
Calif.
Federal Telecommunication Laboratories,
Nutley, N. J.
Food Machinery & Chemical Corp.
Becco Chemical Div., Buffalo, N. Y.
Westvaco Chlor-Alkali Div., South
Charleston, W. Va.
Foote Mineral Co., Paoli, Pa.
Ford Motor Co., Dearborn, Mich.
General Electric Co., Schenectady, N. Y.
Chemistry & Chemical Engineering
Component, General Engineering
Laboratory
Chemistry Research Dept.
General Physics Research Dept.
Metallurgy & Ceramics Research Dept.
General Instrument Corp., Newark, N. J.

(Sustaining Members cont'd)

General Motors Corp.
Brown-Lipe-Chapin Div., Syracuse, N. Y. (2 memberships)
Guide Lamp Div., Anderson, Ind.
Research Laboratories Div., Detroit, Mich.
General Transistor Corp., Jamaica, N. Y.
Gillette Safety Razor Co., Boston, Mass.
Gould-National Batteries, Inc., Depew, N. Y.
Grace Electronic Chemicals, Inc., Baltimore, Md.
Great Lakes Carbon Corp., New York, N. Y.
Hanson-Van Winkle-Munning Co., Matawan, N. J. (3 memberships)
Harshaw Chemical Co., Cleveland, Ohio (2 memberships)
Hercules Powder Co., Wilmington, Del.
Hill Cross Co., Inc., New York, N. Y.
Hoffman Electronics Corp., Evanston, Ill.
Hooker Chemical Corp., Niagara Falls, N. Y. (3 memberships)
Houdaille Industries, Inc., Detroit, Mich.
Hughes Aircraft Co., Culver City, Calif.
International Business Machines Corp., Poughkeepsie, N. Y.
International Minerals & Chemical Corp., Chicago, Ill.
Jones & Laughlin Steel Corp., Pittsburgh, Pa.
K. W. Battery Co., Skokie, Ill.
Kaiser Aluminum & Chemical Corp.
Chemical Research Dept., Permanente, Calif.
Div. of Metallurgical Research, Spokane, Wash.
Kennecott Copper Corp., New York, N. Y.
Keokuk Electro-Metals Co., Keokuk, Iowa
Libbey-Owens-Ford Glass Co., Toledo, Ohio
P. R. Mallory & Co., Indianapolis, Ind.
McGean Chemical Co., Cleveland, Ohio
Merck & Co., Inc., Rahway, N. J.
Metal & Thermit Corp., Detroit, Mich.
Minnesota Mining & Manufacturing Co., St. Paul, Minn.
Monsanto Chemical Co., St. Louis, Mo.
Motorola, Inc., Chicago, Ill.
National Cash Register Co., Dayton, Ohio
National Lead Co., New York, N. Y.
National Research Corp., Cambridge, Mass.
National Steel Corp., Weirton, W. Va.
New York Air Brake Co., Vacuum Equipment Div., Camden, N. J.
Northern Electric Co., Montreal, Que., Canada
Norton Co., Worcester, Mass.
Olin Mathieson Chemical Corp., Niagara Falls, N. Y.
High Energy Fuels Organization (2 memberships)
Pennsalt Chemicals Corp., Philadelphia, Pa.
Phelps Dodge Refining Corp., Maspeth, N. Y.
Philco Corp., Philadelphia, Pa.
Philips Laboratories, Inc., Irvington-on-Hudson, N. Y.
Pittsburgh Metallurgical Co., Inc., Niagara Falls, N. Y.
Poor & Co., Promat Div., Waukegan, Ill.
Potash Co. of America, Carlsbad, N. Mex.
Radio Corp. of America, Harrison, N. J.
Ray-O-Vac Co., Madison, Wis.
Raytheon Manufacturing Co., Waltham, Mass.
Reynolds Metals Co., Richmond, Va. (2 memberships)
Rheem Semiconductor Corp., Mountain View, Calif.
Schering Corporation, Bloomfield, N. J.
Shawinigan Chemicals Ltd., Montreal, Que., Canada
Speer Carbon Co.
International Graphite & Electrode Div., St. Marys, Pa. (2 memberships)
Sprague Electric Co., North Adams, Mass.
Stackpole Carbon Co., St. Marys, Pa.
Stauffer Chemical Co., New York, N. Y.
Sumner Chemical Co., Div. of Miles Laboratories, Inc., Elkhart, Ind.
Sylvania Electric Products Inc., Bayside, N. Y. (2 memberships)
Tennessee Products & Chemical Corp., Nashville, Tenn.
Texas Instruments, Inc., Dallas, Texas
Metals & Controls Div., Attleboro, Mass.
Three Point Four Corp., Yonkers, N. Y.
Titanium Metals Corp. of America, Henderson, Nev.
Tung-Sol Electric Inc., Newark, N. J.
Udylite Corp., Detroit, Mich. (4 memberships)
Universal-Cyclops Steel Corp., Bridgeville, Pa.
Upjohn Co., Kalamazoo, Mich.
Victor Chemical Works, Chicago, Ill.
Western Electric Co., Inc., Chicago, Ill.
Wyandotte Chemicals Corp., Wyandotte, Mich.
Yardney Electric Corp., New York, N. Y.

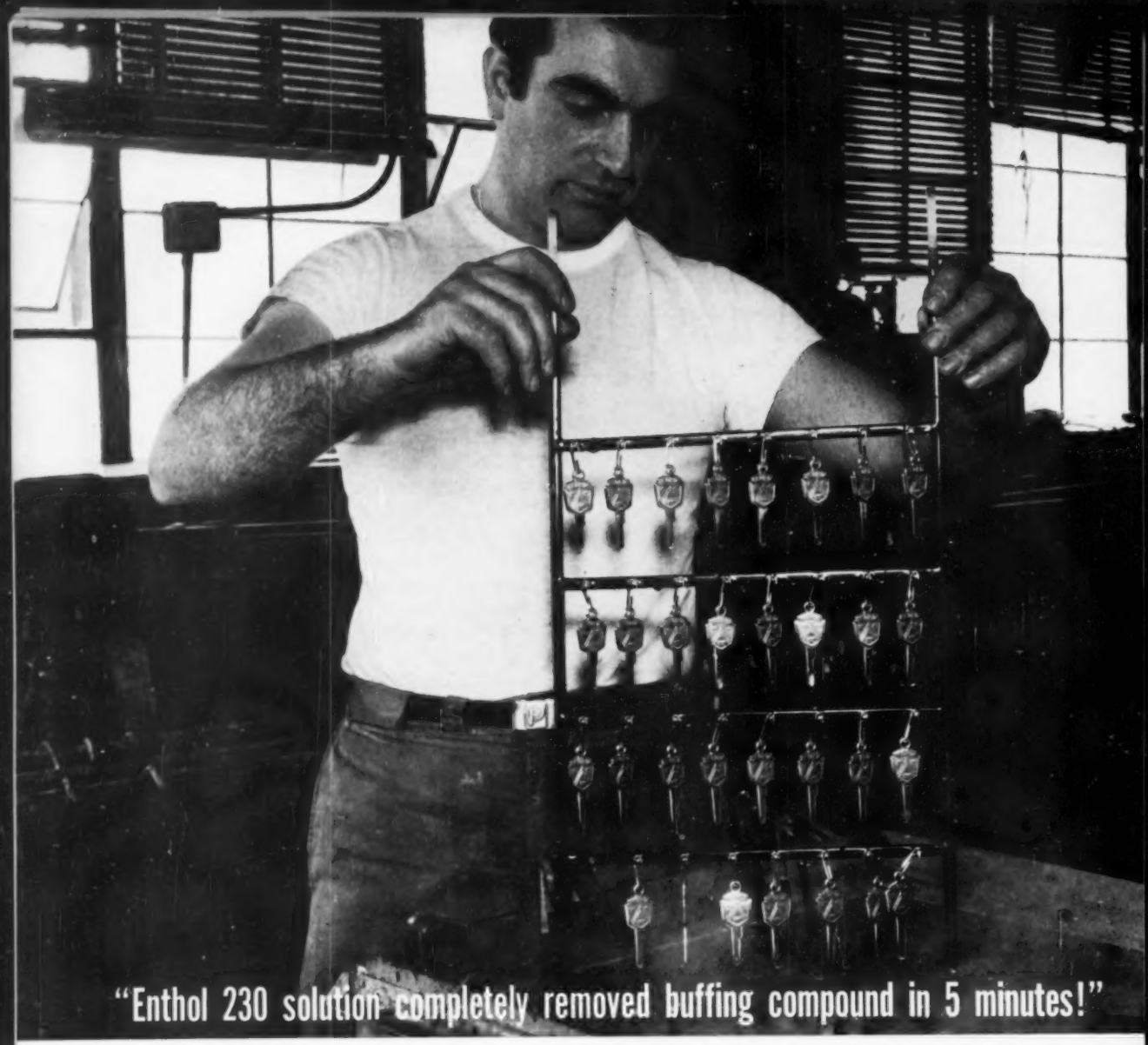

"Enthol 230 solution completely removed buffing compound in 5 minutes!"

At Regal Plating Company, Providence, R. I., these brass keys have just been soaked for 5 minutes in a 3.5% by volume solution of Enthol 230 at 180° F. Buffing compound packed in design work and crevices has been effectively dissolved away.

Regal joins a growing list of platers who have discovered the efficiency of new Enthol 230 in cleaning out the deep crevices, engravings, and filigree work in ornate costume jewelry. As for economy, Regal reports that an 85-gallon tank of cleaning solution required only 3 gallons of Enthol 230 for make-up and 1 gallon for replenishment over a 6 week period! The "ammonia wash" used previously, could not compete with this low operating cost.

Whatever your buffing compound removal problem, this new, mildly alkaline, liquid detergent should solve it. Enthol 230 solutions penetrate and dissolve even hardened buffing compounds, and, in many instances, have eliminated hand brushing of parts. The solutions have extremely long life and high tolerance to contamination by dissolved soils. Enthol 230 solutions can clean steel, zinc die castings, aluminum, copper, brass, white metal, lead, nickel plate, gold, and silver. They are excellent for use in ultrasonic cleaning. Write today for complete information, to Enthone, Inc., 442 Elm Street, New Haven, Conn.

ASARCO

ANOTHER PRODUCT OF *Enthonics* RESEARCH

ENTHONE

A Subsidiary of American Smelting and Refining Company